

**DESIGN OF COMPOSITE PROTEIN MICROCRYSTALS FOR THE
SUSTAINED ORAL DELIVERY OF ANTIGENS**

By
Noelia E. Almodóvar Arbelo

A thesis submitted in partial fulfillment of the requirements for the degree of

MASTER OF SCIENCE
in
CHEMICAL ENGINEERING

UNIVERSITY OF PUERTO RICO
MAYAGÜEZ CAMPUS
2015

Approved by:

Madeline Torres Lugo, PhD
President, Graduate Committee

Date

Maribella Domenech Garcia, PhD
Member, Graduate Committee

Date

Magda Latorre Esteves, PhD
Member, Graduate Committee

Date

Silvina Cancelos, PhD
Graduate School Representative

Date

Aldo Acevedo Rullan, PhD
Chairperson of the Department

Date

Copyright © 2015
By
Noelia Almodóvar Arbelo

ABSTRACT

Oral immunization is a promising method to decrease access of allergens and pathogens to the body. Oral delivery of antigens is challenged by the anatomical conditions of the gastrointestinal tract, such as degradation by the acidic environment of the stomach and protein breakdown by proteases. The use of protein composite microcrystals to deliver antigens to the gastrointestinal tract was proposed to challenge these difficulties. Composite microcrystals were composed of an antigen in the form of crystalline protein and a biodegradable polymeric carrier, alginate. This work focused on testing the application of this mechanism with the model protein lysozyme, insulin and ovalbumin, as well as testing the protein release behavior in simulated gastrointestinal conditions of lysozyme microcrystals from the alginate matrix. It was hypothesized that by using a protein in crystalline form, the release in simulated gastrointestinal conditions of the protein in alginate beads would be controlled and sustained. Alginate beads and microbeads were created via ionic crosslinking with calcium. Successful crystallization of lysozyme was performed in these systems demonstrating that calcium-alginate served as an adequate matrix for lysozyme protein crystallization. Protein release behavior of solvated and crystallized protein from alginate beads when exposed to simulated gastric and intestinal fluid was compared. Composite microcrystals released the majority of its content in simulated intestinal fluid and a smaller quantity in simulated gastric fluid. Protein transport of the liquid protein from the alginate matrix was characterized by the power law as pseudo Fickian, while the composite system was found to be anomalous, where the release is characterized by a combination of polymer relaxation and diffusion. Release kinetics studies showed that crystalline protein was released slower and in a sustained way than its liquid counterpart, independently from the alginate content being used as indicated by a smaller diffusion coefficient. The

proposed crystallization method was furthermore applied to insulin and ovalbumin. Insulin was found to crystallize in covalent crosslinked alginate beads. Ovalbumin, on the other hand, preferably crystallizes on the surface of calcium alginate beads. These results showed a potential new approach for the oral delivery of proteins.

RESUMEN

La inmunización a través de la vía oral es una forma prometedora de reducir el acceso de agentes alérgicos y patógenos al cuerpo. La degradación de antígenos por el ambiente ácido del estómago y el rompimiento de proteínas por las proteasas son barreras anatómicas del sistema gastrointestinal que limitan la absorción de estos al cuerpo. Por estas razones para que el cuerpo desarrolle una respuesta inmune es necesario proteger el antígeno y liberar mayores cantidades del mismo. Para combatir estas dificultades se propuso el uso de microcristales de proteína compuesta para la liberación de antígenos al sistema gastrointestinal. Los microcristales combinados estaban compuestos de un antígeno en forma de cristal de proteína, y alginato, un polímero biodegradable, que sirve de matriz para llevar los microcristales al lugar de acción, a la misma vez que protege el antígeno. La hipótesis esperada es que al usar la proteína en forma cristalizada, la liberación de la proteína en condiciones simuladas gastrointestinales sería controlada y sostenida.

Este trabajo se enfocó en probar este mecanismo con las proteínas modelos lisozima, insulina y ovoalbúmina. A la misma vez es de nuestro interés probar el comportamiento de liberación de proteína de esta proteína cristalizada en condiciones que simulan el sistema gastrointestinal. Esferas y microesferas de alginato fueron creadas con calcio como agente entrecruzante. Se cristalizó exitosamente la proteína lisozima en estos sistemas. Los resultados demuestran que alginato entrecruzado por calcio sirvió como sistema adecuado para la cristalización de lisozima.

Se hicieron pruebas de la liberación de la proteína cristalizada de esferas de alginato en líquido simulado gástrico e intestinal para probar cómo este sistema se comportaría para la

liberación del antígeno por la vía oral. Esto se comparó con la liberación de la matriz de alginato de la proteína en forma líquida, que se observa con mayor frecuencia en la literatura. El alginato resultó ser un polímero adecuado para la liberación de antígeno al intestino, ya que liberó la mayoría de su contenido en el fluido intestinal simulado. El transporte de proteínas líquidas de la matriz de alginato se caracterizó por la ley de potencia como Fick, mientras que la de proteína cristalizada se caracterizó como anómala. Al examinar la cinética de liberación temprana de la matriz de alginato, se determinó que la proteína cristalina se liberó de la matrix de alginato más lentamente y de forma sostenida que sus análogos de proteína líquida. Esto fue confirmado con el cálculo de los coeficientes de difusión para estos dos sistemas.

El sistema de liberación de antígeno propuesto se aplicó a la insulina y la ovoalbúmina. En el caso de la insulina, la cristalización de proteínas en bolitas de alginato ocurrió en polímeros de alginato entrecruzados covalentemente. Se encontró que ovoalbúmina prefiere cristalizar en la superficie o cerca del borde de las esferas de alginato. Estos resultados demuestran una nueva forma de liberar proteínas oralmente.

ACKNOWLEDGEMENTS

I wish to recognize several persons who in one way or another helped me in this project. I wish to dedicate this section to acknowledge their support. Their guidance and support made this work possible. First, I have to thank God for guiding me, opening doors and blessings through my life. I would like to express my gratitude to Dr. Madeline Torres for allowing me to be a part of this innovative project during my master studies. I appreciate the advice, supervision and guidance during this journey, which contributed, significantly to my professional and personal development. Thank you for the honest discussions, tireless editing and advice. Thank you for providing me with the tools to develop both personally and professionally in the past two years and a half and for teaching me how to approach research with an open mind. I would like to thank to my graduate committee members Dr. Maribella Domenech and Dr. Magda Latorre for their comments and corrections on this thesis.

I also wish to thank all my CBEN lab colleagues for the unique and wonderful experiences we shared, which have allowed me to grow in different areas of my life. I want to give special thanks to Janet, Fernando, Karem, and Marisel for making this experience a fun one. I hold dearly in my memories all of the conversions we had. Camilo thank you for being a great collaborator and helping me with the Confocal Microscope various times.

I am grateful to the NIH RISE 2 BEST Program for the financial support and educational development given. All the seminars received helped me visualize myself as the kind of professional I want to be. Rosalie and Mairim, thank you for always checking up on anything that was needed during this project.

Also I express my foremost gratitude to my family, Nelson, Elizabeth, Natalia and Nelson Jr., for the love and support in every decision. You guys are the best family anyone could

ask for. I am genuinely grateful to my husband Jayson. I am glad that we started this journey together. You have been an unconditional fountain of support in my life.

Finally, I offer acknowledgements to the funding agency that have allowed this work possible: U.S. National of Health (NIH) under Award No NIHINBRE2PORR016470-09 (INBRE Program) and NIH RISE2BEST Program under Award No NIH-R25GM088023.

TABLE OF CONTENTS

ABSTRACT	iii
RESUMEN	v
ACKNOWLEDGEMENTS	vii
LIST OF FIGURES	xii
LIST OF TABLES.....	xv
1 JUSTIFICATION	1
2 BACKGROUND.....	3
2.1 Oral/Mucosal Immunization.....	3
2.1.1 Anatomy of the Gastrointestinal Tract	5
2.2 Protein for Antigen Delivery	9
2.2.1 Model Proteins	10
2.2.2 Protein Crystallization	12
2.3 Biodegradable Polymers for Oral Immunization.....	16
2.3.1 Alginate	17
3 LITERATURE REVIEW	21
3.1 Approaches to Oral Immunization and Antigen Delivery	21
3.1.1 Sodium Alginate for Protein Delivery and Crystallization	22
3.2 Protein Crystallization Studies	25
4 OBJECTIVES	29
5 MATERIALS	31

6	METHODS	32
6.1	Alginate Bead and Microbeads Formation.....	32
6.2	Microbead Size Analysis.....	34
6.3	Lysozyme Crystallization in Alginate Beads and Microbeads.....	34
6.4	Fluorescent Alginate and Lysozyme.....	37
6.5	Lysozyme Release from Beads.....	39
6.6	Insulin Crystallization	41
6.7	Ovalbumin Crystallization	43
7	RESULTS AND DISCUSSION	45
7.1	Alginate Bead and Microbeads Characterization	45
7.2	Lysozyme Crystallization in Alginate Systems.....	48
7.3	Fluorescent Lysozyme and Alginate Crystallization	51
7.4	Lysozyme release behavior from alginate system	54
7.5	Insulin Crystallization in Alginate Systems	68
7.6	Ovalbumin Crystallization in Alginate Systems.....	71
8	CONCLUSION AND RECOMENDATIONS	74
	REFERENCES	77
	Appendix A: Microbead Size Analysis	84
	Appendix B: Lysozyme Crystallization in Alginate Beads.....	86
	Appendix C: Protein Release from Alginate Systems	87

Appendix D: Insulin Crystallization via Hanging drop method and in Alginate Beads92

Appendix E: Ovalbumin Crystallization93

LIST OF FIGURES

Figure 1 Peyer's Patches Immune Response.....	8
Figure 2 Lysozyme Crystal and Structure.....	10
Figure 3 Insulin Crystal and Structure.....	11
Figure 4 Ovalbumin Crystal and Structure.....	12
Figure 5 Common Crystallization Methods.....	15
Figure 6 Guluronic acid and mannuronic acid in Alginate.....	17
Figure 7 Eggbox model.....	18
Figure 8: BETE Nozzle Alginate Microbead Formation Set-up.....	33
Figure 9: Varied Alginate Bead size from 1.5mm to 5um.....	46
Figure 10 Box Plots for the three batches of alginate microbeads with three different concentrations.....	47
Figure 11 Lysozyme crystallization in solution and inside alginate beads.....	49
Figure 12 Decrease in size crystallization of lysozyme in alginate beads and microbeads.....	51
Figure 13 Fluorescent Alginate Beads with Lysozyme Crystallization.....	52
Figure 14 3D Confocal Picture of alginate matrix with embedded Lysozyme crystals.....	52
Figure 15 Single Lysozyme crystal in Alginate Matrix.....	53
Figure 16 Z-Stack view of Alginate Microbead with two Lysozyme crystals within structure....	54
Figure 17 Protein quantity per polymer content.....	57
Figure 18 Release Profiles for Solvated and Crystallized Protein from 2, 3, 4% w/v Aginate Beads in Simulated Gastric Fluid.....	59
Figure 19 Release Profiles for Solvated and Crystallized Protein from 2, 3, 4% w/v Aginate Beads in Simulated Intestinal Fluid.....	59

Figure 20 Protein Fraction Release per mg of polymer for Solvated and Crystallized Protein in Simulated Gastric Fluid.....	60
Figure 21 Protein Fraction Release per mg of polymer for Solvated and Crystallized Protein in Simulated Intestinal Fluid.....	60
Figure 22 24 hours of Protein Release Profiles of Crystallized and Liquid Lysozyme from Alginate Beads in SGF (left) and SIF (right)	61
Figure 23 Baker-Lonsdale Model Fitting for 3% Alginate bead with crystalline protein (line is the model fitting, dot is the experimental data).	67
Figure 24 Insulin Crystal Formation by Method 1 (sodium phosphate, left) and Method 2 (sodium citrate, right).....	70
Figure 25 Insulin Protein Crystallization in Alginate Beads. Complete bead (left). Close up (right).....	70
Figure 26 Ovalbumin Crystallization obtained from egg white purification process. (Left) SDS PAGE Electrophoresis of liquid before ovalbumin crystallization and after. (Right)	72
Figure 27 Ovalbumin Crystallization in alginate beads	73
Figure A.1 Size Analysis for Alginate Microbead.....	84
Figure A.2 Histograms of 2, 2.5, 3.0%w/v AlgNa Microbeads Diameter Distribution in Minitab.....	85
Figure B.1 Lysozyme Crystallization in Alginate Beads.....	86
Figure B.2 Alginate Crystallization Procedure for 3%w/v Alginate Bead.....	86
Figure B.3 Alginate Crystallization for 1-4%w/v Alginate Beads.....	86
Figure C.1 Short term Protein Release in SGF: Solvated Protein and Crystallization protein.....	87
Figure C.2 Protein Release with fitted model for 2, 3, 4%w/v Alginate Beads with Liquid Protein.....	88

Figure C.3 Residual Data Analysis with Fitted Model for 2, 3, 4% ² /v Alginate Beads for Liquid Protein.....	89
Figure C.4 Protein Release with fitted model for 2, 3, 4%w/v Alginate Beads with Crystallized Protein.....	90
Figure C.5 Residual Data Analysis with Fitted Model for 2, 3, 4% ² /v Alginate Beads for Liquid Protein.....	91
Figure D.1 Insulin Crystals by Hanging Drops and Inside Alginate Beads.....	92
Figure E.1 Ovalbumin Crystallization.....	93

LIST OF TABLES

Table 1 Examples of commercially available licensed oral vaccines	5
Table 2 : Environment of the gastrointestinal tract's segments.....	7
Table 3 General Overview of Biodegradable Polymers.....	16
Table 4 Protein Crystallization Conditions	35
Table 5 Loading Efficiency of Crystallized and Liquid Protein into Alginate Beads	56
Table 6 Average n values for transport behavior.....	63
Table 7 Diffusion from Alginate Matrices	65
Table 8 Results from Baker-Lonsdale Model for Diffusion Coefficient	67
Table 9 Main Proteins found in Egg White.....	72
Table A.1 Yield of the Microbead Preparation Process by the BETE Nozzle Spray.....	85

1 JUSTIFICATION

The gastrointestinal tract is a gate for the introduction of pathogens and a site for strong inflammatory responses due to food allergies. The prevention of diseases through the actuated stimulation of the immune system is thus a promising alternative to decrease the access of such pathogens to the body. One alternative is the creation of mucosal immunity by oral/mucosal vaccination. This is relevant especially since mucosal vaccine administration has been demonstrated to induce immune responses not only in the mucosal site, but also system-wide.¹ Furthermore, administering vaccines through the oral route provides varied benefits like convenience in administration and patient compliance.

One of the main challenges of creating oral mucosal vaccines is the difficulty in delivering antigens to the mucosa. Antigens as well as other proteins easily degrade in the gastric acid of the stomach and through the action of proteases. As a consequence, large doses of antigens are needed to cause an immune response.² To overcome these challenges, we propose the development of protein composite microcrystals that can serve as a delivery avenue to antigens through the gastrointestinal tract. The rationale of this system reside in that proteins in their crystalline form are more robust in harsh environments when compared to their solvated counterparts. Also, they can pack more protein in the same volume.³ Therefore, the use of a polymer matrix to carry the microcrystals to the site of action while protecting them from the harsh environments of the gastrointestinal tract is of great interest. The polymer can also be selected to stimulate an immune response, making it a potential adjuvant.

There are various biodegradable, natural polymers that can serve to encapsulate and deliver these composite microcrystals. Several examples are agarose, chitosan and alginate. Alginate was

selected because it has many advantages, including biocompatibility, low toxicity, and relatively low cost. This natural polymer is also widely used in the biomedical field. For this particular project, it is very useful because of its ability to crosslink by addition of divalent cations such as calcium, providing a matrix with controlled diffusion properties. Also, its size and shape can be manipulated to form microbeads.⁴

This project focused on the encapsulation, crystallization and release of the crystallized proteins lysozyme, insulin and ovalbumin at a micron scale through the use of alginate microbeads. Lysozyme was chosen as a suitable model protein because its crystallization has been well documented in literature. This technique will then be applied to insulin and ovalbumin. Insulin is a small protein that serves as a therapeutic hormone used daily in the medical treatment of diabetes by millions of people.⁵ This protein was chosen because it has been previously crystallized and it can serve also as a model protein. Ovalbumin is known to be the main responsive antigen for the development of egg allergies and is normally used in immunotherapy. Ovalbumin was selected as the test protein for the goal of developing an oral mucosal vaccine. It is hypothesized that the alginate microspheres can be used to crystallize and control the release of the protein in a simulated gastrointestinal tract environment. Because composite microcrystals can be obtained from any protein that can be crystallized, the results of this study will aid in the future formulation of other composite crystals as well.

2 BACKGROUND

Vaccination has been historically known to be efficient in eradicating diseases. Using an oral vaccine is an approach to counterattack the pathogens that gain access to the body through the gastrointestinal (GI) tract. To be able to design and implement the proposed mucosal vaccine, it is necessary to understand the anatomy of GI tract, and the immunological processes in the mucosa. The proposed oral mucosal vaccine will both have an antigen, in the form of a crystallized protein, and an adjuvant in the form of a biodegradable polymer. Therefore, this chapter will include information on oral immunization, biodegradable polymers, protein crystallization techniques and the advantages of using a protein in its crystalline form, rather than solvated.

2.1 Oral/Mucosal Immunization

Vaccines are beneficial because they activate the immune system to produce its own antibodies against an antigen, resembling a disease infecting the body. The aim of vaccination is to provide immunity against a benign form of a pathogen that will trigger an immunological memory. Because of this immunological memory, if the body encounters a secondary exposure to the pathogen, the infection will be terminated before the disease starts. Vaccines are usually composed of an antigen and an adjuvant. The antigen will encourage the production of one of five immunoglobulin (Ig) antibodies (IgA, IgG, IgD, IgM, IgE) with a specific immunological role in the body.⁶ The adjuvant delivers the antigen and helps in stimulating a strong immune response often allowing smaller amounts of the antigen to be used in the vaccine.⁷

Mucosal immunization can be administered through oral, nasal, sublingual, rectal or vaginal routes. We have chosen to focus on the oral route since the allergens and pathogens we would like to immunize against gain access to the body through the gastrointestinal tract. Administering vaccines

orally is safe, convenient, and positive for patient compliance.⁸ There are challenges with this route of administration as there are with any of the mucosal routes. The quantity of dosage that actually reaches the mucosal area is small making systemic circulation minimal. Antigens and proteins can be denaturalized or degraded by proteases in the GI tract thus, requiring large doses of the antigen makes it non attractive.^{9, 10} For these reasons, the most common route for antigen administration is parenteral (intramuscular), which bypasses the acid environment of the stomach, and can be administered in lower doses. Antigens administered in this way are taken by dendritic cells into the closest lymph node, where a cellular immune response is started and a systemic immunity is given.¹¹

However, intramuscular vaccine administration alone provides poor gut mucosa immunity, and is less effective when infection occurs at mucosal surfaces.⁹ The immune responses generated in the systemic lymphoid organs are qualitatively distinct from the ones in the gut associated lymphoid tissues (GALT), because the types and distribution of defensive cells in both systems is different and varies greatly in number.¹² The gut mucosal surfaces are filled with their own lymphoid tissue and immune system cell resources because of its importance in food nutrient absorption. Additionally, immune responses that are started on the mucosa membranes can provide immunization both in the mucosa and systemically, because immunization starts locally in the GALT and spreads to other lymph nodes.¹³ This makes oral vaccination an important tool for disease prevention.

There are several examples of commercially available oral vaccines that have been successful in disease prevention worldwide. These are licensed oral vaccines for Typhoid, Cholera, Rotavirus and Polio¹⁴, shown in Table 1 by their composition, and the antibodies (Ig) that they stimulate to cause an immune response. These vaccines are taken orally and immunize the mucosa of the GI tract where the infection occurs. For example, the rotavirus, an agent that causes diarrhea, responsible for the death of over 500,000 children each year in developing countries, spreads by the fecal-oral route.¹⁵ The virus is

shed by an infected person and then enters a susceptible person's mouth to cause infection. This oral vaccine induces protective immunity against viral infection through the induction of mucosal IgA (which provides protection at the mucosal surface) and systemically neutralizing IgG.¹⁶

Table 1 Examples of commercially available licensed oral vaccines

(Modified from Reference 14)

Pathogens	Trade name	Composition	Immunological Mechanism
Rotavirus	RotaTeq (Merck); Rotarix (GlaxoSmithKline)	Live attenuated, monovalent or pentavalent rotaviruses	Mucosal IgA and systemic neutralizing IgG
Salmonella Typhi	Vivotif (Crucell); Ty21A	Live attenuated S. typhi bacteria	Mucosal IgA, systemic IgG and Cytotoxic T lymphocyte
Poliovirus	Orimune; OPV; Poliomyelitis vaccine	Live attenuated trivalent, bivalent and monovalent viruses	Mucosal IgA and systemic IgG
Cholera	Dukoral (Crucell); Shanchol (Shantha Biotechnics)	Inactivated V. cholera O1 classical and El Tor biotypes	Toxin-specific and lipopolysaccharide specific IgA

The worldwide impact of these vaccines has motivated scientists to design and discover new potential oral vaccines. By exploring the anatomy and the immunological process in the gastrointestinal tract, we can learn what anatomical barriers need to be overcome for oral mucosal vaccine delivery. This can help us choose the adequate design for an oral vaccine.

2.1.1 Anatomy of the Gastrointestinal Tract

Since the gastrointestinal tract plays a major role in nutrients absorption, it has various physical barriers that protect the body from any foreign material. These aid us in preventing diseases, but

difficult the ability to administer vaccines. The anatomy of the GI tract is divided into two main parts: upper and lower. The upper gastrointestinal tract consists of the mouth, esophagus, and stomach. The lower gastrointestinal tract consists of the small (duodenum, jejunum, and ileum) and large intestine (colon, rectum, anal canal). The environment of the GI tract changes from one segment to the next. For example, the pH of the stomach is acidic (pH~1) and the pH of the small intestine is slightly basic (pH~7).¹⁷ So when designing an oral vaccine, these factors have to be taken in consideration. The acidic environment of the stomach can be detrimental for proteins and induce denaturation. These also can be further degraded by enzymes in the stomach (pepsin) and in the intestine (proteases). To counteract these problems in supplying a vaccine orally, large amounts of antigen have to be supplied and the antigen has to be protected.¹⁸

The residence time in each segment varies, as well as the surface area as seen in Table 2. As the value of residence time and surface area increases, better absorption of the antigens can be expected. The site with the longest residence time is the large intestine followed by the Ileum. The site with the largest surface area is the Ileum. Therefore it is not surprising that this is the site where most of the nutrients from food are absorbed, making it the ideal site for oral vaccine delivery. The residence time in this segment is ~7 hours and its surface area is the highest of the GI tract, meaning that a vaccine will be in contact with the gut wall and lymphoid tissues for the longest time in this segment.¹⁷ Additionally, the ileum is the site of the lower GI that is most filled with gut associated lymphoid tissues (GALT), such as the Peyer Patches.⁶

Table 2: Environment of the gastrointestinal tract's segments.

(Source Reference 17)

Gastrointestinal Tract Segments	pH	Residence Time	Surface Area (m²)
Stomach	1-2	90min	3.5
Small Intenstine: Jejunum	5.5-7	1.5-2h	184
Small Intenstine: Ileum	7-7.5	5-7h	276
Large Intenstine	7-7.5	1-60h	1.5

The mucosa of the Ileum (Figure 1) contains the Peyer's Patches which are the best site for antigen delivery and screening. These are lymphoid tissues that have immune system cells of the GALT. Peyer's Patches have a dome like appearance and its entrance are covered by Microfold (M) cells, which have a thin shape to increase absorption.¹⁹ Antigens administered orally that arrive to the Ileum will interact with the M cells of the Peyer Patches. M cells allow the passage of antigens through the gut wall into the Peyer Patch. Dendritic (DC) cells, which constantly examine the intestinal lumen for antigens, inspect this foreign material and present it to the B and T lymphocytes. They then secrete antibodies (Ig) and cytokines that travel through the lymph nodes and into the blood stream. The antibodies can then travel back to the intestinal epithelium to provide specific protection for that antigen at the surface of the gut mucosa.²⁰

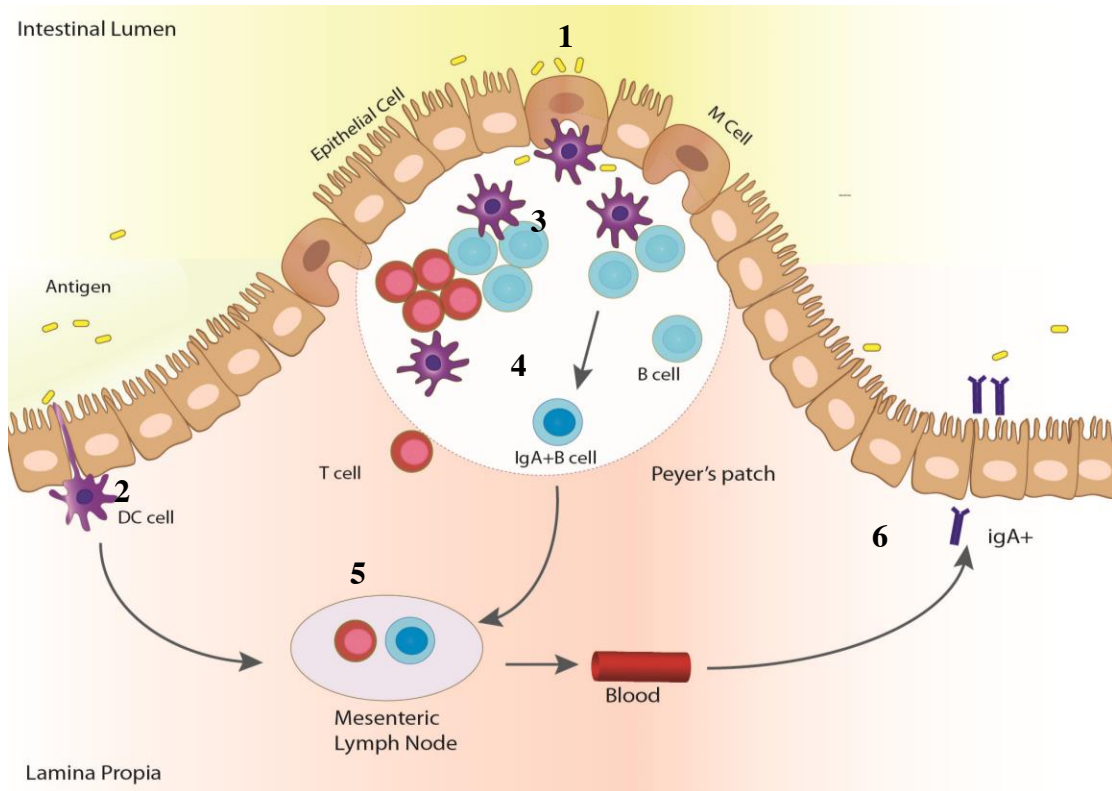


Figure 1 Peyer's Patches Immune Response.

Peyer Patches have a dome-like appearance. M cells allow the passage of antigens and pathogens into the Peyer's patch (1). Dendritic cells (2) examine this foreign material and present it to the B and T cells (3), which secrete specific antibodies (Ig) and cytokines (4) for that antigen. Antibodies and cytokines are taken into the mesenteric lymph node and into the blood stream (5). The antibodies can then travel back to the intestinal epithelium to provide specific protection at the surface of the intestinal lumen (6). Modified from Reference 20.

Each antibody has a specialized function. IgA for example is the main antibody in the mucosa lining of the gastrointestinal tract, so if a pathogen enters the gut mucosa wall, it will induce the production of IgA. IgG facilitates the engulfment and further destruction by phagocytes of the extracellular microorganisms and toxins. IgE, in contrast, reacts in response to parasitic infestations

and allergens. This antibody triggers strong inflammatory reactions to counterattack parasites or in response to an allergic reaction.⁶ When a person develops an allergy to a foreign material, the body finds the organism to be an intruder and reacts with immune responses that cause various allergic symptoms (inflammation). In the case of a pathogenic infection symptoms would occur.²¹ Our aim when designing a vaccine is to sensitize the body to an identified protein by delivering it to the M cells, which can be targeted by a particle size of less than 10 μ m.²² The immune response would be to counterattack its presence by developing antibodies and an immune memory, which makes vaccines effective.

Based on these physiological challenges for delivering vaccines orally, the adequate vaccine design for oral mucosal immunization would include at least the following qualities. Firstly, provide protection of the antigen against the proteases and gastric acid of the stomach. Secondly, an adjuvant, which helps create a stronger immune response. Thirdly, provide release of large doses of the antigens in the intestinal lumen. Fourthly, have an adequate antigen size for M cell interaction. To elucidate these challenges, we have selected a system which will be composed of a protein in its crystallized form to serve as the antigen and a biodegradable polymer to serve as the adjuvant. The polymer will provide protection of the antigen in the harsh environment of the GI tract, help create a stronger immune response, control the size of the antigen, and release its content in the intestinal lumen. The crystalline protein will release larger doses of the antigen in the same volume, provide a slower dissolution of the antigen, and provide stability to the antigen.

2.2 Protein for Antigen Delivery

The antigens chosen in this project are the proteins lysozyme, insulin, and ovalbumin. Lysozyme and insulin have been particularly selected because of their usefulness in protein

crystallization. Ovalbumin on the other hand is an immune responsive protein that is used to model vaccine adjuvants and allergic reactions. These proteins are going to be supplied in their crystalline form because it will add benefits in delivering the oral vaccine.

2.2.1 Model Proteins

Lysozyme is an egg white protein. Although this protein does not produced a specific immune response to a disease, it was chosen as a model protein in this project because it can readily crystallize into multiple crystal forms.²³ Lysozyme is an enzyme which hydrolyzes polysaccharides in bacterial cell walls. Hen egg white lysozyme is composed of a single chain of 129 amino acids and has a molecular weight of 14,296 Da.²⁴ Extensive information on lysozyme crystallization has been obtained by measuring its solubility as a function of salt concentration along with other factors, such as crystal form, pH, temperature and salt type. For these reasons this protein is widely used in studying protein crystallization.

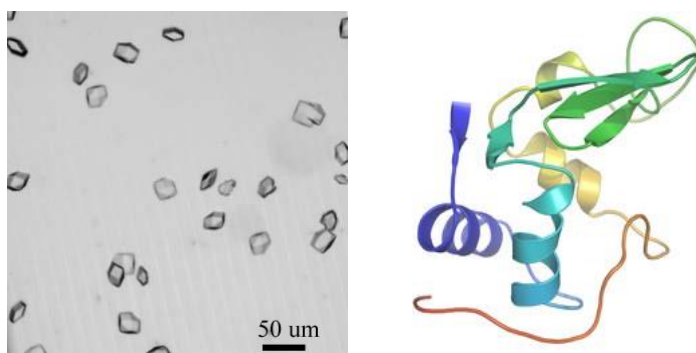


Figure 2 Lysozyme Crystal and Structure

Left: Picture of Lysozyme Crystal. Right: Lysozyme Molecular Structure, courtesy of Protein Data Bank 30

Insulin is an important protein for the therapeutic treatment of diabetes of millions of people every day. Even though there are researchers looking at delivering this protein in its solvated form through the gastrointestinal tract for diabetes treatment²⁵, we decided to use this protein as a model

protein because its crystallization protocol has been well studied by the scientific community. Insulin was one of the first proteins to be studied by crystallography to determine its structure. It has been crystallized in different conformations such as monoclinic, rhombohedral, cubic, and tetragonal.⁵ A crystallized formulation of insulin is currently used in the pharmaceutical market to treat diabetes.

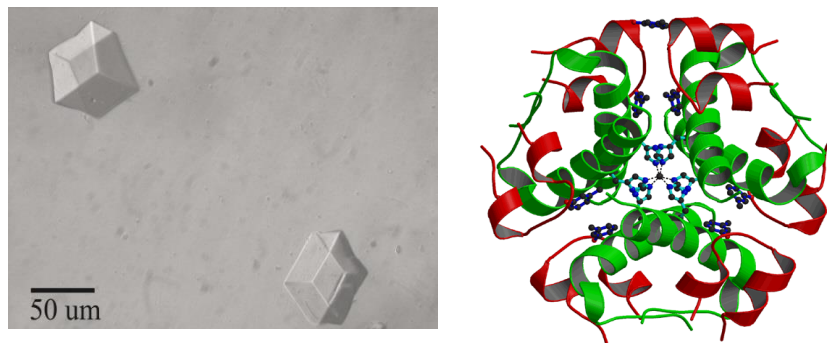


Figure 3 Insulin Crystal and Structure

Left: Picture of Insulin Crystal. Right: Insulin Molecular Structure, courtesy of Protein Data Bank 30.

Ovalbumin is the main component of egg white protein. This protein is of interest in this project because it is one of the causes of egg allergy. Egg allergy is common in early childhood, and although remission can occur during transition into adulthood, 12% of food allergies are attributed to egg. Complications of having an allergy to egg include the medical contraindication to vaccination of the seasonal and pandemic influenza vaccines and yellow fever vaccine because of their egg contents.²⁶ It is also commonly used for immunotherapy and for modeling allergy behaviors. This protein is a protein that is mildly immunogenic and readily available, so it is widely used when testing for novel vaccines efficiency in generating an immune response.^{27,28} Ovalbumin has a molecular weight of about 45,000 Da and an isoelectric point of pH 4.6. Native ovalbumin changes to S-ovalbumin, a more thermostable form, when exposed to heat or alkaline pH conditions. It is also susceptible to surface denaturation by shaking. It was first isolated in crystalline form by Hofmeister

(1887) by adding an equal volume of saturated ammonium sulfate solution to egg white and then evaporating the solution at room temperature.^{29,30}

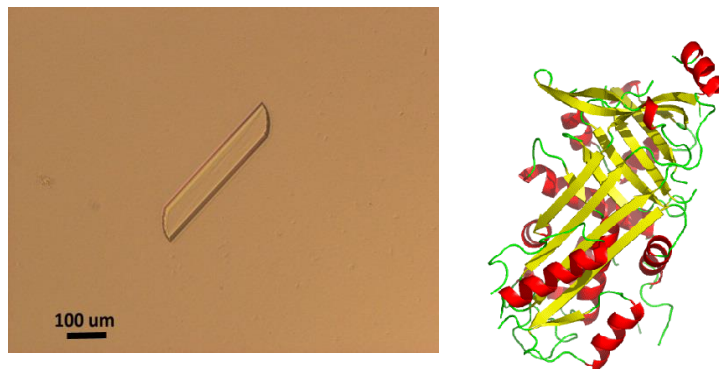


Figure 4 Ovalbumin Crystal and Structure

Left: Picture of Ovalbumin Crystal. Right: Ovalbumin Molecular Structure, courtesy of Protein Data Bank 3O.

2.2.2 Protein Crystallization

Crystallization of therapeutic macromolecules can offer significant advantages. In the pharmaceutical industry, the crystallization of active pharmaceutical ingredients (API) is commonly used to provide various benefits. Crystallization is used as a powerful tool to isolate and purify pharmaceuticals. The concentrated crystals are beneficial to deliver certain drugs which require high doses at the delivery site (for example, the gut wall).³¹ The stability of the drug in crystalline form is much higher than that of the soluble or amorphous form, which has an impact on properties such as the dissolution rate.³² These same principles apply when using protein crystallization for protein delivery. This is the case for the only currently FDA approved protein in its crystallized form, insulin. As explained earlier, insulin is an important protein in the treatment of diabetes. It is currently used by pharmaceuticals companies for subcutaneous delivery in its crystallized form because the insulin crystals dissolve slowly, which is beneficial for slow release of insulin into the blood stream. The size

and morphology of the crystal affects how fast the insulin is released, which helps explain why many conformation forms of this protein have been studied.

Protein crystallization is most commonly used to study the structure of protein molecules by X-ray crystallography. Industrially, crystallization is used as a purification step and for biological catalysis³³, but apart from insulin, crystallized proteins are not currently being used for antigen/drug delivery. The reason for this is that crystallizing a protein at a bench scale is a complicated task by itself and the structural fragility of proteins makes it complicated to upscale.³⁴ Because great potential exist for protein crystallization applications in the pharmaceutical industry, studies on upscaling protein crystallization are being performed.²⁹

To successfully crystallize any protein, an understanding of the nucleation and growth of these crystals is necessary. Protein crystals are molecular protein segments orderly packed into defined crystal lattice space groups. They are held together by hydrogen bonds and electrostatic interactions of the amino acid side chains with solvent molecules that are restrained between molecules during crystal structure formation. Crystal formation is also defined by nonspecific interactions like hydrophobic and van der Waals interactions.³⁴ To obtain the crystal, the protein solution is exposed to a salt that will serve as a precipitant as it “salts-out” the protein. This salting out principle allows small ions to form bonds with water molecules, therefore dehydrating the protein. As the ionic strength of the solution increases, the solubility of the protein decreases. If the concentration of ions becomes high the proteins are driven to neutralize its surface charge by interacting with one another.

The crystallization process is a thermodynamic and kinetic process. Thermodynamically, crystallization requires bringing the macromolecule to supersaturation. The protein should therefore be concentrated to the highest possible concentration without causing aggregation or precipitation of the macromolecule. Introducing the sample to a precipitating agent can promote the nucleation of protein

crystals and further three-dimensional crystal growth.³⁵ Thermodynamically, the crystalline form is an energetically favorable and stable state. Kinetically, the process of crystal nucleation and growth depend on the solubility and supersaturation of the protein in its environment. Differences between the supersaturated chemical potential of the molecule and its chemical potential in the saturated solution are the driving force in protein crystallization,³⁴ shown by the following equation.

$$\Delta\mu = k_b T \ln \frac{C}{C_s} \quad \text{Equation 1}$$

where k_B is the Boltzmann constant, T the absolute temperature, C the actual concentration before crystallization, and C_s the concentration of the protein at equilibrium.

There are a number of techniques to achieve protein crystallization. The techniques relevant to this thesis are the hanging drop method and crystallization in hydrogel matrices by counter diffusion. The hanging drop method is a way to test the crystallization conditions of proteins. This method uses vapor diffusion to equilibrate a drop of a solution of protein, buffer, and precipitant with a reservoir of buffer and precipitant in a sealed environment (Figure 5). The amount of precipitant in the drop at first is not enough to cause nucleation and crystallization, but as the system equilibrates the drop volume decreases causing the protein and precipitant concentration to increase.³⁶

Protein crystallization in hydrogel matrices by counter-diffusion is a technique that eliminates convection and establishes diffusion as the primary mechanism of mass transport. Usually, the protein is put at one side or inside of the polymer, while the precipitant solution is situated outside the polymer. Slow diffusion through the polymer matrix of the protein and precipitant occurs, which promotes nucleation and subsequent crystal formation, instead of an agglomerated precipitation. An

example of this technique can be seen in counter diffusion crystallization, such as the one in the Granada Box method (Figure 5B). This method consists of various set ups. One consists of filling a capillary with the polymer and the protein of interest. This capillary is then put in a solution of the precipitating agent. The crystal formation occurs along the capillary in the section where the protein and precipitating agent meet. This method provides added benefits in crystallization, such as protein purification and slow diffusion of crystallizing agents.³⁷

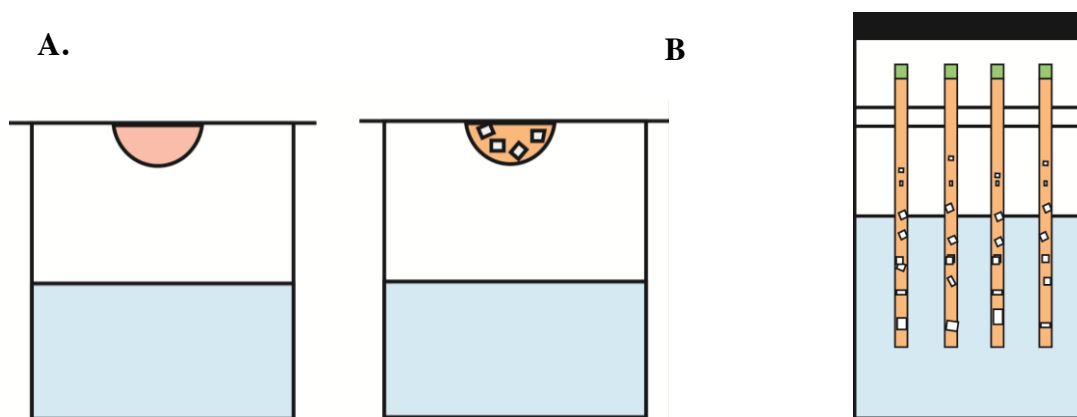


Figure 5 Common Crystallization Methods.

A) Vapor Diffusion Crystallization. The protein is deposited in a drop on a glass cover and put on top of a bath with the precipitating solution. As the precipitant solution diffuses into the drop, the protein crystallizes. **B) Crystallization in Hydrogel with Granada Box.** The protein can be either added to the capillary or to one side of the capillary plug. The capillary is then situated in a bath of the precipitant solution. Crystallization occurs along the capillary.

Crystallizing proteins in hydrogels is a viable and repeatable technique. Taking this into consideration for our vaccine system, the adequate adjuvant would be a polymer that allows protein crystallization to form in it, so that it is protected from the harsh environment of the GI tract. It would also release the protein contents in the intestine and not in the stomach, and would serve as an adjuvant

to the antigen. The adjuvant chosen should have a stable long shelf life, be non toxic, biodegradable, and cheap to produce, as well as being able to promote an appropriate immune response.³⁸

2.3 Biodegradable Polymers for Oral Immunization

Biodegradable polymers have been used for biomedical applications because they can be enzymatically degraded by the body once they have accomplished their purpose. They are also non toxic and capable of controlled rates of degradation. There is a large variety of biodegradable polymers, as seen in Figure 4, and each has their own benefits for different biomedical applications. Each polymer has specific (chemical, biological, and degradation) properties to provide efficient therapy.³⁹ For example, if the drug you want to deliver is targeted for the stomach, chitosan might be the ideal polymer since it releases its contents at low pH. Agarose is an ideal polymer for protein crystallization, but it does not possess the qualities for adequate antigen delivery because it is non immunogenic and will release the antigen in the stomach. Polylactics have been investigated, but are also non immunogenic, which can be problematic for adjuvant applications. We believe that alginate is the best choice to be used as a vaccine adjuvant in our system, since it is immunogenic, allows proteins to be crystallized in its matrix, and behaves differently in varied pH environments favoring intestinal antigen release.

Table 3 General Overview of Biodegradable Polymers

Biodegradable Polymers	Properties for biomedical applications
Synthetic Polymers	
Poly lactics	Demonstrate good cell adhesion and proliferation making it a potential candidate for tissue engineering applications. It can also form high strength fibers.
Natural Polymers, Polysaccharides	

Chitosan	Ability to act as a permeation enhancer through its interaction with the cell membrane resulting in a structural reorganization of tight-junction associated proteins. It also has mucoadhesive properties.
Alginate	Rate of content release can be varied by varying the protein/drug polymer interaction with the polymer, as well as varying the amount of crosslinking. ³⁹

2.3.1 Alginate

Sodium Alginate (AlgNa) is an anionic polymer that can be obtained naturally from seaweed and brown algae. This polysaccharide forms a family of linear block copolymers of mannuronic acid (*M*) and its epimer guluronic acid (*G*) units. The difference between both is their conformation and the position of the carboxyl group. These are linked together in various proportions and arrangements of *M* and *G* units along the chain (Figure 4). The regions in an alginate strand can have the same repetition of monomers (*MMM* or *GGG*) or an alternating sequence (*MGM*). A repetition of *M*-monomers is referred to as an *M*-block, while a repetition of *G*-monomers is referred to as a *G*-block.^{40, 41}

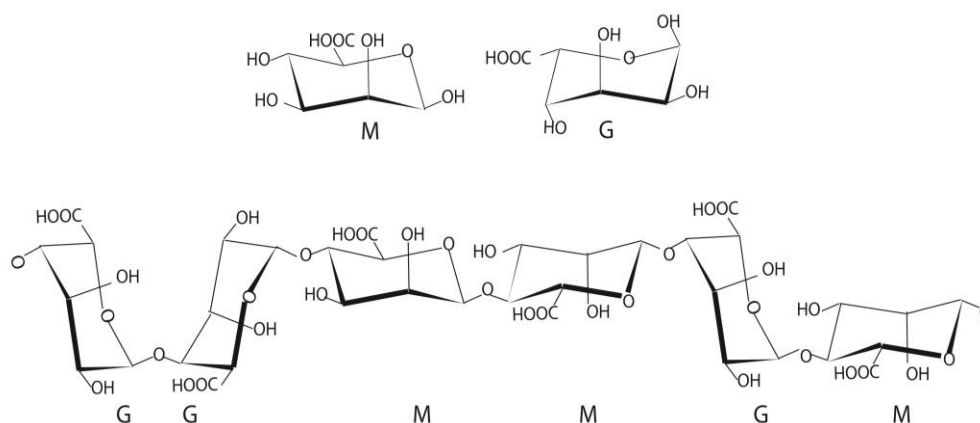


Figure 6 Guluronic acid and mannuronic acid in Alginate.

The figure shows the conformations and chemical structure of the two monomers of alginate; *G* and *M*, and their binding site when linked together. A *GG*-block will form a cavity structure as shown, which makes it ideal for ionic binding. Modified from Reference 40

AlgNa has been widely used in biological applications since it has a low toxicity, water-solubility, and biocompatibility, and it is relatively cheap. Alginate, particularly *G*-blocks and *MG*-blocks, chelate by selectively binding divalent cations, such as calcium, and forming hydrogels under mild conditions. The gel formation is mainly driven by *G*-blocks which associate to tightly held junctions when divalent cations are present.⁴² The Eggbox Model (Figure 4) describes how *G*-blocks merge together forming chelates with divalent ions. It was called the egg box model in reference to how calcium ions are situated in guluronic cavities like eggs in a carton, as illustrated in figure 4.⁴³ This crosslinking only occurs with the *G* blocks in the strand, because of the orientation of the carboxyl group. The rigid structure of a *G*-block shows higher affinity towards divalent cations than *M*, or *MG* blocks as the cavity created between *G*-monomers functions as an ion binding site. Alginates with high *G* blocks yield stronger gels. Therefore, the gel strength and porosity can be adjusted by adjusting the composition of alginate.⁴⁴

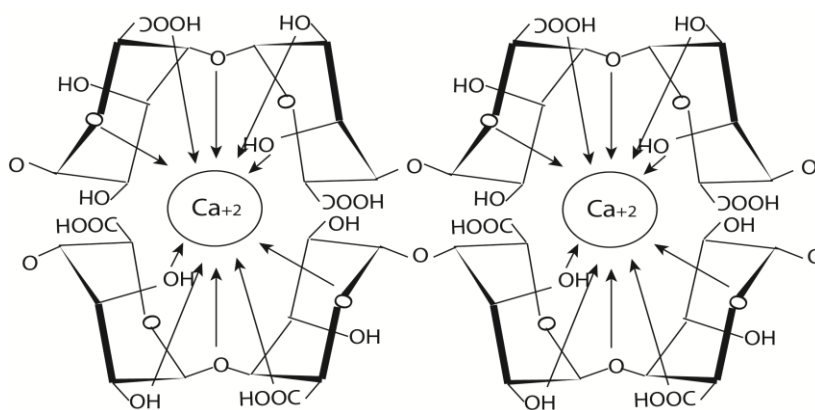


Figure 7 Eggbox model.

One calcium ion requires four *G*-units for cross-linking to occur. When calcium content is increased, more crosslinking of the alginate matrix occurs, providing the polymer with structural strength. Modified from Reference 43.

Alginate hydrogels of high guluronic content (higher than 60%) offer strength, low shrinkage and high stability. These properties make alginate an interesting material for tissue engineering applications and drug delivery. Due to the free hydroxyl and carboxyl groups distributed along the backbone, alginate is a suitable candidate for chemical modifications. Chemical modification of free hydroxyl group of alginates could be done by oxidation, reductive amination, and, copolymerization, whereas chemical modification of free carboxyl group can be done by esterification, and amidation.^{42,45} This makes alginate a very versatile polymer, with a lot of potential for different applications, one being potential directly targeting M cells by putting receptors on the surface of the alginate.

Peptides are commonly coupled to alginate by carbodiimide chemistry. Still, this may not be needed since alginate with high manuronic acid content is known to be immunogenic. Alginates with a guluronic acid content of 50% or above are recognized as not eliciting an immune response. High manuronic alginates (70-85%) may stimulate the innate immune system through membrane-binding receptors and have been showed to stimulate mouse Peyer patch cells.⁴⁶ Based on this, this polymer is viable to serve as an adjuvant for an oral vaccine.

Alginate is non-toxic and safe for human use. An example of alginate currently used in the pharmaceutical industry is in the acid reflux medicine Gaviscon, which helps protect the lining of the esophagus from stomach acid. Another important property of alginate is its behavior in different pH environments. This polymer is anionic and will collapse in acidic conditions (shirking) and will swell in basic environments (relaxed). This makes it an ideal adjuvant for oral vaccine administration, since it will protect the antigen while traveling through the stomach and release its contents in the intestine.⁴⁰ The release from alginate beads can be characterized by diffusion of the protein through the pores of the polymer network and/or degradation of the polymer network. The driving force for the diffusion

is the concentration gradient of molecules in solution. For larger molecules such as proteins, diffusional resistance occurs, although even large proteins will leak out of the gel beads with a rate depending on their molecular size, and pH of the solution.⁴⁷

3 LITERATURE REVIEW

3.1 Approaches to Oral Immunization and Antigen Delivery

Delivering proteins orally would have important applications in therapeutic treatment and disease prevention.⁴⁸ Scientists have turned to designing oral protein delivery systems as a technique to protect the protein and to modulate its release. There are several oral protein delivery systems currently being researched such as liposomes, vesicles, nanoparticles, and biodegradable polymers. Liposomes, for example, have been researched to deliver ovalbumin through oral administration in mice, showing that it was efficient in inducing oral tolerance by varying liposome composition.⁴⁹ The challenge with using liposomes as adjuvants is that they exhibit poor stability in vivo, and poor storage properties making them less desirable for protein delivery technologies than polymers.⁵⁰

The most common factor between protein delivery systems is the small particle size. Particles (>5 μ m) are going to be retained in the Peyer's Patches, stimulating a mucosal response. Smaller particles would move to other lymphoid organs inducing a more systemic immune response. A decrease in diameter leads to improved transport across the epithelium.²²

Hydrogels that are sensitive to pH have attracted attention for oral delivering of proteins, since the gastrointestinal tract has varied environments. Some of these polymers fall into the category of polysaccharides, such as chitosan and alginate. The favorable properties like biocompatibility, biodegradability, pH sensitiveness, mucoadhesiveness has enabled these polymers to become the choice of the pharmacologists as oral delivery matrices for proteins.

Many researchers have used chitosan for microparticles in mucosal drug delivery because of mild encapsulation conditions and mucoadhesive properties.^{39, 51} However, chitosan suffers from limited solubility at physiological pH and causes pre-metabolism of drugs in intestinal and gastric fluids in the

presence of proteolytic enzymes. To overcome these drawbacks chitosan has to be chemically modified or delivered with another polymer.⁵² Since this could affect protein crystallization, we have chosen to focus on alginate as the adjuvant in our vaccine.

3.1.1 Sodium Alginate for Protein Delivery and Crystallization

George et al.⁵³ suggested the use of crosslinked alginate as a hydrogel matrix for protein delivery. The biodegradable polymer alginate has been chosen for this project to protect and deliver the protein. Alginate provides a variety of advantages that are very suitable for our vaccine system such as mucoadhesion, ease of formation, structural similarity to extracellular matrix and ability to be used to crystallize proteins.³

Sodium alginate, being an anionic polymer with carboxyl end groups, is a good mucoadhesive agent. Mucoadhesive microspheres exhibit a prolonged residence time at the site of application contributing to improved therapeutic performance of the drug. Allamneni et al.⁵⁴ has studied the mucoadhesive properties of alginate. They varied the alginate concentration to increase the mucoadhesive properties of microspheres to achieve a substantial increase in length of stay in the GI tract of a drug called glipizide, used for treatment of type 2 diabetes. The mucoadhesive properties of the microspheres were evaluated by an in vitro wash-off test in rat stomach mucosa. They showed that by increasing the polymer alginate concentration from 2 to 5%w/v, the bioadhesive property of the microspheres also increased from 36 to 58%.

The molecular weights of sodium alginates range between 32,000 and 400,000 g/mol making it a great polymer to be used for varying the release kinetics of a protein release system. Varying the crosslinking time and alginate concentration can change the release of the content of alginate gels.

Aslani et al.⁵⁵ showed permeability studies of acetaminophen in alginic acid gels. The study found that acetaminophen permeability in the gel films decreased with increasing divalent cation concentration and cross-linking time until an apparent optimum was reached. Bhopatkar et al.⁵⁶ used alginate beads containing the model protein hemoglobin (Hb). Release studies were conducted in simulated gastric fluid (SGF) and subsequently in simulated intestinal fluid (SIF) at 37°C. The beads were stable in the gastric fluid, but released their protein upon transfer to intestinal fluid. This release coincides with the burst and disintegration of beads, which signals that they can be applied to releasing vaccines in the intestine.

The behavior of alginate microspheres filled with ovalbumin has been studied both in vitro and in vivo. Hariyadi et al.⁵⁷ examined the in vitro release of ovalbumin from alginate microspheres by changing the alginate concentration and examining two crosslinkers barium and calcium chloride at different concentrations. The study revealed that protein release decreased by decreasing alginate concentration. The crosslinker used also had an effect on the release behavior. Alginate microspheres produced using barium chloride had faster release behavior of ovalbumin in simulated GI tract conditions. This behavior was adjudicated to an increase in the porosity of microspheres form with barium chloride. The in vivo release of ovalbumin and alginate microbeads has been studied by Bowersock et al.⁵⁸ Their aim was to find if ovalbumin-alginate microspheres administered orally were successful in activating IgA and IgG antibody production. A group of BALB female mice were administered ovalbumin-alginate microsphere and another group with blank spheres. Serum was collected at day 0 and 2 weeks after the final inoculation and assayed by ELISA for ovalbumin specific IgA and IgG antibodies. Mice that were inoculated with ovalbumin in alginate microspheres by oral administration had a good immune response with increased serum IgG and IgA titers to ovalbumin and increased antibody secreting cells compared to mice that received plain microspheres.

It was concluded that the microspheres were effective in releasing the antigen upon oral administration to cause this stimulation in immune response.

As we mentioned in the previous chapter, alginate can serve as an adjuvant to stimulate immunological activity of cells by chemical modifications of alginate with RGD or by using an alginate with high mannuronic acid content. Suzuki et al.⁵⁹ administered intradermal RGD-modified alginate microparticles to mice and showed evidence of cell targeting by enhancing immunogenicity, in particular cellular responses such as IFN- γ cytokine secretion and lymphocyte proliferation. Mata et al.⁶⁰ demonstrated the effect on intestinal immunological activity by varying the mole fraction of mannuronate residues of alginates in contact with Peyer's patch cells of mice. Alginates with high mannuronate content (mole fraction of 0.69–0.86) showed immunological activity, but alginates with lower mole fraction than 0.31 did not.

Some disadvantages of alginate beads are low drug encapsulation efficiency and rapid release of the small loaded molecules as shown by Halder et al.⁶¹. Low encapsulation efficiency and loading capacity of alginate beads are attributed to the gel porosity, which can cause a leaking of some molecules. If the crosslinking is done with the protein mixed with the alginate, further drug diffusion into the crosslinking solution from the gel network can occur.⁶² Other researchers have remediated these problems by combining alginate with other polymers. Zhang et al.⁶³ used alginate–chitosan microspheres to develop a system for insulin delivery. The chemical stability of insulin released from the microspheres was well preserved after the microspheres were treated with the simulated gastric fluid containing pepsin for 2 hours and in simulated intestinal fluid. Martins et al.⁶⁴ used alginate mixed with dextran sulphate to avoid insulin release at pH 1.2, protecting the protein from the acidic environment and reducing the total insulin released at pH 6.8. In this research, we have remediate the

before mentioned problems by using the protein in a crystallized form, which will allow an increase in drug encapsulation efficiency and a slower release of the protein. Also the protein will be added to the bead once is formed to avoid the protein diffusing into the calcium chloride solution while crosslinking.

The possibility of using alginate beads for protein crystallization was tested in an experiment performed by Willaert et al³, which show a process for crystallization of lysozyme inside an alginate bead with size of 2mm. The protein was added into an alginate bead by diffusion, which allows protein purification, improving the quality of the crystals obtained. Then the crystallizing agents were diffused into the beads. This permitted crystallization to occur by counter-diffusion, in which alginate bead matrix provided an adequate environment for the crystallization of the lysozyme protein. Although the goal of this research was to obtain crystals for X-ray diffraction, we believe that this system shows promise for antigen delivery. In this system, the particle size was 2mm, our goal is to implement this method of crystallization in alginate microbeads in a size of less than 20um.

3.2 Protein Crystallization Studies

Crystallization of pharmaceuticals drugs has been used in industry as a way to deliver a drug in a controlled, stable way. Examples of drugs being currently formulated in this form are: atorvastatin calcium, a drug used for the treatment of high cholesterol ⁶⁵, piroxicam, a non-steroidal anti-inflammatory drug ⁶⁶, and for sulfathiazole⁶⁷, a local antimicrobial agent. Alternative, insulin is the only crystalline protein FDA approved for therapeutic use.⁶⁸ The potential applications and benefits of crystallized proteins both in drug and antigen delivery have branded crystallized proteins as “diamonds in the rough” for therapeutic formulations.³⁴ They are not currently used in biomedical applications, because protein crystals are brittle and harder to crystallize than active pharmaceutical ingredients, but

by crystallizing them in hydrogels systems they are going easier to process. The most notable commercially available technology of crystallized proteins is called Cross-Linked Enzyme Crystal (CLEC®) developed by the Altus Company. The CLEC process mainly consists of two steps including batch crystallization of enzymes and chemical intercrosslinking of enzyme microcrystals with glutaraldehyde. This technology has not been successfully applied to the oral delivery of enzymes, but it has applications in enzyme immobilization for industrial processes.³¹

Hydrogels like silica, agarose, and PEG have been used for protein crystallization and subsequent structure determination by X-ray crystallography.³⁷ Gels influence crystal growth by diminishing convective mixing. They control the agglomeration and precipitation of proteins by allowing slow diffusion of reactants. The role of gels in crystallization techniques also serves to remove the effect of gravity, as they are able to prevent both particle sedimentation and fluid motion in the mother solution.⁶⁹ Van et al.²⁴ found that agarose plays a dual role in protein crystal growth, as an impurity and impurity filter. It promotes two-dimensional crystal nucleation up to 25% as an impurity, but at the same time reduces the concentration of other impurities on the crystal surface, by a factor of approximately 1/7. Because of this, crystal growth in gels is successful in obtaining large, high quality protein crystals. Gavira et al.⁷⁰ used the different crystallization set ups to obtain lysozyme and insulin crystals in PEG polymers, in which the polymer serve as a membrane to control the diffusion of the crystallization precipitant into the protein. Lysozyme crystals grown at 5 and 7% hydrogel concentration were characterized by having a crystal shape composed of prismatic and pyramidal faces. An important observation was that when the PEG concentration was increased to 10%, the crystal had a rounder shape. Insulin crystals were grown in a similar way along the capillary to a final size of approximately $460 \times 420 \times 420 \mu\text{m}^3$.

In the case of ovalbumin, protein purity is also an important concern for successful crystal growth. For this reason, studying the ovalbumin crystal structure in hydrogel systems is beneficial. For example, Dumetz et al.⁷¹ studied the ovalbumin crystallization and aggregation in PEG polymers. Although the crystallization was done in a solution of PEG and not meant for protein delivery, PEG promoted the crystallization of needle-like crystals. Ovalbumin crystal shape is characterized by typically having length-width-thickness ratio of 8:1:0.2 in both the monoclinic and triclinic crystal forms.⁷² Bulk protein crystallization of ovalbumin can also be applied industrially as shown by Judge et al.²⁹ They were successful in crystallizing ovalbumin from a mixture of lysozyme, ovalbumin, and conalbumin at 1-L batch scales in ammonium sulfate solutions at 30°C.

The viability of protein crystallization for therapeutic formulations has been broadly summarized by Basu et al.⁶⁸ from the Altus Company. Shi et al.⁷³ reported the possibility of using protein crystals for controllable release of therapeutics by measuring the dissolution rates of spherical crystals of Recombinant human interferon α -2b (rhIFN). Zinc ions play an important role in forming rhIFN crystals, giving the crystal structural integrity. In vitro rhIFN dissolution from spherical crystals with varied zinc contents was performed and measured at time intervals in artificial extracellular fluid. They found a strong dependence of the dissolution rates on the proportion of zinc co-crystallized. A higher molar ratio of zinc to rhIFN resulted in a lower initial burst and release rate. This correlates with published research of insulin crystals^{74, 75}, in which the dissolution behavior of protein crystals were depended on their own structures. They adjudicate differences in the dissolution behavior to the ordered fraction within the crystals, where molecules are more densely packed than in the amorphous phase, demonstrating that protein crystals are potential candidates for local sustained release application. We believe that by using both a polymeric microbead and a protein crystallized, our

vaccine system will have not only a sustained release of the protein, but it will be a potential vaccine that can be delivered orally.

4 OBJECTIVES

The impact this work will have will aid in the research and development of vaccines delivered via the GI tract. This work aims to design and implement an oral vaccine method by using alginate microbeads for the encapsulation of a crystallized protein that will cause an immune response once it is in the targeted mucosal site in the body. It is hypothesized that alginate microbeads can be used to crystallize and control the release of the protein. The first model protein to be used in the project is lysozyme, because its crystallization protocol is well known. The second model protein to be tested is insulin, which has been widely studied and previously crystallized. The third protein is ovalbumin, which will be our test protein and has been used for immunization therapy of allergies to egg white. Both insulin and ovalbumin have never been crystallized inside alginate beads, so this research will also be innovative in protein crystallization research.

The overall objective of the proposed work is to design and apply a crystallization method to successfully encapsulate protein crystals within alginate microbeads in the desired size range. The specific objectives for this research are:

- Create an alginate system in the size range of 5-25um that provides a matrix for encapsulation of protein crystals that can be delivered through the gastrointestinal tract and have an adequate release of the protein.
- Characterize the particle distribution of the microbeads for various gelation conditions.
- Find the optimal crystallization conditions for insulin and ovalbumin by the hanging drop method.
- Crystallize the various model proteins within the alginate system.
- Confirm, using fluorescence microscopy, the integration of the crystal inside the alginate bead structure.

- Perform release studies of the system and investigate the relationship between polymer properties and release kinetics.

5 MATERIALS

The polymer used is Low Viscosity Sodium Alginate (AlgNa) (#Cat ICN-15472583). This polymer was purchased from Fisher Scientific (Pittsburg, Pennsylvania). Calcium chloride (#Cat 223506), and fluorescein-amine isomer I (#Cat 201626) were purchased from Sigma-Aldrich (St. Louis, Missouri). Anhydrous ethanol (#Cat A405P1), ethyl-3-(3-dimethylaminopropyl) carbodiimide hydrochloride (EDC) (#Cat PI-22980), Texas Red sulfonyl chloride (#Cat PI-46115), acetonitrile (#Cat A955), and sodium carbonate (#Cat S263) were purchased from Fisher Scientific (Pittsburg, Pennsylvania).

The proteins were all used as received from the manufacturer. No further protocol was used to purify them. Product purity was certified by the manufacturer >90% for the three proteins. Lysozyme (#Cat L-6876), insulin from bovine pancreas (#Cat I-5500), and ovalbumin from chicken egg white (#Cat A-5503) were purchased from Sigma-Aldrich (St. Louis, Missouri). Crystallization buffers used were sodium acetate (#Cat ICN-15472583), tris(hydroxymethyl)aminomethane hydrochloride (#Cat PR-H5121), and sodium phosphate (#Cat S379-212) all purchased from Fisher Scientific (Pittsburg, Pennsylvania). The precipitating agents were sodium chloride (#Cat S271-10), sodium phosphate dibasic (#Cat S379-212), and ammonium sulfate (#Cat BP212R-1) were bought from Fisher Scientific (Pittsburg, Pennsylvania). All of the solutions, except the proteins, were filtered with a 0.45µm pore size Nylon filter (Fisher Scientific, #Cat 09-719-007, Pittsburg, Pennsylvania). The proteins were filtered using a sterile syringe filter with a 0.22 µm pore size hydrophilic PVDF membrane from Millipore (#Cat SLGV033RS, Billerica, Massachusetts).

6 METHODS

6.1 Alginate Bead and Microbeads Formation

Low viscosity alginate (#Cat ICN-15472583, Fisher Scientific, Pittsburg, Pennsylvania) was used through out all of the experiments in the concentrations of 1-4%w/v. An alginate solution was made by weighting the desired amount of sodium alginate and slowly adding it to deionized water (DI) at room temperature. The polymer solubilized after mixing for two hours. An adjuvant system was created with two different sizes of beads. The first was in the size of 1mm which will be called beads for the purposes of this thesis. This bead size helped in clearly visualizing if the conditions used cause adequate protein crystallization inside the polymer. The second one was in the size range of 5-20um, which will be called microbeads. This was a smaller sized bead which can be used as the vaccine of interest with an adequate size for M cell interaction. Beads were made according to Gombotz et al⁴⁰, in which alginate beads were formed by dripping the polymer gel using a with a 23 ½ gauge syringe into 50mL of a 1M calcium chloride solution (#Cat 223506, Sigma-Aldrich, St. Louis, Missouri). The shape of the beads was formed by ionic cross linking of the carboxyl groups with the calcium ions once the polymer solution was in contact with the crosslinker. These were allowed to mix with the calcium chloride solution at 60rpm using a magnetic stirrer (Eppendorf, Isotemp, Hamburg, Germany) for two hours at room temperature before they were collected with a mesh size of 250um and washed with deionized water. The formed beads were in the size range of 1-2mm.

To decrease the alginate bead size and form microbeads, a spray nozzle was used, obtained from the company BETE (XAER model, Greenfield, MA) as performed Kwok et al⁷⁶ with some modifications. This nozzle was used as established by the manufacturer, which is very specific on the pressure allowed. The nozzle does not have options to change the settings. This is why it is important

to use the compressed air and peristaltic pump to control the size of the microbeads. A diagram of the polymer atomization nozzle set up is shown in Figure 4. One side of the nozzle has a feed opening for the polymer, which was supplied through a peristaltic pump (setting 7) (Cole-Palmer, Masterflex, Vernon Hills, IL). The polymer feed had a concentration of 2%w/v. The other side of the nozzle had a compressed air inlet (pressure 250psig), which was used to control the size of the microbeads. This side of the nozzle was connected to a compressed air tank. Polymer mist obtained from the nozzle was gathered in a round crystal plate (100mm in diameter) with 20 mL of 0.1M calcium chloride solution. The polymeric microbeads were allowed to crosslink with the calcium chloride solution for two hours to ensure that they were completely crosslinked. Microbeads were gathered and passed through a mesh size of 20 μ m three times to ensure they were in the desired size range of <20 μ m. The obtained microbeads were labeled in their corresponding size range (<20 μ m or >20 μ m). These were washed with DI water, further concentrated using an Amicon 4k column (Millipore Corp., #Cat UFC800324, Billerica, Massachusetts), and centrifuged at 8,000rpm for 5 minutes using an Eppendorf 5430R Centrifuge (Hamburg, Germany).

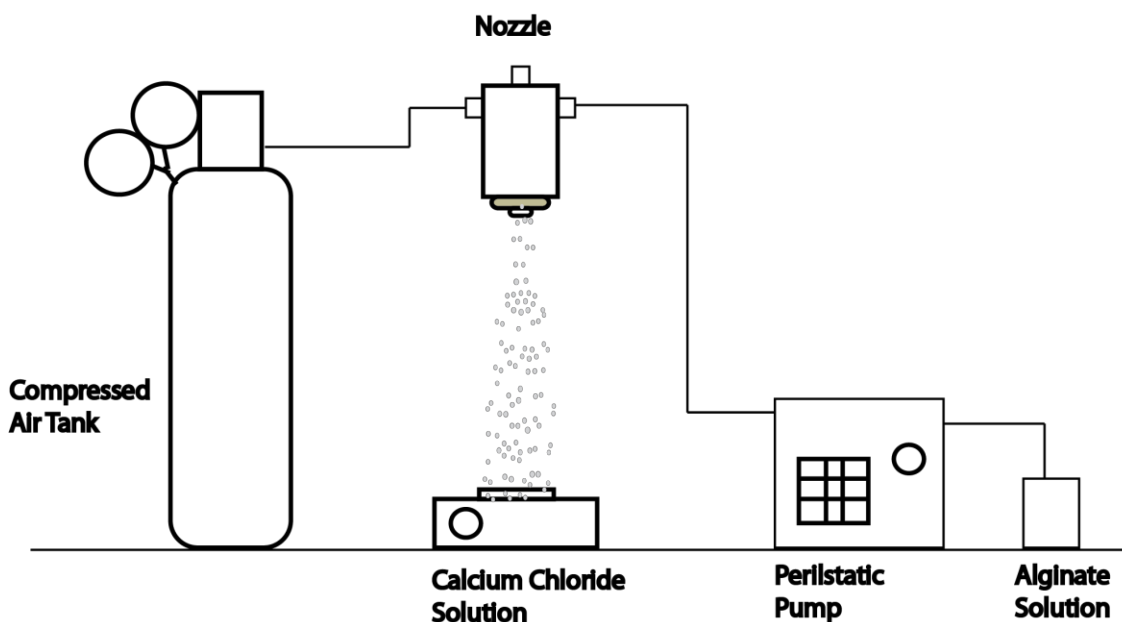


Figure 8: BETE Nozzle Alginate Microbead Formation Set-up.

Low viscosity alginate solution was supplied into a BETE nozzle by using a peristaltic pump. Compressed air was supplied into the nozzle causing a mist to emerge, which was gathered by a plate filled with calcium chloride cross-linker.

6.2 Microbead Size Analysis

The microbeads obtained by the aforementioned process were analyzed to determine their size depending on the alginate concentration. Pictures of the resulting microbeads were taken with an optical microscope (Olympus CKX31, Tokyo, Japan) to determine microbead size distribution. The background of the picture was eliminated using the program Infinity Analyze from the microscope (Lumenera Corporation, Ontario, Canada). Once the background was eliminated, the picture was analyzed with Image J. By measuring the scale bar pixels, the diameter of the microbeads was found. Image J can detect differences in color between the picture background and microbeads, and measure the area of each particle in the same color. Once the area of each microbead was found, the corresponding diameter was calculated. This detailed process is shown in Appendix B. The microbead diameter was exported to Minitab where the size distribution curves were plotted for three different alginate viscosities (3.0, 2.5, 2.0%w/v). To make this statistical analysis valid, the experiment was repeated three times (i.e. three different batches with one picture per batch).

6.3 Lysozyme Crystallization in Alginate Beads and Microbeads

Once the delivery system was made, we focused on integrating the antigen of interest into the alginate beads and microbeads. As mentioned this was be done by crystallizing the mentioned proteins inside cross-linked alginate. Protein crystallization conditions are defined typically by three factors, the protein to be crystallized, a buffer or solvent to establish a pH environment, and a precipitating salt. For the three proteins chosen, the crystallization conditions are summarized in Table 4.

Table 4 Protein Crystallization Conditions

Protein	Buffer	Precipitant
Lysozyme	0.05M Sodium Acetate, pH=4.5	7%w/v Sodium Chloride
Insulin	A. 0.1 M Tris/HCl, pH=9 B. 0.02M HCl	A. 0.5M Sodium Phosphate B. 0.005M Zinc Chloride, 0.05M Trisodium Citrate, and 20% Acetone.
Ovalbumin	0.1 M sulfuric acid, pH 4.6	5.5%w/v Ammonium Sulfate

Lysozyme (#Cat L-6876, Sigma-Aldrich, St. Louis, Missouri) was used as the first model protein because its crystallization conditions are well known and has been crystallized in alginate beads previously. The crystallization of this protein was first tested in solution. A 60mg/mL lysozyme solution was made by adding the weighted protein to a 0.05M sodium acetate buffer (pH=4.5) (#Cat ICN-15472583, Fisher Scientific, Pittsburg, Pennsylvania). The solution was filtered using a sterile syringe filter and 0.22 μm pore size hydrophilic PVDF membrane (#Cat SLGV033RS, Millipore, Billerica, Massachusetts). The precipitating salt was 7%w/v sodium chloride (Fisher Scientific, #Cat S271-10, Pittsburg, Pennsylvania) dissolved in DI water. Costar 96-well plates (#Cat HR3-277Sigma, St. Louis, Missouri) were used for this crystallization. Equal volumes (100uL) of 60mg/mL lysozyme and 7%w/v sodium chloride were added to the well at room temperature. Crystallization of the lysozyme was appreciated after 1 hour.

Crystallization in alginate beads was performed as established by Willaert et al³. The process constitutes of allowing the protein to diffuse into an alginate bead, after which the precipitating salt was added to allow crystal formation to occur inside the polymer matrix. Beads (12 beads) were added into a Costar 96-well plate (Sigma, #Cat HR3-277, St. Louis, Missouri) and softly washed with 100uL of 0.05M sodium acetate buffer (pH=4.5) for 2 hours, changing the buffer every 30 minutes. This was

done to ensure there was not excess water inside the bead that could affect the crystallization. This solution was removed and 100uL of 60mg/mL lysozyme dissolved in sodium acetate buffer were added into each well for diffusion of the protein into the bead to occur for 4 hours. After the allotted time, the protein that did not diffuse into the bead was removed and the precipitating salt was added (100uL of 7%w/v sodium chloride). The bead was allowed to be in contact with the salt at this concentration for 30 minutes, after which the 7%w/v sodium chloride was removed. Subsequently, 100uL of 40mg/mL of lysozyme in 2%w/v sodium chloride were added. The crystallization was allowed to occur for 12 hours. All of the steps of this crystallization were done at room temperature.

The procedure was modified for lysozyme crystallization in microbeads, because diffusion occurs faster and they were harder to handle due to their small size. The microbeads were first centrifuged (5 min, 25C, 7,800rpm) using a 50kDa Amicon membrane filtration column (Milipore #Cat UFC905024, Billerica, Massachusetts). They were washed by adding 10mL of the 0.05M acetate buffer (pH=4.50) into the column for 10 minutes and centrifuging at the same conditions. 5mL of 60mg/mL of lysozyme were added into the filtration column and the protein was allowed to be in contact with the microbeads for 2 hours. The microbeads were centrifuged for 5 minutes at 7,800rpm at 4°C and 50uL of the microbeads and the amount of protein solution that was still left in the column were placed in a 96well plate, where 100uL of the 7%w/v of sodium chloride were added with 0.2M Calcium Chloride. The microbeads have to be added with a small quantity of protein, so the protein does not diffuse out of the microbead before crystallizing. Crystallization of lysozyme in alginate microbeads can be observed after 30 minutes of adding the precipitating salt.

6.4 Fluorescent Alginate and Lysozyme

Confocal microscopy (Olympus iX81, Tokyo, Japan) was employed to confirm that the crystal was embedded in the polymer matrix. The visualization of the crystallization of lysozyme in alginate beads and microbeads was performed by labeling both the protein and the polymer with different fluorescent labels. Alginate was labeled by covalent binding 1-ethyl-3-(3-dimethylaminopropyl) carbodiimide hydrochloride (EDC) (#Cat PI-22980, Fisher Scientific, Pittsburg, Pennsylvania) and fluorescein-amine Isomer I (#Cat 201626, Sigma, St. Louis, Missouri). EDC is an agent that crosslinks a carboxyl functional group, such as the ones in alginate, with an amine functional group, like the ones in fluorescein-amine, allowing the alginate to become fluorescent. This is called a carbodiimide reaction and can be very versatile for binding the mannuronan groups in alginate with amines, such as the ones in chitosan and RGD peptides. EDC is water soluble and very reactive, particularly in the pH-interval 3.5-4.5. The high water content in alginate allowed EDC to dissolve when mixed. EDC (25mg) was added to 50mL of a sodium alginate solution (2%w/v) with pH adjusted with 0.1M HCl to 4.5-5.0. This solution was mixed and cooled in ice for 15 minutes. 50 mg of fluorescein-amine were put in a 10mL amber bottle and dissolved with 5 mL of pure anhydrous ethanol (#Cat A405P, Fisher Scientific, Pittsburg, Pennsylvania). Once dissolved, they were also put in an ice bath and cooled for 15 minutes. The cooling was done to slow the reaction of EDC until both solutions were completely mixed (5mL of fluorescein-amine with 50mL of EDC-sodium alginate) and agitated at 60rpm using a magnetic stirrer (Eppendorf, Isotemp, Hamburg, Germany) for two hours at room temperature. The solutions were allowed to react for 72 hour at room temperature for optimum and thorough carboxyl-EDC-amine reaction. Once the reaction was allowed to complete, free fluorescent molecules were removed by dialysis. Dialysis was performed with membranes from Spectrum Laboratories (Spectra/PorDialysis Membrane, MWCO: 12-14000 kDa) at room temperature. The alginate

fluorescein-amine solution was dialyzed against 1L of a water/ethanol solution in a ratio of 4:1, with continuous replacement of this solution until no trace of fluorescein-amine was found in the solvent. This was confirmed by taking a 200uL sample, placing it in a 96-well plate and reading it in a Molecular Devices Microplate Reader (Gemini EM, Sunnyvale, CA, USA) at 498nm. This reading was confirmed three additional times, after adding the water/ethanol solution to the dialysis gave a reading equal to a mixture of water/ethanol. The emission wavelength of fluorescein-amine is 498nm. The fluorescent alginate complex was sensitive to light, so it was covered at all times.

Lysozyme was labeled using Texas Red sulfonyl chloride (#Cat PI-46115, Fisher Scientific, Pittsburg, Pennsylvania). The procedure for conjugating the protein to Texas Red fluorescent dye is described by Hermanson in its book "Bioconjugate Techniques"⁷⁷. Lysozyme was dissolved in 0.1 M sodium carbonate (#Cat S263, Fisher Scientific, Pittsburg, Pennsylvania), pH 9.0, at a concentration of 5 mg/mL. Texas Red was dissolved in acetonitrile (#Cat A955, Fisher Scientific, Pittsburg, Pennsylvania) at a concentration of 20 mg/mL. 50 uL of the Texas Red solution was mixed with 1mL of the protein solution. The reaction was allowed to occur at room temperature for one hour. This is a covalent conjugate addition reaction in which the sulfonyl chloride (SO₂Cl) group in Texas Red easily forms conjugates with amine groups in proteins. The lysozyme-Texas Red solution was dialyzed in water to remove free Texas Red. Dialysis was performed with membranes from Spectrum Laboratories (Spectra/PorDialysis Membrane, MWCO: 12-14000 kDa) at room temperature. The alginate lysozyme-Texas Red solution was dialyzed against 1L of a water/ethanol (4:1) solution, with continuous replacement of the water/ethanol solution until no trace of Texas-Red was found in the solvent. This was confirmed by taking a 200uL sample, placing it in a 96-well plate and reading it in a Molecular Devices Microplate Reader (Gemini EM, Sunnyvale, CA, USA) at 562 nm. The emission wavelength of Texas Red is 562nm. This reading was confirmed three additional times, after adding

the water/ethanol solution to the dialysis gave a reading equal to a mixture of water/ethanol. The crystallization protocol was then followed for alginate beads with minor adjustments. Fluorescent alginate was mixed with regular alginate (1:9) and fluorescent lysozyme was mixed with regular lysozyme (0.5:9.5) before starting the crystallization. Once dissolved to the concentrations established for crystallization, the protein was filtered using a sterile syringe filter and 0.22 μm pore size hydrophilic PVDF membrane (#Cat SLGV033RS, Millipore, Billerica, MA, USA). The crystallization was then followed as previously mentioned.

6.5 Lysozyme Release from Beads

This experiment was performed by testing the protein release crystallized and liquid lysozyme protein in different beads. Three alginate concentrations were used to make the alginate beads (2, 3, and 4%w/v). The alginate beads were made as established in Section 6.1. Six different bead types were made: 2%w/v alginate with crystallized or liquid protein, 3%w/v alginate with crystallized or liquid protein, 4%w/v alginate with crystallized or liquid protein. 4 repetitions of each bead type were done through this experiment. Protein loading was performed for 4 hours by imbibition, in which each bead was allowed to be in contact with 100 μL 60mg/mL lysozyme solution in a 96 well plate (one bead per well). After 24 hours, the protein solution that was not absorbed from the beads that were going to be crystallized was removed and 7%w/v sodium chloride was added for 30 minutes and removed. Subsequently a solution of 40mg/mL lysozyme in 2%w/v sodium chloride was added. Crystal formation was confirmed to occur by using a light microscope (Olympus CKX31, Tokyo, Japan). For the beads that did not have the protein in crystalline form, the step of adding the salt was omitted.

All of alginate beads types were put in a 96-well plate (one bead per well) to perform this experiment. Beads were exposed to two different fluids for 8 hours each, one simulating the acid

environment of the stomach (low pH) and one simulating the intestine environment (high pH). Testing in the simulated fluid was done first for SGF with the six bead types (4 repetitions for each) and then in SIF with a new batch of six bead types (4 repetitions each). Simulated Gastric Fluid (SGF) was made with hydrochloric acid solution (pH 1.2, USP 29). Simulated Intestinal Fluid (SIF) was made with phosphate buffer and sodium hydroxide (pH 6.8, USP 31). The 96-well plate with the beads was placed to be stirred by an orbital shaker (100 rpm) situated inside an Incubator (Thermo Scientific, Imperial III, Pittsburg, PA, USA) with a constant temperature of 37°C. 100uL of the either SIF or SGF were added. At established time intervals (2min, 4min, 6min, etc) throughout the experiment, 100uL aliquots of the solution were taken and fresh SGF or SIF were replaced as needed to maintain a constant volume. Protein content in these aliquots was quantified with a Coomassie Blue (Bradford) Assay kit (#Cat 23236, Fisher Scientific, Pittsburg, PA) and absorbance measured with a spectrophotometer at 595 nm (Multiskan Go, Thermo Scientific, Waltham, Massachusetts). The measurement was carried for each bead type, with their own four repetitions, for the different established time intervals. Protein release was determined by measuring the protein content liberated from each bead in the established time frame. Cumulative protein released was calculated by summing the protein release of each time frame and normalizing it with the total protein release for each bead. Loading Efficiency (LE) was determined by dissolving 4 different beads for each bead type in 1.5 mL of PBS (pH 7.4) for 2 days. The bead was incubated at room temperature under magnetic stirring (250 rpm) to help dissolve it. After 24 h, protein content was quantified by measuring the absorbance of the dissolved particle solution at 595 nm using the Coomassie Blue Bradford Assay Kit as previously mentioned. Because they were already diluted in 1.5mL of volume, the solution was analyzed without further additional dilution. The protein content of the lysozyme solution added to the beads was analyzed in the same way, but the solution was dissolved in 3mL of deionized water before measuring.

LE was determined from the ratio of released lysozyme of each bead to the total amount of lysozyme added for imbibition into the bead.

6.6 Insulin Crystallization

The crystallization of insulin was performed with two different crystallization protocols, with differences in the solvent used and the precipitating salt. The crystallization conditions for insulin bovine pancreas (#Cat I-5500, Sigma-Aldrich, St. Louis, MO, USA) were found by the hanging drop method. For the first crystallization protocol, two protein concentrations were tested 15 and 20mg/mL. The protein was dissolved in 0.1 M Tris(hydroxymethyl)aminomethane hydrochloride (#Cat PR-H5121, Fisher Scientific, Waltham, Massachusetts) (tris/HCl; pH= 9). The pH of the solution was adjusted with 0.1 N hydrochloric acid (#Cat A144C, Fisher Scientific, Pittsburg, PA, USA) or 0.1 N sodium hydroxide (#Cat S5881, Sigma, St. Louis, MO, USA). Once dissolved the insulin solution was filtered. The precipitating agent used was sodium phosphate dibasic (#Cat S379-212, Fisher Scientific, Waltham, Massachusetts) dissolved in 0.1 M tris/HCl in three different concentrations (0.5 M, 0.4M, 0.3M). For the hanging drop method, 24-well plates and borosilicate cover glasses were purchased from Hampton Research (#Cat HR3-142 and HR3-277, Aliso Viejo, California) to set up the crystallization. The well was filled with 1.0mL of the sodium phosphate solution. A 2uL drop (1uL of insulin solution plus 1uL of precipitant solution) was mixed and placed in the cover glass. High vacuum grease was carefully applied to the edge of the wells. The cover glass was overturned and placed on top of the high vacuum grease, carefully pushing it down to be sure that there are no air pockets between the grease seal and the cover glass. The crystallization was allowed to occur for 24 hours at room temperature.

Crystallization in the alginate crosslinked bead was followed in a similar way as with lysozyme crystallization. First, alginate beads were washed with deionized water for 2 hours. Subsequently, the beads were put one per well into a 96-well plate. A solution of 20mg/mL of insulin dissolved in 0.1 M Tris(hydroxymethyl)aminomethane hydrochloride was made. 200uL of this solution was added per well and allowed to be in contact with each bead for 2 hours. After the allotted time, the protein that did not diffuse into the bead was removed and the precipitating salt was added (200uL of 7%w/v sodium phosphate dibasic). The bead was allowed to be in contact with the salt overnight. Then crystallization inside the bead was examined. All of the steps of this crystallization were done at room temperature.

The second crystallization protocol for insulin used was tested via the hanging drop method, where the insulin protein was dissolved in 0.02M HCl (pH=4.5) at a lower concentration of 5mg/mL of bovine insulin. The insulin solution was filtered using a sterile syringe filter with a 0.22 μ m pore size hydrophilic PVDF membrane. The precipitating agents used were sequentially added in equal amounts: 0.005M Zinc Chloride, 0.05M Trisodium Citrate, and 20% Acetone (#Cat 229997, S4641, 179124, respectively, Sigma-Aldrich, St. Louis, MO, USA). 1mL of this was added to a 24-well plate. 1uL of the protein solution was added into a circular cover glass along 1uL of the precipitating agent. High vacuum grease was carefully applied to the edge of the wells. The cover glass was overturned and placed on top of the high vacuum grease, carefully pushing it down to be sure that there are no air pockets between the grease seal and the cover glass. The crystallization was allowed to occur for 24 hours at room temperature.

6.7 Ovalbumin Crystallization

Purified crystalline ovalbumin was prepared from chicken egg white using a method similar to Sorensen and Hoyrup (1915) as modified by Judge et al (1995).²⁹ An egg dozen was bought from the local supermarket. The yolk and white were separated and the egg white was frozen (-20C). Frozen egg white (1g) was thawed and gently mixed to degrade membrane material. An equal volume of saturated ammonium sulfate solution (55g ammonium sulfate/100g water) was added slowly to an Erlenmeyer flask while magnetic stirrer (Eppendorf, Isotemp) for 5 minutes at room temperature. The solution was left standing for 2 hours at room temperature, after which the white precipitate that formed was removed by centrifugation (14,000g, 25°C, 30 min) in an Eppendorf 5430R Centrifuge (Hamburg, Germany) and discarded. The filtrate was adjusted to pH 4.6 with 0.1 M sulfuric acid, briefly stirred, and left to crystallize overnight at room temperature in an incubator at room temperature. Crystalline ovalbumin was separated from the liquor by centrifugation (14,000g, 25°C, 10 min) in an Eppendorf 5430R Centrifuge (Hamburg, Germany) and dissolved in water (15 mL). Saturated ammonium sulfate solution was then slowly added until a slight permanent turbidity was observed (23-25 g ammonium sulfate/100 g water). The solution was briefly stirred to promote nucleation and allowed to crystallize overnight. After centrifugation, crystals were washed and stored in a 10:7 by volume saturated ammonium sulfate-water mixture at 4°C.

An SDS PAGE was performed to ensure the obtained crystals corresponded to pure ovalbumin. The SDS-PAGE was done following the protocol of the Bio-Rad Company. Ovalbumin crystals were dissolved in water. Protein concentration was determined with Coomassie Blue (Bradford) Assay kit (#Cat 23236, Fisher Scientific, Waltham, Massachusetts). Each solution sample containing more than 0.5 µg/mL of protein (5µL) was combined with 2.5 µl of 4X LDS sample buffer, and DI water to make a total volume of 10 µl. The samples were heated in 70°C water for 10 minutes and then loaded

onto a 4-20% Mini-PROTEAN® TGX™ Gel (Bio-Rad Laboratories, Philadelphia, PA). About 5 µl of protein ladder solution was loaded onto the gel as a molecular weight standard. Electrophoresis was performed using an Mini-PROTEAN TETRA Cell Systems (#Cat 165-8000, Bio-Rad Laboratories, Philadelphia, PA) at 200 V and 130 mA for 50 minutes with the upper and lower buffer chambers filled with 800mL of SDS running buffer (1x), made of 100 mL of 10x stock with 900mL of deionized water. After electrophoresis, the gel was placed in a clean tray and rinsed with 200 ml DI water to remove residual SDS using a single-speed orbital mixer. This washing procedure was repeated 3 times with DI water replaced every 5 minutes. The Blue Stain Reagent was added to the gel and 1 hour was allowed for complete staining. After staining, the membrane was cleaned through a series of water wash steps, in which the stain reagent was replaced with several DI water changes for a 1-2 hour period to obtain clear protein staining.

7 RESULTS AND DISCUSSION

7.1 Alginate Bead and Microbeads Characterization

Sodium Alginate beads of millimeter size were produced by placing drops of the polymer in contact with a crosslinking agent. There are various ways to crosslink alginate such as ionic and covalent crosslinking. The most common method to prepare hydrogels from an aqueous alginate solution was to combine the solution with ionic cross-linking agents, such as divalent cations. The ionic crosslinker calcium was chosen, with the advantage that the alginate morphology is maintained (i.e maintains the spherical shape after dropping) when it comes in contact with the calcium chloride solution.

Divalent cations are believed to solely bind to guluronate blocks of the alginate chains, as the structure of the guluronate blocks allows a high degree of coordination of the divalent ions. When the alginate solution was dripped from a syringe at a slow rate into a calcium chloride solution, a sphere formed. The beads obtained through this method had a size range between 1.0-2.0mm (Figure 9A).

Alginate microbeads can be obtained with different techniques, such as emulsions, spray-drying, microfluidics, and by using an atomizer. Each of these methods has advantages over the others. Microfluidics for example produced microbeads with a narrow size range^{78, 79}, while emulsions easily allowed the inclusion of two or more polymers in a microbead.⁸⁰ The factors to keep in mind to choose any method over the other are cost, ease of microbead production, possible microbead agglomeration, and final use. Two methods were employed to produce alginate microbeads. The first was an oil-in-water emulsification technique. This preparation method involved the use of harsher chemical reagents such as iso-octane. The resulting suspension contained large amounts of amorphous materials

and a small portion of microbeads covered in oil, which could be problematic to remove for protein crystallization later on. The second method was to use a polymer atomization process to obtain microbeads, for which a set up was established. Varying the pressure provided by the compressed air allowed the alginate to be sprayed as a mist, which could be gathered by a calcium chloride bath. The atomizing procedure was successful in producing microbeads within the desired size range without any other contaminants that could affect protein crystallization. The challenge with this process was that particle size was heterogeneous. Based on previous research⁷⁶, narrower particle size could be obtained by lowering alginate concentrations (<1%w/v). As seen experimentally, protein crystallization in microbeads with less than 2%w/v alginate was difficult to achieve, so an alginate with 2%w/v was used. Given that a narrow size distribution was desired, the obtained product was filtered through a 20um mesh. Microbeads that stayed on top of the mesh are shown in Fig 9B, which have an average size of 100um. The microbeads that fell through the mesh, Fig 9C, had a size between 5-20um, and were not agglomerated.

The yield from the BETE Spray System was measured by weighting the dried quantity of alginate that was supplied to the system and compared with the weight of the microbeads after they were synthesized and dried in at room temperature overnight. Results showed a yield of 23.30% of alginate recuperation in the microbeads after filtration. The rest of the alginate formed into microbeads >20um, with a minor quantity staying in the equipment as left over from the procedure.

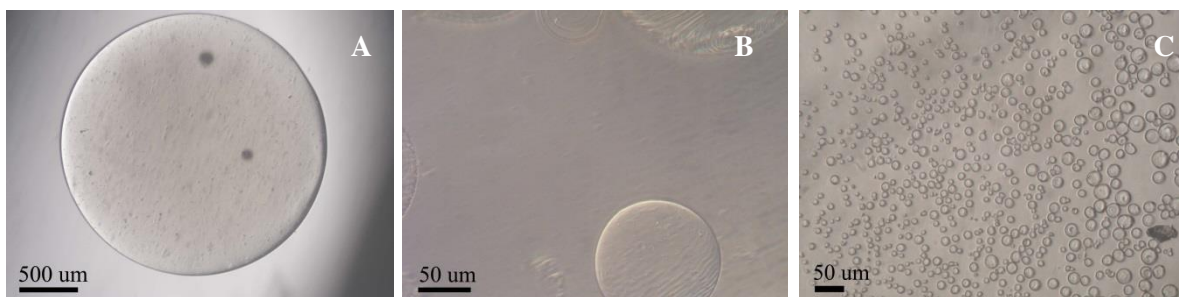


Figure 9: Varied Alginate Bead size from 1.5mm to 5um.

(A) 2%w/v Alginate Bead 1.5mm. Scale: 100um (B) 2%w/v Alginate Microbead 100um

Scale: 50um (C) 2%w/v Alginate Microbead 5-20um Scale: 50um.

The size of the microbeads was analyzed at different alginate concentrations (2-3%w/v). The process for microbead size analysis can be appreciated in Appendix 1, where microbead size analysis was done with Image J. Results demonstrated that the mean alginate microbead diameter for the 2.0% AlgNa microbead was 12.33 μ m (\pm 4.006 μ m). For the 2.5% AlgNa microbead, mean diameter slightly increased to 13.05 μ m (\pm 3.47 μ m). The mean microbead diameter for the 3.0% AlgNa microbead was 13.33 μ m (\pm 5.20 μ m). A summary of all the mean diameter size and standard deviation for the three concentrations can be observed in the box plot illustrated in Figure 10. Statistical analysis indicated that there was no statistical difference between the three. All of the three concentrations alginate microbeads fell within the same size range of 5-20 μ m. Similar results were obtained by Kwok et al.⁷⁶ with a Turbotak atomizing nozzle system.

In conclusion, alginate beads were easily obtained with calcium chloride ionic crosslinking. Alginate microbeads were found to be better produced by polymer atomization, for which a set up was established. Although this procedure did not provide a narrow size distribution, the microbeads obtained for the three alginate concentrations studied were within the desired size range of 5-20 μ m.

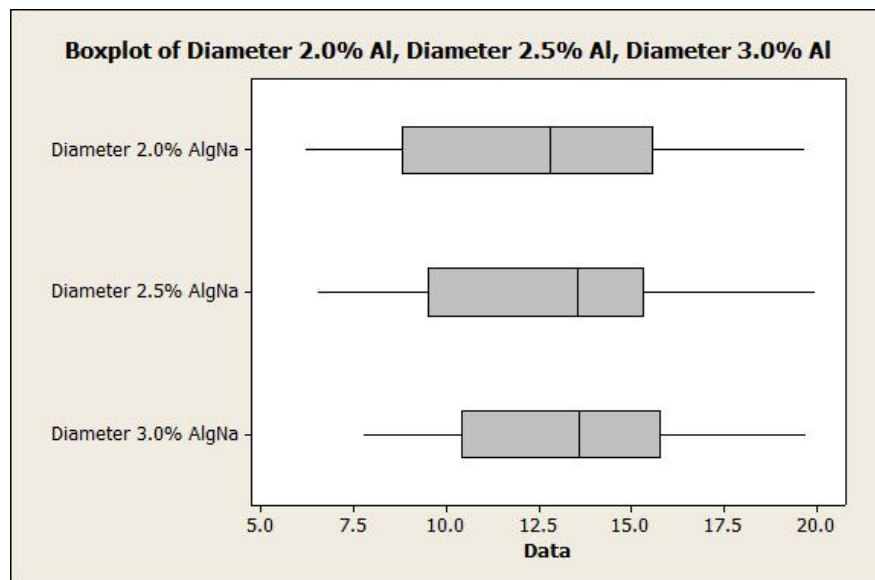


Figure 10 Box Plots for the three batches of alginate microbeads with three different concentrations

7.2 Lysozyme Crystallization in Alginate Systems

Lysozyme crystallization (Figure 8A) was characterized by a pyramidal tetragonal structure.⁷⁰ Crystallization of lysozyme was successful for the conditions of 0.05M Sodium Acetate Buffer with a pH of 4.50, 7%w/v sodium chloride. These conditions were chosen as the adequate lysozyme crystallization conditions to examine in alginate beads. Large beads allowed more control of the crystallization and helped in clearly visualizing protein crystallization.

Protein loading was conducted in two different ways, incorporation of the protein into the alginate solution prior to crosslinking the alginate bead or by imbibition of the protein to an already formed bead. The first method is commonly used in literature^{25, 40} to load proteins into alginate, before crosslinking the bead. This method was found to not be useful for lysozyme, because it formed a white precipitate once added to an alginate solution. The second method proved to be successful to load the lysozyme protein into alginate. The process of imbibition constituted on protein loading the alginate bead by taking up surrounding protein fluid. This latter method has the advantage that an additional protein purification step is added, because large protein impurities and aggregates can be physically excluded by the polymer matrix, because of their size.³ Once the alginate bead was loaded with the protein, it had a slight orange color (Appendix B). Caution was taken not allow the bead to oversaturate with protein, since it could cause an amorphous crystallization. After protein imbibition, adding the precipitating salt crystallized the protein. The initial salt concentration (7%w/v) allowed nucleation of the protein to occur inside the bead, while the precipitating salt meets the protein. After the precipitating agent was added, an interface of protein agglomeration was seen in the edge of the bead (Appendix B). With time, crystal nucleation was observed with a higher concentration in the center of the bead. The second salt concentration (2%w/v with 40mg/mL lysozyme) allowed for crystal growth. The final crystal growth was appreciated inside of the bead (Figure 11B & 11C). For

lysozyme, this occurred in a time frame of an hour. Crystallization was caused by the development of a nucleation front.⁸¹

As observed experimentally (Appendix A), increasing gel concentration from 2%w/v to 4w/v resulted in a larger number of crystals of smaller size. There are two possible explanations for this behavior, this growth could be due to an increase in calcium ions in the structure (i.e. lysozyme is known to interact with calcium) and/or as there is more polymer in the bead, therefore there are more available crosslinking sites, which difficult the rate of diffusion of the protein out of the bead allowing more protein to be crystallized inside of it. Willaert et al.³ found similar results when increasing the alginate content, more nucleation as more polymer was added. They adjudicated this behavior to alginate acting as a protein nucleation promoter. This behavior is due to the reduction of polymer matrix pore size as the polymer concentration is increased. The confinement of these smaller pores limits the cluster size of protein agglomerates as well as the size of the impurities, and increases the contact of the protein with other protein chains, therefore increasing protein nucleation.

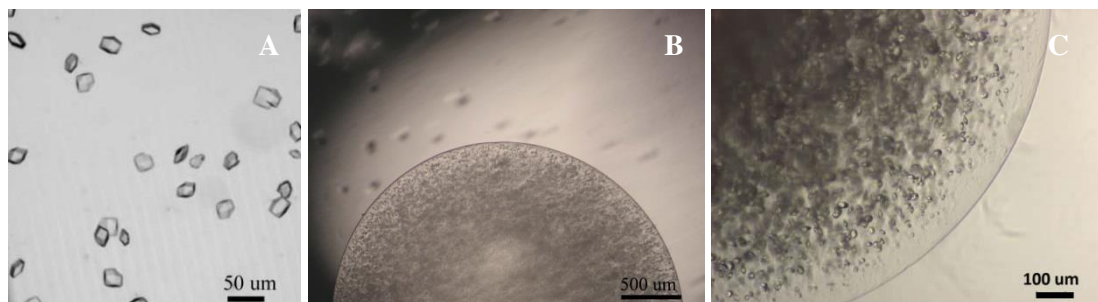


Figure 11 Lysozyme crystallization in solution and inside alginate beads.

A) Lysozyme Crystals. Scale Bar: 50µm B) Lysozyme Crystallization in alginate bead. Scale Bar: 500µm C) Close-up of lysozyme crystals in alginate beads. Scale Bar: 100µm

Crystallization in alginate microbeads (<20um) was followed with the aforementioned procedure. This process had never been done in literature before; therefore, the crystallization procedure for large beads was implemented with various changes to be able to manage small microbeads. At this scale, crystallization proved to be more difficult to achieve. The keys to be able to crystallize in this small scale were to do only the 60mg/mL lysozyme loading, centrifuging the microbeads with the protein at 4°C before adding the precipitating salt, and adding 0.2M Calcium Chloride with the precipitating salt. The first step ensured that the microbead was not over saturated with the protein. The cold temperature in the second step aided in promoting protein nucleation. The third step was experimentally discovered and reported as well by Sugahara et al.⁶⁹ Adding calcium chloride helps the microbead to stay crosslinked during crystal formation.

After performing the crystallization under the aforementioned conditions, small crystals were found embedded in the alginate microbead (Figure 12B). The crystal shape of the small crystals was generally round. This behavior has been observed by other researchers in protein crystallization with PEG⁷⁰ and silica gels⁸². As explained by Gavira et al.⁷⁰, protein crystals grown in high concentration gel media lose structural faces due to the homogenization of the surface energy between the gel and the protein crystal. It is believed that this behavior can be attributed to the incorporation of gel fibers into the crystal structure.

The aforementioned behavior can be further appreciated in the crystallization of lysozyme in a microbead (<20um), where a monocrystal appeared (Figure 12C). Microbeads of the polymeric phase served to locally concentrate the protein and provide an interface for nucleation to occur.³ It can be noted that as the size of the alginate beads decreased, less crystals appeared inside the microbead. These results showed a promising approach for obtaining crystals in alginate microbeads, which could have major implications not only in antigen delivery, but in X-ray crystallography, where obtaining a

single protein crystal is highly desirable. In conclusion, fewer crystals appeared as the size of the bead was lowered. To demonstrate that the protein crystal was inside the bead, a fluorescent counterpart of the system was created to be visualized by confocal microscopy.

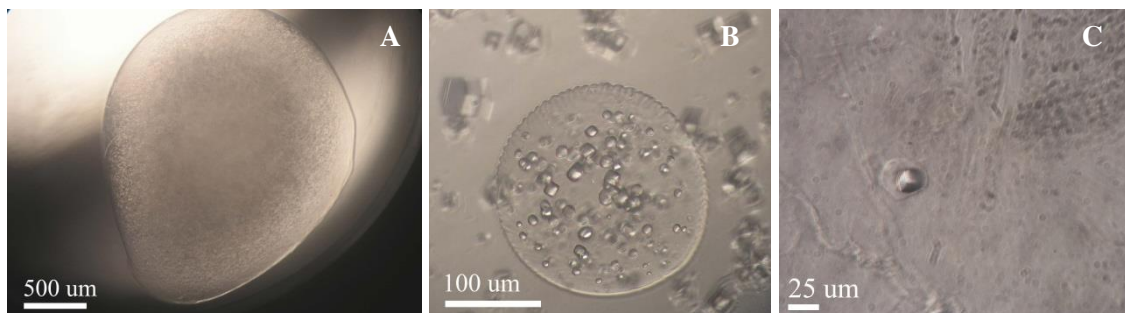


Figure 12 Decrease in size crystallization of lysozyme in alginate beads and microbeads

A) Crystallization of lysozyme in the low viscosity alginate 1.5mm bead, showing a large quantity of crystallized protein. Scale Bar: 500um B) Crystallization of lysozyme in 200um beads, where crystals can be appreciated in less quantity. Scale Bar: 100um C) Crystallization of lysozyme in an alginate microbead, where a single crystal can be appreciated. Scale Bar: 25um

7.3 Fluorescent Lysozyme and Alginate Crystallization

Crystallizing with fluorescent macromolecules can add unwanted impurities, but as shown in Figure 13A, the fluorescent dye labels appeared not to interfere with the crystallization process. The crystallization of fluorescent lysozyme in alginate was performed in beads and microbeads and captured by confocal microscopy. Alginate-fluorescein-amine complex had a green fluorescence with an emission in the 488nm wavelength. Lysozyme-Texas Red complex had a red fluorescence in the 568nm wavelength. Figure 13B illustrates a green fluorescent alginate bead with homogeneously distributed red fluorescent lysozyme crystals. Protein crystals were homogeneously distributed through

the polymer matrix, with no noticeable preference to growing at one point in the bead. A 3D reconstruction image showed that the protein crystals (Figure 14) were surrounded by an alginate matrix in the bead (green colored), with stronger lysozyme content (red) in some areas than others. It was confirmed by a z-stack picture (Figure 16) that the protein crystals were surrounded and embedded within the alginate matrix.

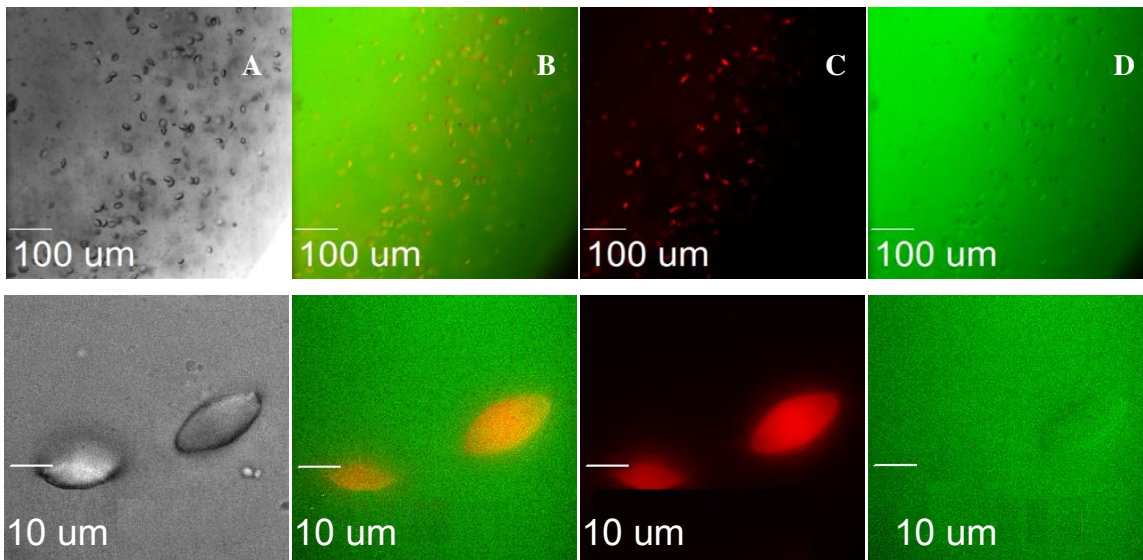


Figure 13 Fluorescent Alginate Beads with Lysozyme Crystallization

A. Open light source picture of lysozyme crystals taken with confocal microscopy. Top: 10X image. Bottom: 40X image. B. Alginate bead with lysozyme crystal 488nm and 568nm light source. Top: 10X. Bottom: 40X. C. Lysozyme Crystal with Texas Red fluorescence without 488nm ray source. Top: 10X. Bottom 40X. D. Crosslinked alginate with fluorescein amine fluorescence without 568nm ray source. Top: 10X image. Bottom 40X image.

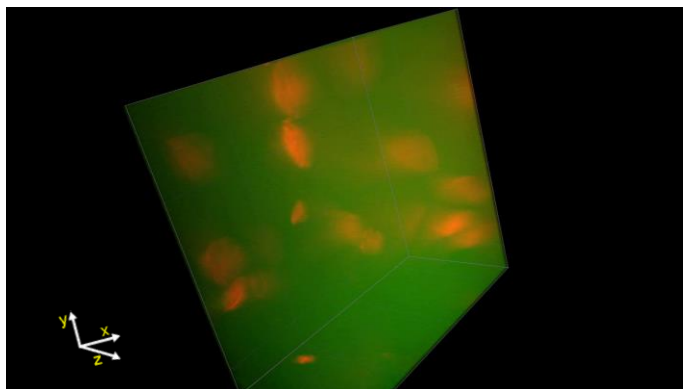


Figure 14 3D Confocal Picture of alginate matrix with embedded lysozyme crystals

A close-up look at the lysozyme crystals demonstrates a rounder morphology of the lysozyme crystal grown within the polymer with crystal faces that were less defined than a lysozyme crystal grown in solution (Figure 15). The study was also performed with alginate microbeads, in which lysozyme crystal growth was also studied as seen in Figure 16. The results of the z-stack confirmed (Figure 16) that the microbead had two lysozyme crystals completely inside of the microbead. Therefore, the polymer delivery system will be efficient in protecting the protein crystals. In conclusion, these results are relevant because they confirm that lysozyme crystals were embedded in the alginate matrix and immobilized by it, as well as giving us an idea on how the protein crystals were distributed in the matrix.

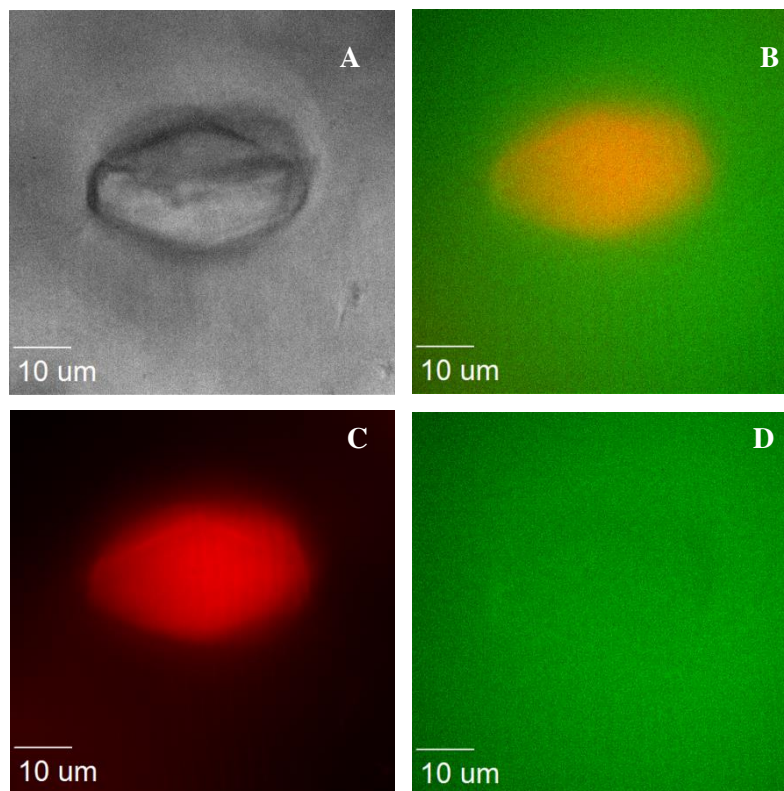


Figure 15 Single lysozyme crystal in Alginate Matrix

A. Open light source picture of lysozyme crystals taken with confocal microscopy. B. Alginate beads (Green-488nm) with lysozyme crystal (Red-561nm) image. C. Lysozyme Crystal with Texas Red fluorescence without 488nm ray source. D. Crosslinked alginate with fluorescein amine fluorescence without 561nm ray source.

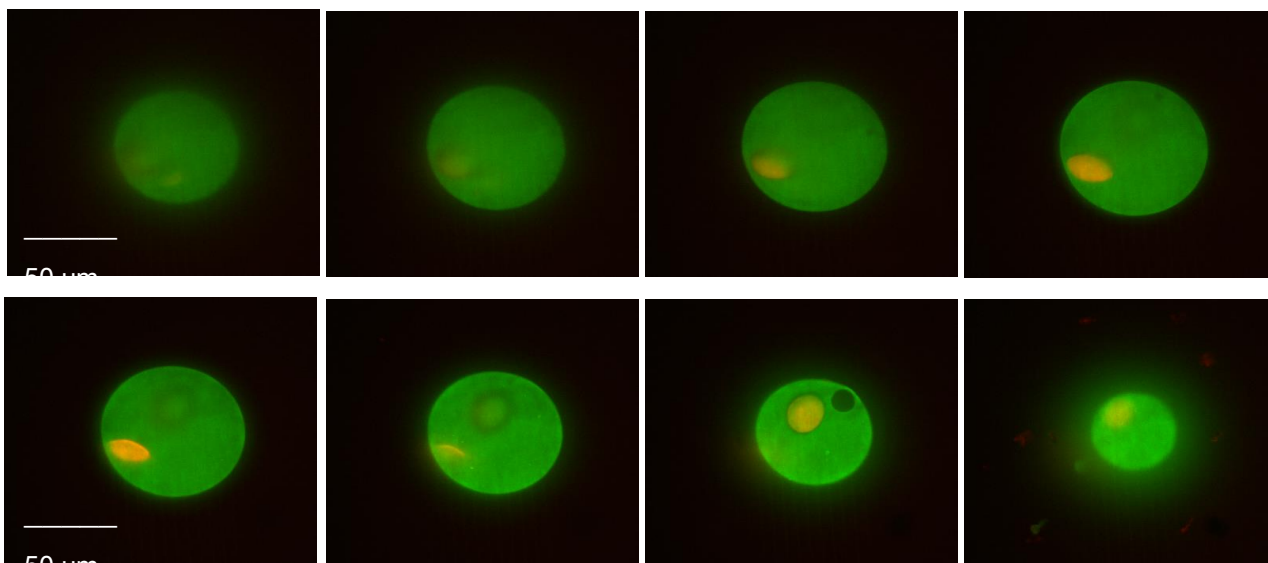


Figure 16 Z-Stack view of Alginate Microbead with two lysozyme crystals within its structure

7.4 Lysozyme release behavior from alginate system

Studying protein release behavior from alginate systems in simulated conditions can give us information on how it will behave in a biological environment. Protein release behavior was measured in environments simulating stomach and intestinal anatomical conditions. The US Pharmacopeia guidelines (USP) established how to perform these tests at a temperature of 37C. Testing in Simulated Gastric Fluid (SGF) was done using a mixture of sodium chloride, hydrochloric acid, and deionized water at a pH of 1.2. In the case of testing the release behavior in Simulated Intestinal Fluid (SIF), a mixture of potassium phosphate, sodium hydroxide and deionized water was used, with an established pH of 6.8.

Protein release from alginate beads with protein in solvated form are commonly found through literature^{57,25}. Therefore, the goal of this study was to investigate the effect in the release behavior

when crystallized lysozyme was embedded in alginate systems beads. Performing the release from alginate beads with crystallized protein and comparing it to the solvated protein can give us valuable information on differences between them. Three different parameters were analyzed and varied during experimentation. The first parameter was to perform protein release in either a SIF or SGF environment to prove that it was an adequate system for intestinal antigen delivery. It was hypothesized that the alginate system would favor protein release in SIF rather than SGF, since published literature^{64, 56, 57} have shown the pH-responsive characteristic of alginate (polymer swelling at high pH and shrinking at low pH).

The second tested variable was whether the release of the protein was affected by the morphology of the protein inside the alginate system (i.e. crystallized or in liquid form). Protein crystals tend to have a slower dissolution, because of their robust structure.⁷³ It was hypothesized that slower release kinetics would be obtained from protein crystals embedded in alginate beads. The third parameter examined was having the alginate bead made with different concentrations (2, 3, 4%w/v). It was hypothesized that the protein will release faster from alginate matrixes with lower alginate content, since as concentration polymer is greater, protein retention increase was expected. In total, there were 6 bead types, 2, 3, 4 %w/v alginate beads with either protein in its crystalline or solvated form. All of the sample beads were tested in four repetitions.

The data obtained was analyzed by measuring the loading efficiency, protein release profiles in both SGF and SIF, type of transport from beads, and diffusion coefficient of the protein from the beads. The loading efficiency (LE) for both crystallized and liquid lysozyme in the alginate bead was calculated by measuring the protein content in each bead and dividing it by the protein added for imbibition. The LE for all the bead types was in the range of 18% to 63% as illustrated in Table 5.

Distinct patterns between the loading efficiencies from beads with crystallized or liquid protein can be appreciated (Figure 17). The LE for the crystallized protein was more than double to that of the liquid protein for each alginate concentration. A One-Way ANOVA (95% Confidence Interval) with a Tukey Post Hoc Statistical Analysis between the LE data indicated that there was a statistical difference between the LE of crystallized and liquid proteins from 2% and 3w/v alginate beads. This confirmed one of the hypothesized benefits of using crystallized protein for antigen delivery. More protein can be encapsulated in the same volume when the protein is crystallized. This behavior can be attributed to the orderly packed arrangement a protein has in a crystal structure.³⁴ Being able to deliver more protein in the same volume will be beneficial to create a stronger immune response with the same delivery carrier.

There was also a difference between the LE of beads made with different alginate concentrations. A slight increase in LE was observed as the alginate concentration was lowered. There was no statistical difference between the LE of different alginate concentrations for the liquid protein, but there was a statistical difference between the LE of crystallized protein from 2% and 3%w/v alginate beads with the 4%w/v alginate bead.

Table 5 Loading Efficiency of Crystallized and Liquid Protein into Alginate Beads

Bead Type	Loading Efficiency (%)	Bead Type	Loading Efficiency (%)
2% Crystallized	63.43 ± 2.25	2% Liquid	25.93 ± 1.38
3% Crystallized	61.53 ± 3.81	3% Liquid	20.58 ± 2.87
4% Crystallized	32.68 ± 2.13	4% Liquid	18.31 ± 5.02

Scientific studies were evaluated to determine how much protein quantity would be necessary to induce an immune response if the system were to be applied in vivo. According to Friedman et al.⁴², the quantity of lysozyme necessary to induce an immune response that leads to creating Peyer's patches immune activity and subsequent oral tolerance to that antigen is 1mg of lysozyme supplied

orally every two days for at least 10 days. The data in Figure 17 demonstrates the protein quantity per polymer content supplied by our system. Correlating this study with Friedman's data, administering 1mg of polymer with crystallized lysozyme could be plausible to create an immune response in vivo with our system.

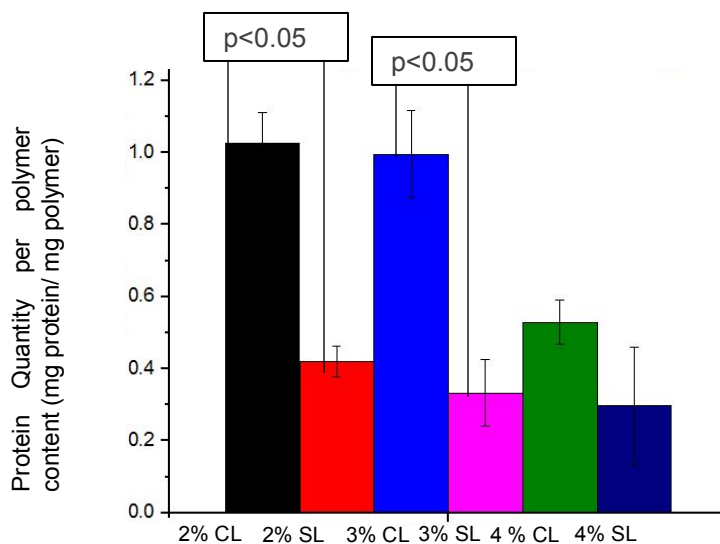


Figure 17 Protein quantity per polymer content. Comparison of Alginate beads with crystallized and solvated protein CL = Crystallized Lysozyme, SL = Solvated Lysozyme (Data representative of 4 alginates beads)

Protein release kinetic studies of each bead type in simulated gastrointestinal fluids (Simulated Gastric Fluid and Simulated Intestinal Fluid) was performed for twenty-four hours each. The release profiles in the SGF environment for both liquid and crystalline lysozyme from 2, 3 & 4%w/v beads can be appreciated in Figure 18 & 20. The release profile in SGF was characterized by an initial rapid release, within the first 10 min, followed by a plateau state, after which no protein was released. The beads with the crystalline protein had an overall protein release of less than 10%, which further confirms the usefulness of this system for intestinal antigen delivery. In the case of the beads with liquid protein, a slight increase in initial release of around 15-20% of its content can be appreciated. After this, no further protein was released. The pH-responsive characteristic of alginate (polymer swelling at high pH and shrinking at low pH) is one of the reasons this polymer was chosen for

intestinal protein delivery. Researchers have observed that alginate efficiently protects its content from an acidic environment by shrinking. The explanation for obtaining a low protein release behavior in both crystalline and solvated protein in SGF can be attributed to the alginate carboxyl group's reaction in an acidic environment. The carboxyl groups ($-\text{COO}^-$ ions) in the polymer are protonated ($-\text{COOH}$) when in contact with low pH, therefore the electrostatic repulsion between chains was reduced and they are able to come closer, forming hydrogen bonds and a tight matrix network.⁴³

In the simulated intestinal environment, for 2%, 3% & 4% alginate beads with liquid protein (Figure 19&21A), the release had an initial burst and release (~40%) in the first 20 minutes, followed by a stable increase of release of protein through time. A burst release is an initial rapid protein release of around 15% of its contents. This behavior is undesirable in controlled release since it is unpredictable, and the amount of burst cannot be significantly controlled. Initial burst release behavior is characteristic of alginate beads when they are exposed to SIF caused by chain relaxation, as seen in studies by Bhopatkar et al.⁵⁶ for alginate beads containing the model protein haemoglobin (Hb). In the case of liquid protein, it can be appreciated that the protein release follows a trend of faster release from alginate beads with higher alginate percentage (Figure 19A). This is consistent with a study done by Hariyadi et al.⁵⁷, where they attributed this behavior to an exposure of microspheres to an acid environment that may change the egg-box structure between alginate and calcium chloride. Our liquid protein is loaded in an acidic environment, so this could also explain why we obtained a slower release in the 2% beads than the 3% and 4% alginate beads with liquid protein. The 2% alginate beads with the protein in crystalline form (Figure 19&21B) had a sustained release that was slower than beads with their content in liquid form. The 3% and 4% beads with protein in crystallized form had a similar initial release in SIF. Overall the crystallized protein had a sustained protein release as confirmed by Figure 19B when compared to liquid protein release (Figure 19A). Variances in the protein release

between alginate beads of different polymer percentages have been adjudicated by other researchers to factors such as the crosslinking of alginate matrixes, protein-polymer interactions, protein size, etc. For the crystallized protein, it is hypothesized that differences in the release between the 2%, 3%, 4% alginate beads are due to the protein crystal structure/size. Further experimentation is needed to confirm this, but previous researchers^{73, 74, 75} have seen that crystallized protein dissolution is dependent on the crystal structure it has.

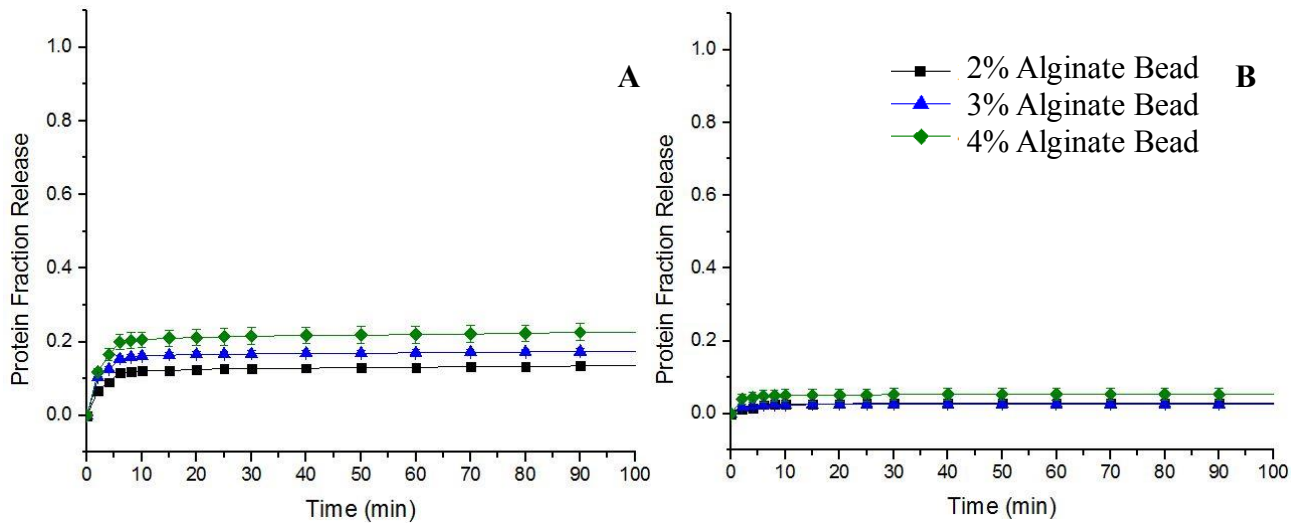


Figure 18 Release Profile for Solvated (A) and Crystallized (B) Protein from 2, 3, 4%w/v Alginate Beads in Simulated Gastric Fluid

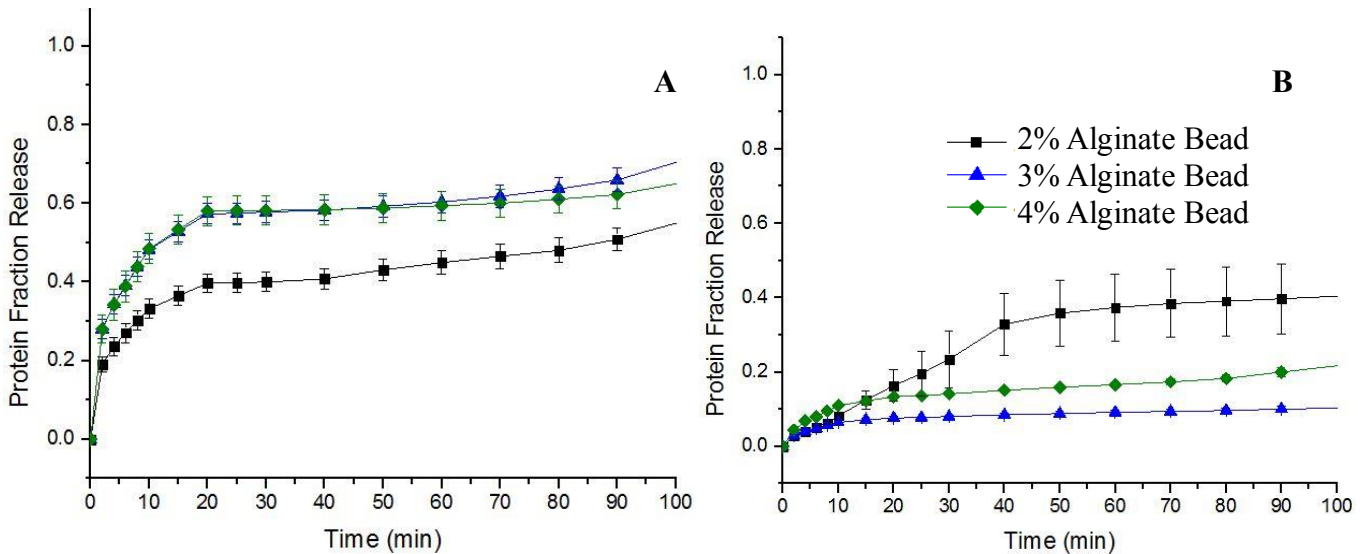


Figure 19 Release Profile for Solvated (A) and Crystallized (B) Protein from 2, 3, 4%w/v Alginate Beads in Simulated Intestinal Fluid

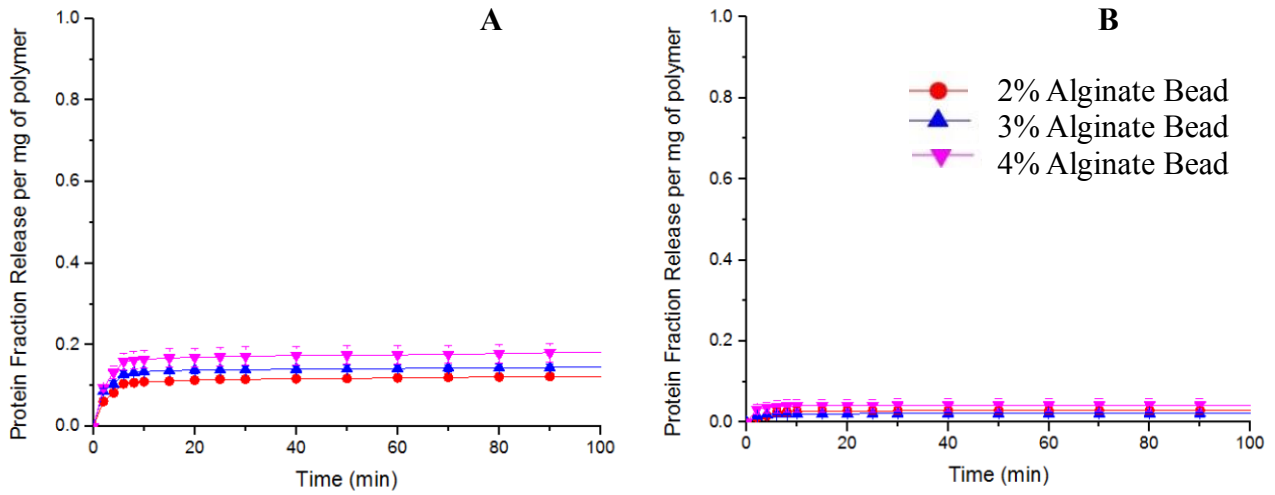


Figure 20 Protein Fraction Release per mg of polymer for Solvated (A) and Crystallized (B) Protein in Simulated Gastric Fluid

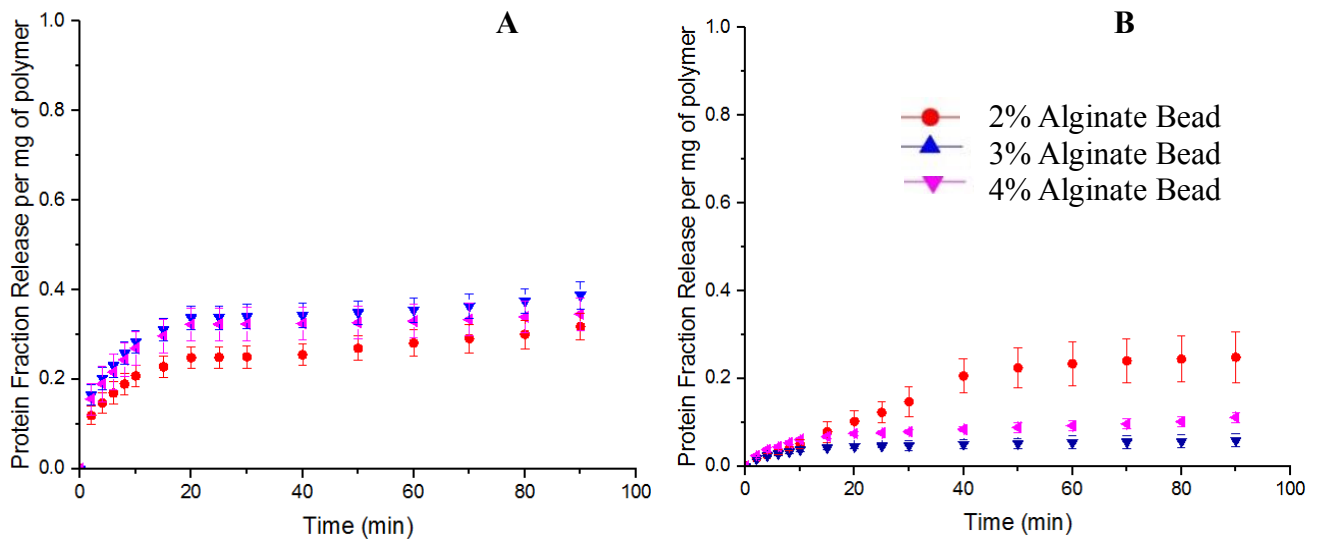


Figure 21 Protein Fraction Release per mg of polymer for Solvated (A) and Crystallized (B) Protein in Simulated Intestinal Fluid

The long-term behavior of the beads (Figure 22) showed that the crystalline protein was efficient in sustained release at 8 and 24 hours, since even at 24 hours the beads with crystalline protein were still releasing protein. These results confirmed our hypothesis that protein release in crystalline form could be sustained, making it ideal for oral immunization. The protein in crystalline

form seems to disrupt chain relaxation of the alginate when in contact with a simulated intestinal environment.

Overall, the release of the protein in crystalline form was more controlled than that of the liquid form, mainly because of the burst and release behavior the alginate has when the protein was in liquid form, which causes a fast initial release. Other researchers had modified this behavior by adding other polymers to alginate,⁸³ but having the protein in crystallized form showed to be a viable alternative. In general, the beads released little content in SGF and more of its content in SIF, confirming that alginate is an ideal polymer for intestinal antigen/protein delivery.

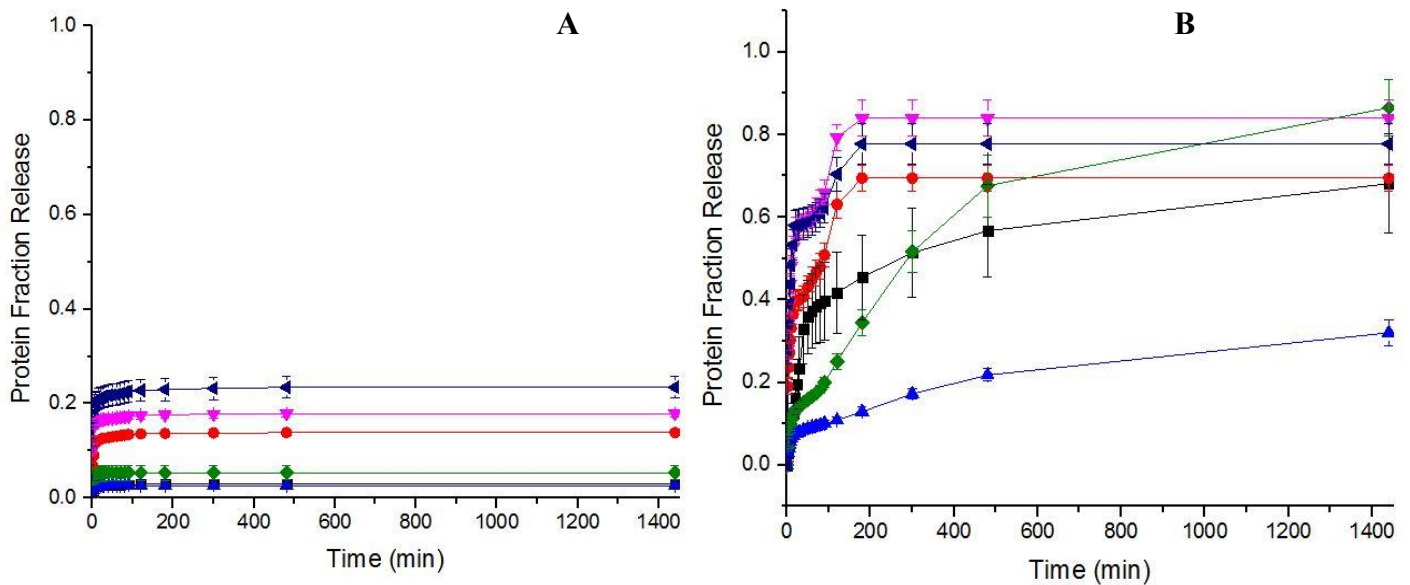


Figure 22 24 hours Protein Release Profiles of Crystallized and Solvated Lysozyme from Alginate Beads in SGF (A) and SIF (B). —■— 2% Crystallized Lysozyme —●— 2% Solvated Lysozyme —▲— 3% Crystallized Lysozyme —▼— 3% Solvated Lysozyme —◆— 4% Crystallized Lysozyme —◄— 4% Solvated Lysozyme

Besides examining the protein release profile, the protein release behavior was studied by examining how protein diffusion and transport occur from alginate systems in these conditions. In order to understand the type of transport phenomenon from each bead, we can analyze the release data

(before 0.6 protein fraction release, in the linear segment of the plot) using the Korsmeyer-Peppas⁸⁴ empirical model, most commonly known as the Power Law (Equation 2).

$$\left(\frac{M_t}{M_\infty}\right) = kt^n \quad \text{(Equation 2)}$$

Here, M_t/M_∞ is the cumulative release at t , t is time, k is a kinetic constant related to the protein-polymer interaction, and n is the exponent parameter, which gives information about the type of transport phenomenon. For spherical systems, these values are described by Siepmann et al.⁸⁵ Values of n less than 0.43 follow a release of Fickian transport, where the system will be diffusion controlled. Values of $n=0.85$ represent non-Fickian Transport (erosion controlled), while values ranging between 0.43 and 0.85 indicate Anomalous transport (combination of diffusion and erosion-controlled release). The values of n have been calculated by linearization of the equation. A statistical analysis was also performed on these n values and the 95% confidence interval was determined. The initial release profile was plotted and with Equation 1 linearized, the slope of the plot provided the n value. The transport phenomenon from the beads that had the liquid protein had an n value of less than 0.43 (Table 6), therefore it was characterized by a porous (approximately Fickian) diffusion behavior. The transport phenomenon from the bead with protein crystallized was characterized by an anomalous transport. This implies that the protein release occurred by diffusion and swelling. Because there was a noticeable difference between both types of beads (crystallized vs solvated protein), it can be concluded that the anomalous transport was mainly controlled by the protein crystals in the alginate beads. This type of transport phenomenon also occurred with some polymer beads that have multi-layers of different polyelectrolytes.⁸⁶ The statistical analysis (Appendix) by ANOVA with 95% Confidence Intervals and post-hoc Tukey test shows there was a statistical difference between the n values of 2%AlgNa crystallized and liquid protein, and the n values from 4% AlgNa beads crystallized

and liquid protein. There was no statistical difference between n values of crystallized and liquid protein in 3% AlgNa beads.

Table 6 Average n values for transport behavior SIF release

Type of bead	n values	Type of transport
2% Crystallized	0.7181 ± 0.0842	Anomalous
2% Liquid	0.3520 ± 0.0301	Porous
3% Crystallized	0.4856 ± 0.0217	Anomalous
3% Liquid	0.3390 ± 0.0196	Porous
4% Crystallized	0.5635 ± 0.0369	Anomalous
4% Liquid	0.34821 ± 0.0313	Porous

The diffusion coefficients were analyzed by two models developed by Siepmann et al.⁸⁷, which served to calculate the diffusion coefficient in spheres, as applied to monolithic systems. A monolithic system is considered to be a matrix system, in which the protein and the release rate controlling material are more or less homogeneously distributed throughout the bead. Therefore, this system can be applied when protein loading was done by imbibition.

There are two conditions when studying the diffusion coefficients in monolithic systems, whether the initial protein concentration in the polymer was below protein solubility, or above protein solubility. The first case can be analyzed by an approximation from Fick's Second Law of Diffusion. The second case can be modeled by employing Baker and Lonsdale model of Higuchi's equation for spherical systems.

In the case of modeling the release of liquid protein, the initial concentration of the protein was below protein solubility, so the first case can be used to analyze this system. Equation (5) can be used to calculate the diffusion coefficient. This equation was derived from Fick's Second Law of Diffusion (3). This equation can be simplified through the early $Mt/M_{inf} < 0.4$ and late time $Mt/M_{if} > 0.6$ approximations.

$$D_A \frac{1}{r^2} \frac{\partial}{\partial r} \left[r^2 \frac{\partial C_A}{\partial r} \right] = \frac{\partial C_A}{\partial t} \quad (\text{Equation 3})$$

By substituting $u = r C_A$ we obtain,

$$D_A \frac{\partial u^2}{\partial r^2} = \frac{\partial u}{\partial t} \quad (\text{Equation 4})$$

$$u(0, t) = 0, t > 0$$

$$u(a, t) = aC_0, \quad t > 0$$

$$u(r, 0) = rf(r), \quad 0 < r < a$$

This substitution allows solving the previous partial differential equation and obtaining the following expression,

$$\frac{M_t}{M_\infty} = 1 - \frac{6}{\pi^2} \sum_{n=1}^{\infty} \frac{1}{n^2} \exp \left[-\frac{Dn^2\pi^2 t}{a^2} \right] \quad (\text{Equation 5})$$

For early diffusion, $M_t/M_\infty < 0.4$

$$\left(\frac{M_t}{M_\infty} \right) = 6 \left(\frac{Dt}{\pi R^2} \right)^{1/2} - \left(\frac{3D}{R^2} \right) t \quad (\text{Equation 6})$$

For late diffusion, $M_t/M_\infty > 0.6$

$$\left(\frac{M_t}{M_\infty} \right) = 1 - \left(\frac{6}{\pi^2} \right) \exp \left(-\frac{\pi^2 Dt}{R^2} \right) \quad (\text{Equation 7})$$

The diffusion coefficient (D) for each trial was determined using both the early approximation and late times approximation equations that were previously described. For the first approximation, the MATLAB Curve Fitting Tool was used to plot points of data collected to Equation (6) and fit the model mentioned that provides the diffusion coefficients for each experiment.

As summarized in Table 7, the diffusion was analyzed for all of the experiment with liquid protein, in which the largest diffusion values were obtained for 3% and 4% alginate matrix with liquid lysozyme with a value of $19.0810 \times 10^{-6} \pm 0.19$ and $19.6164 \times 10^{-6} \pm 0.04$ (cm^2/s), respectively for the SIF protein release. These values were consistent with what was observed in the protein release profiles, in which the 3% and 4% alginate beads with liquid protein released its protein content, the fastest. The smallest diffusion value obtained was $9.1931 \times 10^{-6} \pm 0.12$ (cm^2/s) for 2% alginate matrix with liquid lysozyme. This behavior was only seen with the protein in liquid form, and can be adjudicated to how the protein was loaded. Since protein loading occurred after the alginate bead was already made, the tight crosslinking could disrupt protein diffusing into the core of the bead. These diffusion values were in the same order as the diffusion coefficients found in literature for protein release from alginate matrices.^{57, 88}

Table 7 Diffusion from Alginate Matrices of solvated protein in SIF

Exp.	$D_{\text{ave}} \times 10^{-6}$ (cm^2/s)	Std Dev (cm^2/s) $\times 10^{-6}$
2% Liquid	9.1931	0.1259
3% Liquid	19.0810	0.1929
4% Liquid	19.6164	0.0405

In the case of modeling the release of crystallized protein from an alginate matrix, the Higuchi model fitted better this type of system, since protein crystals were in a supersaturated state, the initial protein concentration was above protein solubility. If the protein is homogeneously distributed within a matrix at an initial concentration that exceeds drug solubility, this system is called monolithic dispersion. Modeling of this type of system was done using an equation with a steady state approach derived by Takeru Higuchi. The conditions and assumptions for using this equation were the

following. Protein transport within the matrix was rate limiting, whereas protein transport within the release medium and water penetration into the system was rapid. The dissolution of protein particles (i.e. crystals) within the matrix was rapid compared to the diffusion of dissolved protein molecules within the system. Perfect sink conditions were provided throughout the experiment. The initial protein concentration in the matrix was higher than the solubility of the protein in the (wetted) system. The size of the particles was much smaller than the thickness of the sphere. The drug was initially homogeneously distributed throughout the matrix.

Baker and Lonsdale developed a model from the Higuchi equation to describe the drug controlled release from a spherical matrix, being represented by the following expression:

$$\frac{M_t}{M_\infty} - \frac{3}{2} \left[1 - \left(1 - \frac{M_t}{M_\infty} \right)^{2/3} \right] = - \frac{3D C_s}{R^2 C_i} t \quad (\text{Equation 8})$$

Where, where M_t and M_∞ denote the cumulative amounts of drug released at time t and at infinite time, respectively; D represents the diffusion coefficient of the drug within the system; C_s represents the protein solubility; C_i represents the initial drug concentration in the system, and R the radius of the sphere.

This equation can be fitted to the experimental data of the release of crystallized protein using SigmaPlot, which was a curve fitting program that is easier to use than Matlab, and has the Baker-Lonsdale equation in its data base. Figure 23 demonstrates how this model fitted to the release data of crystalline protein from 3%w/v alginate beads. Fitted data for the release of crystalline protein from alginate beads of 2 and 4% w/v was provided in Appendix C. This model fitted the data from the 3%w/v The results from the model fit, as well as the calculated diffusion are summarized in Table 8.

The lowest diffusion value was obtained for 3%w/v alginate bead with crystalline protein was $1.88793 \times 10^{-8} \text{ cm}^2/\text{s}$, but a statistical analysis showed that all of the diffusion values were statistically similar. When comparing the diffusion from alginate beads with protein in crystalline and liquid form, the smallest values for diffusion were obtained for crystalline protein. Even so, having the protein in its crystalline form provides the bead with added stability and a minor initial burst release than their liquid counterparts.

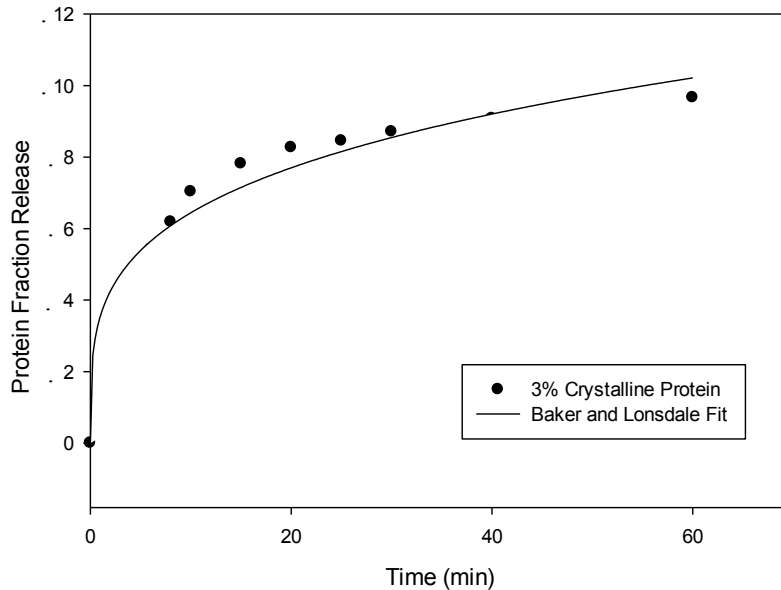


Figure 23 Baker-Lonsdale Model Fitting for 3% Alginate bead with crystalline protein (line is the model fitting, dot is the experimental data).

Table 8 Results from Baker-Lonsdale Model for Diffusion Coefficient for crystallized protein in SIF

Experiment	Diffusion (cm^2/s)	Standard Deviation
2% Crystallized	2.72×10^{-7}	3.08×10^{-5}
3% Crystallized	1.88×10^{-8}	4.87×10^{-5}
4% Crystallized	1.43×10^{-7}	6.77×10^{-4}

It can be concluded that an alginate matrix can be used to provide adequate protein immobilization and stability during transport to the intestinal section of the GI tract, because of its efficient protein retention in SGF and liberation in SIF. The transport from crystallized proteins can be characterized as anomalous, while the transport from liquid protein is pseudo Fickian. Overall the crystallized protein resulted to have a slower diffusion of the protein in the different alginate concentration beads than their liquid counterparts.

7.5 Insulin Crystallization in Alginate Systems

Insulin crystallization has been one of the most researched protein crystallizations since different confirmations of the crystal structure lead to varying dissolution rates, which is beneficial for insulin formulations. We experimented with two methods for insulin crystallization at different pH and precipitating agents. The first method used sodium phosphate as precipitating agent. This crystallization occurred within 24 hours and had various crystal sizes depending on the protein and precipitant concentrations used (Appendix D). For example, insulin crystals grown in the condition of 15mg/mL of Figure 24A (top) showed a smaller crystal size than those grown in a solution of 20mg/mL Figure 24B (bottom). The obtained insulin crystal conformation was similar to the ones found by Ootaki et al.⁸⁹, such as cube and dodecahedron form (Figure 24A top) and rhombic dodecahedron conformation (Figure 24A bottom).

The procedure was then applied to alginate beads. The insulin diffused into the alginate bead structure and was precipitated by sodium phosphate. Although the environment in the alginate bead appeared to be ideal for insulin crystallization, the bead structure disintegrated. The reason for this behavior can be explained how phosphate groups behaved around calcium ions. Phosphate groups in

the precipitating agent can compete with carboxylate groups in alginate for calcium ions, therefore debilitating the bead structure, as seen in Appendix D. This process did not occur rapidly, but was problematic when crystallizing the protein, since as the protein was crystallized; the bead was losing its rigid structure. Alternatives in the procedure for insulin crystallization were searched.

The second crystallization method applied for insulin used zinc ions to cause crystal formation. Insulin and zinc enjoy a multivalent relationship, where zinc influences its crystal structure upon precipitation. Crystallization was performed by the sequential addition of zinc chloride, 25%w/v acetone, and sodium citrate buffer, which is the primary precipitating agent of the group. The resulting crystals (Figure 24B) had a cubic shape. If more zinc ions were added, other conformations were obtained.

This process was then applied to alginate beads. The crystallization was performed by the process of imbibition. Once the final precipitating agent (sodium chloride) was added, the bead disintegrated after 4 hours. The reason for this was that sodium citrate also has affinity with calcium ions. This behavior was also seen with alginate beads made with zinc chloride, which are softer in nature. Because the crystallization protocol of insulin has either one of these precipitating agents, we opted to make alginate beads that were not ionic cross-linked with divalent ions. The procedure applied involved using glutaraldehyde as the crosslinker. Glutaraldehyde covalently crosslinks alginate hydroxyl groups. To strengthen this interaction alginate was first precipitated with methanol and then crosslinked with glutaraldehyde as shown by Kulkarni et al.⁸⁸ Once the bead formed, it had to be washed greatly, because insulin can bind to glutaraldehyde during the imbibition process. The second method of crystallization was applied to the alginate bead, and after 24 hours, insulin crystal formation could be appreciated inside the bead (Figure 25). The bead had less nucleation, when compared to lysozyme crystallization in beads. This was probably due to the glutaraldehyde in the alginate bead. As

shown, crystallization of insulin in alginate beads was better performed in alginate systems that do not have calcium ions or divalent crosslinking, such as covalent crosslinked alginate beads.

One of the most common protein precipitating agents is sodium phosphate, therefore it is in our interest in future applications with other proteins, to use covalent crosslinked alginate beads like this one, to crystallize such proteins.

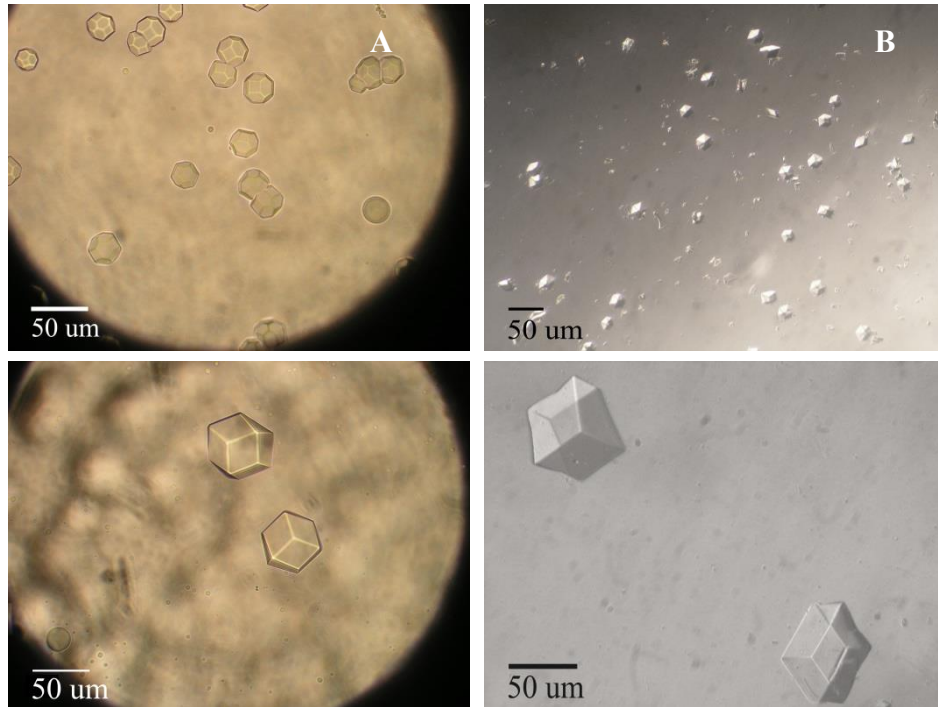


Figure 24 Insulin Crystal Formation by A) Method 1 (sodium phosphate as precipitating salt) and Method 2 (sodium citrate as precipitating salt)

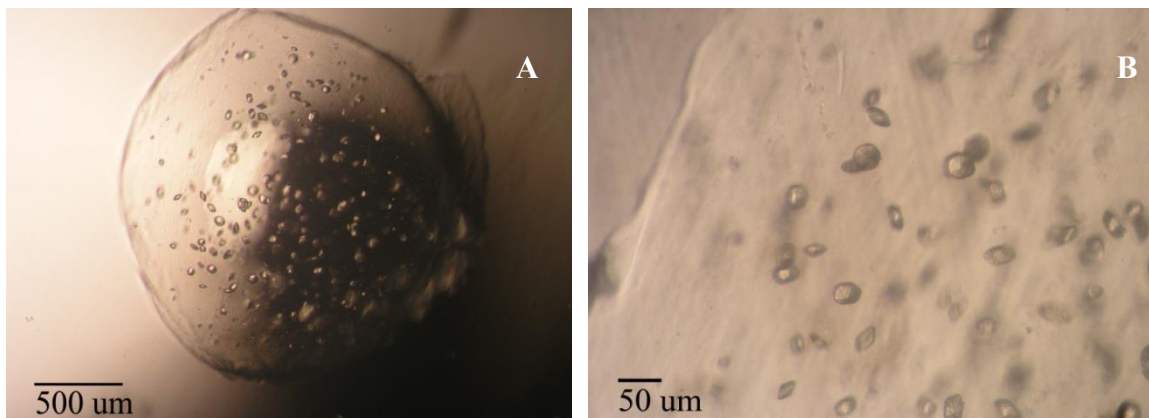


Figure 25 Insulin Protein Crystallization in Alginate Beads. A) Bead with insulin crystals. B) Insulin crystals close up.

7.6 Ovalbumin Crystallization in Alginate Systems

The ovalbumin crystallization was well studied in the 1900s when Hofmeister crystallized it by adding equal volumes of saturated ammonium sulfate solution to egg white and then evaporating the solution at room temperature since it was readily available. The crystallization procedure has not varied much since then. Researchers that have crystallized this protein in recent years⁷¹ have done so by first isolating the protein from egg white. Although companies guarantee protein purity, the protein stability is sensitive to temperature changes, leading to S-ovalbumin formation (a heat-stable form of ovalbumin). Impurities in ovalbumin greatly affect its crystallization, which could lead to amorphous precipitation.

The protein isolation procedure was followed and subsequently crystallized by the addition of calcium ions. The crystal obtained has a shape of elongated crystals which is in accordance to the crystals obtained by Miller et al.⁷² in which crystal length-width-thickness ratio was 8:1:0.2. An SDS page was followed to confirm that the crystal structure was ovalbumin crystallized. The membrane shown in Figure 26 (right), demonstrated the protein liquid (fifth column) from which ovalbumin was crystallized. This mother liquor has a variety of proteins that have molecular size in accordance with the main proteins of egg white (Table 9). The third and fourth columns have dissolved crystalline ovalbumin. Ovalbumin, which has a molecular weight of 45kDa, appears to have been selectively crystallized from the other proteins. The results from the SDS Page indicated that the crystallized protein was in fact ovalbumin.

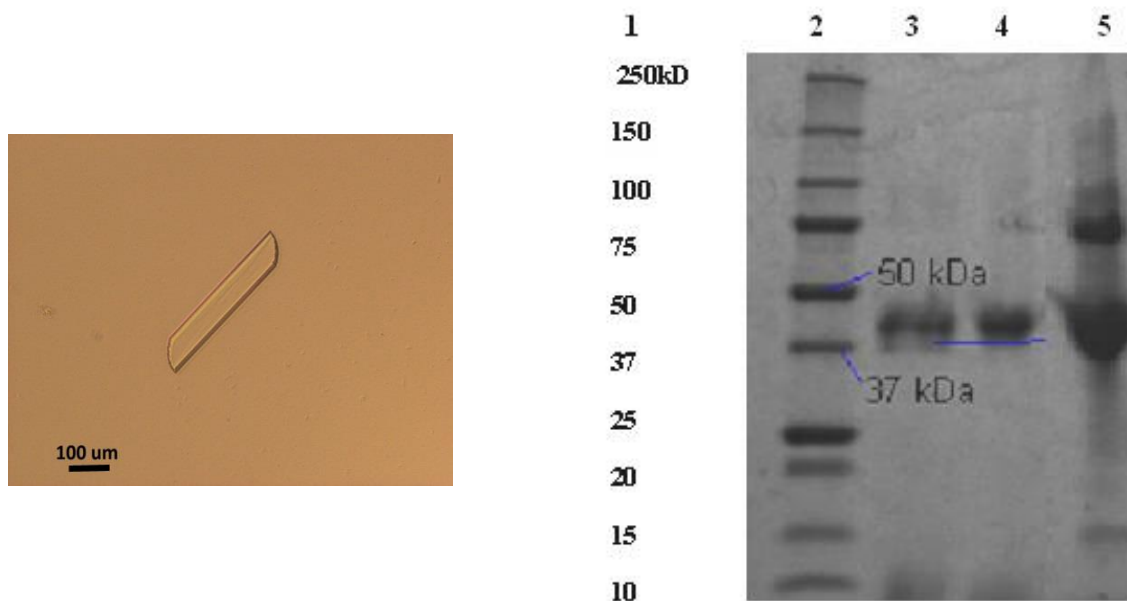


Figure 26 Ovalbumin Crystallization obtained from egg white purification process. (Left) SDS PAGE Electrophoresis of liquid before ovalbumin crystallization and after. (Right)

Column 1&2: Bio Rad Dual Color Marker, Column 3&4: Crystallized Column 5: Mother Liquor before Crystallization.

Table 9 Main Proteins found in Egg White

Egg White Main Proteins	Molecular Weight (kDa)
Ovomucin	5500-8800
Ovotransferin	77.7
Ovalbumin	44.5
Ovomucoid	28.0
Lysozyme	14.3

The crystallization procedure for ovalbumin was then followed in alginate beads with minor adjustments. Crystals that had been obtained by the protein purification method were dissolved and diffused into alginate beads. When the precipitating agent was added, the ovalbumin tended to crystallize outside of the bead or inside very close to the edge of the bead (Figure 27). An explanation as to why this could happen is that ovalbumin has a negative charge, an isoelectric point of 4.7. Cegnar et al.⁹⁰ showed that for a polyanion such as alginate (having a pKa of guluronic and mannuronic acid

3.6 and 3.4, respectively). It is probable that because both are negatively charge they are repelling each other, making it difficult for the protein to be inside the alginate bead. Another alternative for incorporating the ovalbumin into the bead are by adding the ovalbumin with the alginate before crosslinking and using a crosslinker agent that is not calcium chloride.

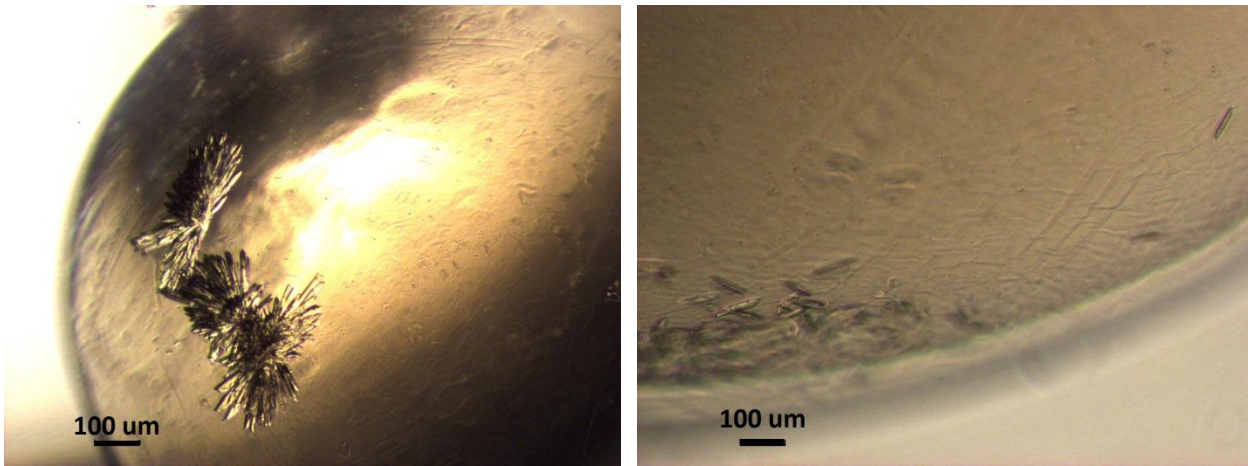


Figure 27 Ovalbumin Crystallization in alginate beads

8 CONCLUSION AND RECOMENDATIONS

This work focused on the design and creation of composite protein microcrystals for oral delivery of antigens. Oral immunization serves as a gateway to prevent allergies and pathogens that gain access to the body through the gastrointestinal mucosa. The design consisted on using a biodegradable polymer called alginate to encapsulate and protect the antigen for the oral delivery to the intestinal section. The antigen was incorporated into the polymer as protein in its crystalline form to give the protein stability. The objectives of this thesis consisted on creating the polymer carrier, crystallizing the model proteins lysozyme, insulin, and ovalbumin, and testing the system protein release capacity in different environments.

The alginate system was successfully created in two sizes, beads and microbeads. The microbeads were developed using a polymer atomizing system to determine particle size and a calcium solution to crosslink the polymer. The microbeads were successfully created in the desired size range (5 – 20um). To create the proposed system, lysozyme protein crystallization was performed in the polymeric beads. The resulting bead had a noticeable polymer crystal nucleation and further crystal growth. It was concluded that the alginate system serves as an adequate environment for lysozyme crystallization. The process was adjusted to be adequate for crystallization in polymer systems of a smaller size (<20um). Crystallized lysozyme in alginate microbeads appeared to have a spherical form due to the alginate. It can be concluded that as the size of the alginate bead decreased, less protein nucleation was noticed. The final microbead obtained had a monocrystal of the protein. Protein crystallization in alginate microbeads at this scale is a new process that has potential applications in protein crystallization as well as antigen delivery.

In general, the lysozyme protein proved to be a great model protein for the testing of the antigen system, since its crystallization could be performed without major complications. Lysozyme crystallized well in the calcium-crosslinked alginate system, because it has affinity with calcium. The protein release test was performed in simulated gastrointestinal fluid conditions. By measuring the loading efficiency, it was found that more protein was encapsulated in the same volume when the protein is crystallized. Being able to deliver more protein in the same volume will be beneficial to create a stronger immune response with the same dosage. In simulated gastric fluid (SGF) the protein release profile obtained was characterized by an initial rapid release, within the first 10 min, followed by a plateau state, after which no protein was further released. Beads with crystalline protein had an overall protein released of less than 10%. It was concluded that having a protein in its crystalline form gives it additional stability and immobility within the polymer matrix. In simulated intestinal fluid (SIF), in contrast, the majority of the beads had a release of more than 60% of their protein content. In general, the beads released little content in SGF and more of its content in SIF. Based on the positive protein retention in SGF and subsequent protein liberation in SIF, it can be concluded that alginate is an ideal polymer for intestinal antigen/protein in delivery.

The protein transport phenomenon from alginate system was characterized as pseudo Fickian for beads with protein in liquid form and anomalous for beads with the protein in crystalline form. By examining the release profile from alginate beads, it was determined that crystalline protein released slower than their liquids counterparts. This was confirmed with the diffusion coefficients calculation, with the largest diffusion values obtained for 3% and 4% alginate matrix with liquid lysozyme with a value of $19.0810 \times 10^{-6} \pm 0.19 \text{ cm}^2/\text{s}$, and $19.6164 \times 10^{-6} \pm 0.04 \text{ cm}^2/\text{s}$, respectively. These values are consistent with what was observed in the protein release profiles, in which the 3% and 4% alginate

beads with liquid protein released its protein content, the fastest. The smallest diffusion value obtained was $1.88793 \times 10^{-8} \pm 0.15 \text{ cm}^2/\text{s}$ for 3% alginate matrix with crystalline lysozyme.

The applicability of this system to other proteins was further studied by testing the crystallization of insulin and ovalbumin in the alginate system. In the case of insulin, protein crystallization in alginate beads occurred, but the crosslinking of the polymer matrix was weakened by the precipitating agents. This was confirmed when the crystallization was performed in alginate beads crosslinked covalently with glutaraldehyde. The crystallization of ovalbumin was performed by first isolating the protein from egg white and additional purification. To perform this crystallization in alginate, it was established that the protein has to be added before crosslinking the polymer matrix, because the protein does not enter the alginate matrix by imbibition. The crosslinking for ovalbumin has to be also done with another agent that is not calcium, such as zinc chloride.

The applications of this system cover a wide range of areas. This system can be used not only in antigen delivery, but also in pharmaceutical drug delivery, and in protein crystallization for X-ray analysis of proteins where it is difficult to obtain a single crystal. It is recommended that if the protein preferably binds to calcium, such as lysozyme, the ionic crosslinked alginate bead should be used for crystallization. If the protein does not preferably binds to calcium or the precipitating agent has strong interactions with calcium, a covalent alginate bead should be used.

REFERENCES

1. Kim, S.-H.; Seo, K.-W.; Kim, J.; Lee, K.-Y.; Jang, Y.-S., The M cell-targeting ligand promotes antigen delivery and induces antigen-specific immune responses in mucosal vaccination. *Journal of immunology* **2010**, *185* (10), 5787-5795.
2. Shukla, A.; Katare, O. P.; Singh, B.; Vyas, S. P., M-cell targeted delivery of recombinant hepatitis B surface antigen using cholera toxin B subunit conjugated bilosomes. *International journal of pharmaceutics* **2010**, *385*, 47-52.
3. Willaert, R.; Zegers, I.; Wyns, L.; Sleutel, M., Protein crystallization in hydrogel beads. *Acta crystallographica. Section D, Biological crystallography* **2005**, *61* (Pt 9), 1280-1288.
4. Lee, K. Y.; Mooney, D. J., Alginate : properties and biomedical applications. *Progress Polymer Science* **2013**, *37* (1), 106-126.
5. Norrman, M.; Schluckebier, G., Crystallographic characterization of two novel crystal forms of human insulin induced by chaotropic agents and a shift in pH. *BMC structural biology* **2007**, *7*, 83-83.
6. Parham, P., *The Immune System*. 3er ed.; Garland Science: 2009; p 506-506.
7. O'Hagan, D. T. *New Generation Vaccine Adjuvants 2007*.
8. Azizi, A.; Kumar, A.; Diaz-Mitoma, F.; Mestecky, J., Enhancing oral vaccine potency by targeting intestinal M cells. *PLoS pathogens* **2010**, *6* (11), e1001147-e1001147.
9. Neutra, M. R. a. K. P. A., Mucosal vaccines: the promise and the challenge. *Nature reviews. Immunology* **2006**, *6* (2), 148--58.
10. Pabst, O. a. M. a. M., Oral tolerance to food protein. *Mucosal immunology* **2012**, *5* (3), 232--9.
11. Pasetti, M. F.; Simon, J. K.; Szein, M. B.; Levine, M. M., Immunology of gut mucosal vaccines. *Immunological Reviews* **2011**, *239* (1), 125-148.
12. Janeway, C. J.; Travers, P.; Walport, M., The mucosal immune system. In *Immunobiology: The Immune System in Health and Disease*, 5 ed.; Garland Science: New York, 2001.
13. Wang, L.; Coppel, R. L. Oral vaccine delivery: can it protect against non-mucosal pathogens? *2008*, p. 729-738.
14. Kim, S.-H.; Jang, Y.-S., Antigen targeting to M cells for enhancing the efficacy of mucosal vaccines. *Experimental & molecular medicine* **2014**, *46* (3), 85-85.
15. Parashar, U. D.; Gibson, C. J.; Bresee, J. S.; Glass, R. I., Rotavirus and severe childhood diarrhea. *Emerging infectious diseases* **2006**, *12* (2), 304-6.

16. Greenberg, H. B.; Estes, M. K., Rotaviruses : from pathogenesis to vaccination. *Gastroenterology* **2013**, *136* (6), 1939-1951.
17. Mojaverian, P., Evaluation of gastrointestinal pH and gastric residence time via the Heidelberg radiotelemetry capsule: Pharmaceutical application. *Drug Development Research* **1996**, *38* (2), 73-85.
18. Shaji, J.; Patole, V., Protein and Peptide Drug Delivery: Oral Approaches. *Indian Journal of Pharmaceutical Sciences* **2008**, *70* (3), 269-277.
19. Lycke, N., Recent progress in mucosal vaccine development: potential and limitations. *Nature Reviews Immunology* **2012**, *12*, 592-605.
20. Hooper, L. V. a. M. A. J., Immune adaptations that maintain homeostasis with the intestinal microbiota. *Nature reviews. Immunology* **2010**, *10* (3), 159--69.
21. American College of Allergy, A.; Immunology, Food Allergies: Egg Allergy.
22. Florence, A., Nanoparticle uptake by the oral route: Fulfilling its potential? *Drug Discovery Today: Technologies* **2005**, *2* (1).
23. Warner, R.; Bailey, C. K., The proteins: Chemistry, biological activity, and methods. New York, Academic Press Inc: 1954; pp 435-435.
24. Van Regenmortel, M. H. V., Structure of Antigens. Taylor & Francis: 1995; pp 93-96.
25. Bowey, K.; Swift, B. E.; Flynn, L. E.; Neufeld, R. J., Characterization of biologically active insulin-loaded alginate microparticles prepared by spray drying. *Drug development and industrial pharmacy* **2013**, *39* (3), 457-65.
26. Marriage, D. E.; Erlewyn-Lajeunesse, M.; Unsworth, D. J.; Henderson, a. J., Unscrambling Egg Allergy: The Diagnostic Value of Specific IgE Concentrations and Skin Prick Tests for Ovomucoid and Egg White in the Management of Children with Hen's Egg Allergy. *ISRN allergy* **2012**, *2012*, 627545-627545.
27. Watarai, S.; Iwase, T.; Tajima, T.; Yuba, E.; Kono, K., Efficiency of pH-Sensitive Fusogenic Polymer-Modified Liposomes as a Vaccine Carrier. *The Scientific World Journal* **2013**, *2013*, 7.
28. Shima, H.; Watanabe, T.; Fukuda, S.; Fukuoka, S.-I.; Ohara, O.; Ohno, H., A novel mucosal vaccine targeting Peyer's patch M cells induces protective antigen-specific IgA responses. *International Immunology* **2014**, *26* (11), 619-625.
29. Judge, R. a.; Johns, M. R.; White, E. T., Protein purification by bulk crystallization: the recovery of ovalbumin. *Biotechnology and bioengineering* **1995**, *48* (4), 316-23.
30. Berman, H. M., The Protein Data Bank. 2000; Vol. 28, pp 235-242.

31. Park, K.; Kwon, I. C.; Park, K., Oral protein delivery: Current status and future prospect. *Reactive and Functional Polymers* **2011**, *71* (3), 280--287.
32. Chen, J.; Sarma, B.; Evans, J. M. B.; Myerson, A. S., Pharmaceutical crystallization. *Crystal Growth and Design* **2011**.
33. Al-Hilal, T. a.; Alam, F.; Byun, Y., Oral drug delivery systems using chemical conjugates or physical complexes. *Advanced drug delivery reviews* **2013**, *65* (6), 845-864.
34. Jen, A. a. M. H. P., Diamonds in the rough: protein crystals from a formulation perspective. *Pharmaceutical research* **2001**, *18* (11), 1483--1488.
35. McPherson, A., Introduction to protein crystallization Methods. *Methods* **2004**, *34* (3), 254-265.
36. McPherson, A., *Crystallization of Biological Macromolecules*. 1999; p 586-586.
37. McPherson, A.; Gavira, J. A., Introduction to protein crystallization. 2014.
38. Petrovsky, N. a. A. J. C., Vaccine adjuvants: Current state and future trends. *Immunol Cell Biol* **2004**, *82* (5), 488--496.
39. Nair, L. S.; Laurencin, C. T., Biodegradable polymers as biomaterials. *Progress in Polymer Science* **2007**, *32* (8-9), 762-798.
40. Gombotz, W.; Wee, S., Protein release from alginate matrices. *Advanced Drug Delivery Reviews* **2012**, *64*, 194-205.
41. Augst, A. D.; Kong, H. J.; Mooney, D. J., Alginate hydrogels as biomaterials. *Macromolecular bioscience* **2006**, *6* (8), 623--33.
42. S.N. Pawar, K. J. E., Alginate derivatization: A review of chemistry, properties and applications. *Biomaterials* **2012**, *33*, 3279-3305.
43. Lee, K. Y. a. M. D. J., Alginate : properties and biomedical applications. *Progress Polymer Science* **2013**, *37* (1), 106--126.
44. Donati, I.; Holtan, S.; Morch, Y. A.; Borgogna, M.; Dentini, M.; Skjaak-Braek, G., New hypothesis on the role of alternating sequences in calcium-alginate gels. *Biomacromolecules* *6* (2), 1031--40.
45. Tripathi, R. a. M. B., Development and evaluation of sodium alginate-polyacrylamide graft-copolymer-based stomach targeted hydrogels of famotidine . *AAPS PharmSciTech* **2012**, *13* (4), 1091--102.

46. Andersen, T.; Strand, B. L.; Formo, K.; Alsberg, E.; Christensen, B. E., Alginates as biomaterials in tissue engineering. **2012**, 227--258.
47. Morch, Y. A.; Donati, I.; Strand, B. L.; Skjaa, k.-B. G., Molecular engineering as an approach to design new functional properties of alginate. *Biomacromolecules* **2007**, 8 (9), 2809--14.
48. Hussain, N., Recent advances in the understanding of uptake of q microparticulates across the gastrointestinal lymphatics. *Advanced Drug Delivery Reviews* **2001**, 50, 107-142.
49. Masuda, K.; Horie, K.; Suzuki, R.; Yoshikawa, T.; Hirano, K., Oral delivery of antigens in liposomes with some lipid compositions modulates oral tolerance to the antigens. *Microbiology and immunology* **2002**, 46 (1), 55--8.
50. Soppimath, K. S.; Aminabhavi, T. M.; Kulkarni, A. R.; Rudzinski, W. E., Biodegradable polymeric nanoparticles as drug delivery devices. *Journal of Controlled Release* **2001**, 70 (1-2), 1--20.
51. Grabovac, V.; Guggi, D.; Bernkop-Schnürch, A., Comparison of the mucoadhesive properties of various polymers. *Advanced drug delivery reviews* **2005**, 57 (11), 1713-1723.
52. Chopra, S.; Mahdi, S.; Kaur, J.; Iqbal, Z.; Talegaonkar, S.; Ahmad, F. J., Advances and potential applications of chitosan derivatives as mucoadhesive biomaterials in modern drug delivery. *The Journal of pharmacy and pharmacology* **2006**, 58 (8), 1021--32.
53. George, M.; Abraham, T. E., Polyionic hydrocolloids for the intestinal delivery of protein drugs: alginate and chitosan--a review. *Journal of controlled release : official journal of the Controlled Release Society* **2006**, 114 (1), 1-14.
54. Allamneni, Y.; Reddy, B.; Dayananda, C.; Venkata, B. R. N.; Chaitanya, K.; Arun, K. K., Performance Evaluation of Mucoadhesive Potential of Sodium Alginate on Microspheres Containing an Anti-Diabetic Drug: Glipizide. *International Journal of Pharmaceutical Sciences and Drug Research* **2012**, 4 (2), 115-122.
55. Aslani, P.; Kennedy, R. A., Studies on diffusion in alginate gels. I. Effect of cross-linking with calcium or zinc ions on diffusion of acetaminophen. *Journal of Controlled Release* **1996**, 42 (1), 75-82.
56. Bhopatkar, D.; Anal, A. K.; Stevens, W. F., Ionotropic alginate beads for controlled intestinal protein delivery: effect of chitosan and barium counter-ions on entrapment and release. *Journal of microencapsulation* **2005**, 22 (1), 91-100.
57. Hariyadi, D. M., Effect of Cross Linking Agent and Polymer on the Characteristics of Ovalbumin Loaded Alginate Microspheres. *Journal of Pharmacy* **2014**, 6 (4), 469--474.

58. Bowersock, T. L.; HogenEsch, H.; Suckow, M.; Porter, R. E.; Jackson, R.; Park, H.; Park, K., Oral vaccination with alginate microsphere systems. **1996**, *39* (2-3), 209--220.
59. Suzuki, S.; Christensen, B. E.; Kitamura, S., Effect of mannuronate content and molecular weight of alginates on intestinal immunological activity through Peyer's patch cells of C3H/HeJ mice. *Carbohydrate Polymers* **2011**, *83* (2), 629--634.
60. Mata, E.; Igartua, M.; Patarroyo, M. E.; Pedraz, J. L.; Hernandez, R. M., Enhancing immunogenicity to PLGA microparticulate systems by incorporation of alginate and RGD-modified alginate. *European journal of pharmaceutical sciences : official journal of the European Federation for Pharmaceutical Sciences* **2011**, *44* (1-2), 32--40.
61. Halder, A.; Maiti, S.; Sa, B., Entrapment efficiency and release characteristics of polyethyleneimine-treated or -untreated calcium alginate beads loaded with propranolol-resin complex. *International journal of pharmaceutics* **2005**, *302* (1-2), 84-94.
62. Setty, C. M.; Sahoo, S. S.; Sa, B., Alginate-coated alginate-polyethyleneimine beads for prolonged release of furosemide in simulated intestinal fluid. *Drug development and industrial pharmacy* **2005**, *31* (4-5), 435-46.
63. Zhang, Y.; Wei, W.; Lv, P.; Wang, L.; Ma, G., Preparation and evaluation of alginate-chitosan microspheres for oral delivery of insulin. *European journal of pharmaceutics and biopharmaceutics : official journal of Arbeitsgemeinschaft für Pharmazeutische Verfahrenstechnik e.V* **2011**, *77* (1), 11-9.
64. Martins, S.; Sarmiento, B.; Souto, E. B.; Ferreira, D. C., Insulin-loaded alginate microspheres for oral delivery – Effect of polysaccharide reinforcement on physicochemical properties and release profile. *Carbohydrate Polymers* **2007**, *69* (4), 725-731.
65. Hájková, M.; Kratochvíl, B.; Rádl, S., Atorvastatin - the World's Best Selling Drug. *Chem. List* **2008**, *102*, 3-14.
66. Childs, S. L.; Hardcastle, K. I., Cocrystals of Piroxicam with Carboxylic Acid. *Crystal Growth & Design* **2007**, *7*, 1291-1304.
67. Bingham, A. L.; Hughes, D. S.; Hursthouse, M. B.; Lancaster, R. W.; Tavener, S.; Threlfall, T. L., Over one hundred solvates of sulfathiazole. *Chem. Commun.* **2001**, 603-604.
68. Basu, S. K.; Govardhan, C. P.; Jung, C. W.; Margolin, A. L., Protein crystals for the delivery of biopharmaceuticals. *Expert opinion on biological therapy* **2004**, *4* (3), 301-17.
69. Garcia Ruiz, J. M.; Charles, J.; Carter, W.; R.M, S., Counterdiffusion Methods for Macromolecular Crystallization. *Methods in Enzymology* **2003**, *368*, 130-154.

70. Gavira, J. A.; Cera-manjarres, A.; Ortiz, K.; Mendez, J.; Jimenez-torres, J. A.; Patin, L. D.; Torres-lugo, M., Use of Cross-Linked Poly(ethylene glycol)-Based Hydrogels for Protein Crystallization. *Crystal Growth & Design* **2014**, *14*, 3239-3248.
71. Dumetz, C.; Chockla, A. M.; Kaler, E. W.; Lenhoff, A. M., Comparative Effects of Salt , Organic , and Polymer Precipitants on Protein Phase Behavior and Implications for Vapor Diffusion. *Crystal Growth & Design* **2009**, *9* (2), 682-691.
72. Miller, M.; Weinstein, J. N.; Wlodawer, A., Preliminary X-ray Analysis of Single Crystals of Ovalbumin and Plakalbumin. **1983**, *258* (9), 5864-5866.
73. Shi, K.; Hongshu, B.; Jiang, Y., Characterization of physicochemical and biological properties of spherical protein crystals for sustained release. *Asian Journal of Pharmaceutical Sciences* **2013**, *8* (1), 58--63.
74. Halder, A.; Maiti, S., Entrapment efficiency and release characteristics of polyethyleneimine-treated or -untreated calcium alginate beads loaded with propranolol-resin complex. *International journal of pharmaceutics* **2005**, *302* (1-2), 84-94.
75. Hallas-Moller, K.; Petersen, K.; Schlichtkrull, J., Crystalline and Amorphous Insulin-Zinc Compounds with Prolonged Action. *Science* **1952**, *116* (3015), 394--398.
76. Kwok, K. K.; Groves, M. J.; Burgess, D. J., Production of 5-15 microns diameter alginate-polylysine microcapsules by an air-atomization technique. *Pharmaceutical research* **1991**, *8* (3), 341-4.
77. Hermanson, G. T., Chapter 10 - Fluorescent Probes. In *Bioconjugate Techniques (Third edition)*, Hermanson, G. T., Ed. Academic Press: Boston, 2013; pp 395-463.
78. Nie, Z.; Xu, S.; Seo, M.; Lewis, P. C.; Kumacheva, E., Polymer particles with various shapes and morphologies produced in continuous microfluidic reactors. *Journal of the American Chemical Society* **2005**, *127* (22), 8058--63.
79. Kong, T.; Wu, J.; Yeung, K.; Wai, K.; Kai, T.; Shum, H. C.; Wang, L., Microfluidic fabrication of polymeric core-shell microspheres for controlled release applications. *Biomicrofluidics* **2013**, *7* (4), 44128.
80. Ribeiro, A. J.; Silva, C.; Ferreira, D.; Veiga, F., Chitosan-reinforced alginate microspheres obtained through the emulsification/internal gelation technique. *European journal of pharmaceutical sciences : official journal of the European Federation for Pharmaceutical Sciences* **2005**, *25* (1), 31--40.

81. Ng, J.; Gavira, J.; Garcia-Ruiz, J., Protein crystallization by capillary counterdiffusion for applied crystallographic structure determination. *J STRUCT BIOL* **2003**, *142* (1), 218-231.
82. Gavira, J. A.; Van Driessche, A. E. S.; Garcia-Ruiz, J.-M., Growth of Ultrastable Protein–Silica Composite Crystals. *Crystal Growth & Design* **2013**, *13* (6), 2522-2529.
83. Gonzalez-Rodriguez, M. L.; Holgado, M. A.; Sanchez-Lafuente, C.; Rabasco, A. M.; Fini, A., Alginate/chitosan particulate systems for sodium diclofenac release. *International Journal of Pharmaceutics* **2002**, *232* (1-2), 225--234.
84. Sciences, H.; Dash, S.; Murthy, P. N.; Nath, L.; Chowdhury, P., Kinetic modeling on drug release from controlled drug delivery systems. *Acta poloniae pharmaceutica* **2010**, *67* (3), 217--23.
85. Siepmann, J. a. S. F., Modeling of diffusion controlled drug delivery. *Journal of Controlled Release* **2012**, *161* (2), 351--362.
86. Adhiyaman, R.; Sanat, K. B., Alginate-Chitosan Particulate System for Sustained Release of Nimodipine. *Tropical Journal of Pharmaceutical Research* **2009**, *8* (5), 433--440.
87. Seipmann, J.; Peppas, N.A., Modeling of drug release from delivery systems based on hydroxypropyl methylcellulose (HPMC). *Advanced Drug Delivery Reviews*. **2001**, *48* (2-3), 139-157.
88. Kulkarni, A. R.; Soppimath, K. S.; Aminabhavi, T. M.; Dave, A. M.; Mehta, M. H., Glutaraldehyde crosslinked sodium alginate beads containing liquid pesticide for soil application. *Journal of Controlled Release* **2000**, *63* (1-2), 97--105.
89. Ootaki, M.; Endo, S.; Sugawara, Y.; Takahashi, T., Crystal habits of cubic insulin from porcine pancreas and evaluation of intermolecular interactions by macrobond and EET analyses. *Journal of Crystal Growth* **2009**, *311* (17), 4226-4234.
90. Cegnar, M.; Ker, V., Self-assembled Polyelectrolyte Nanocomplexes of Alginate, Chitosan and Ovalbumin. *Acta chimica Slovenica* **2010**, *57* (2), 431--41.

Appendix A: Microbead Size Analysis

The alginate microbead size analysis was done for three different alginate percentages (2, 2.5, 3.0%w/v). Pictures were taken with a microscope from three different samples of microbeads at Alginate concentrations of 3%, 2.5%, and 2%. An analysis by Image J for each microbead recognized the boundaries for each one, numerates them, and calculates the area. With the area, the diameter was calculated and plotted in histograms. The yield was calculated by weighting the dried polymer that was supplied and comparing it to the dried weight of the microbeads produced from that polymer quantity.

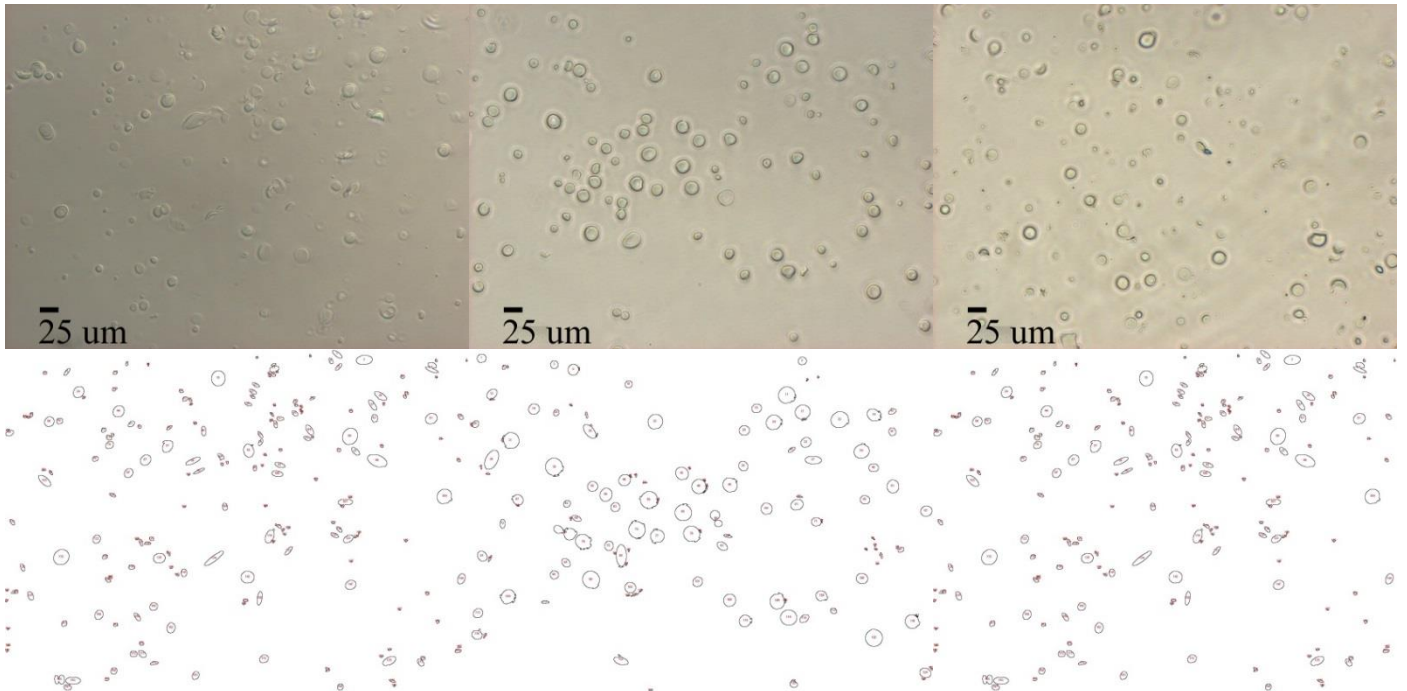


Figure A.1 Size Analysis for Alginate Microbead

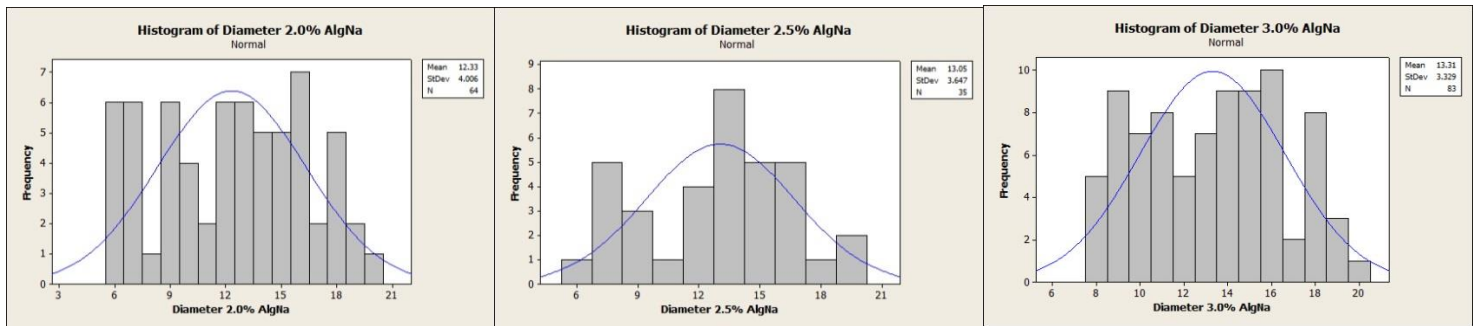


Figure A.2 Histograms of 2, 2.5, 3.0% w/v AlgNa Microbeads Diameter Distribution in Minitab

Table A.1: Yield of the Microbead Preparation Process by the BETE Nozzle Spray			
Alginate Concentration	Microbeads Weight (g)	Alginate Weight (g)	Yield (%)
2% AlgNa	0.213	0.9141	23.30
2.5% AlgNa	0.1941	0.6487	29.92
3% AlgNa	0.1529	0.5688	37.44

Appendix B: Lysozyme Crystallization in Alginate Beads

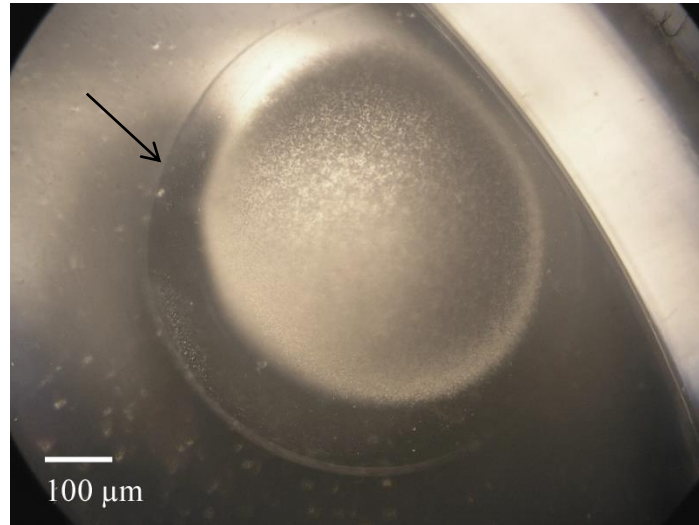


Figure B.1 Interface of lysozyme nucleation inside of the alginate beads.

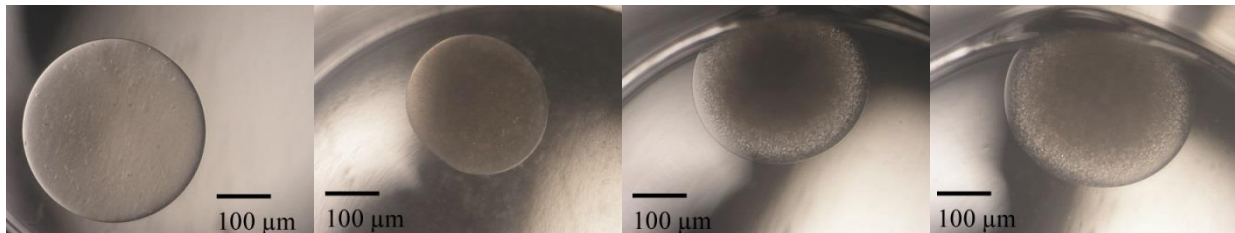


Figure B.2 Alginate Crystallization Procedure for 3% w/v Alginate Bead

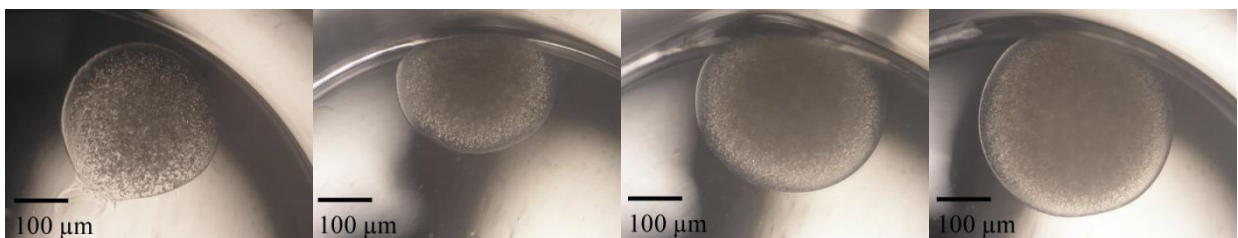


Figure B.3 Alginate Crystallization for 1-4% w/v Alginate Beads

Appendix C: Protein Release from Alginate Systems

The following plots demonstrate protein release (dot) fitted with the appropriate models (line).

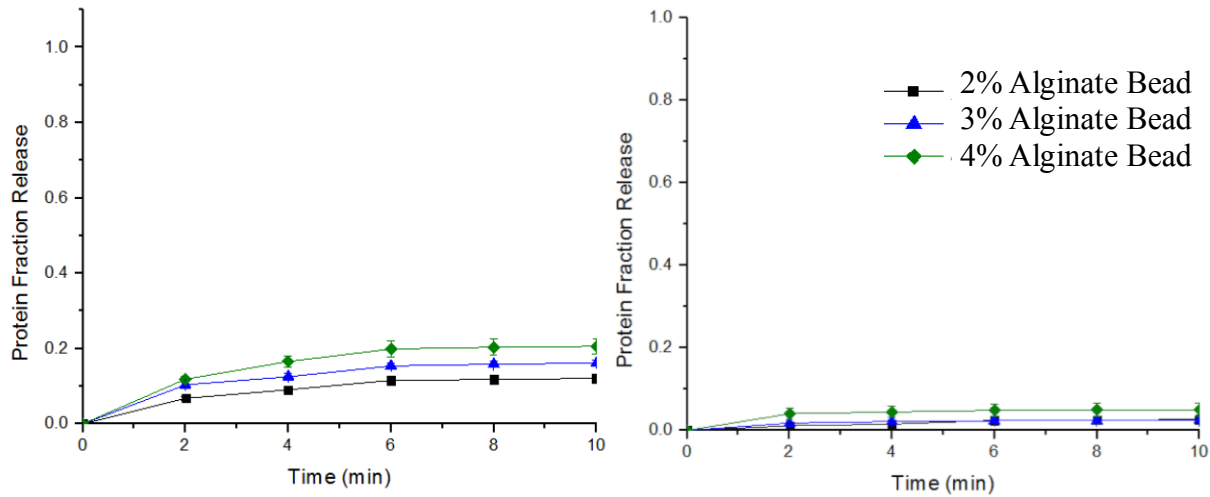


Figure C 1 Short term (first 10 mints) protein release in SGF: Solvated Protein (left) and Crystallized protein (right).

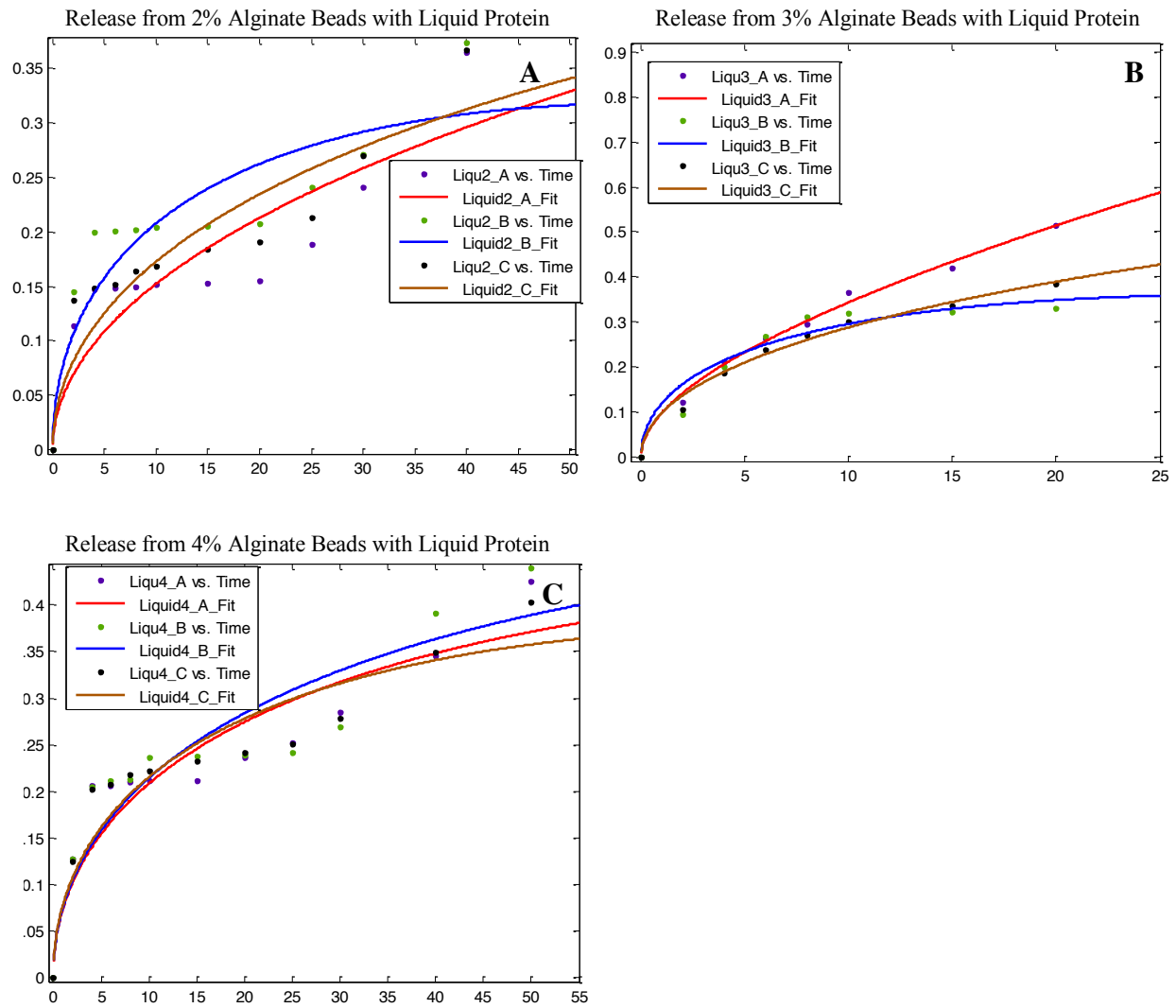


Figure C 2 Protein Release with fitted model for 2 (A), 3 (B), 4 (C)%w/v alginate beads with liquid protein. Line corresponds to model. Symbol corresponds to data (different symbols for each run).

Residual Data Analysis of Results with Model Fit:

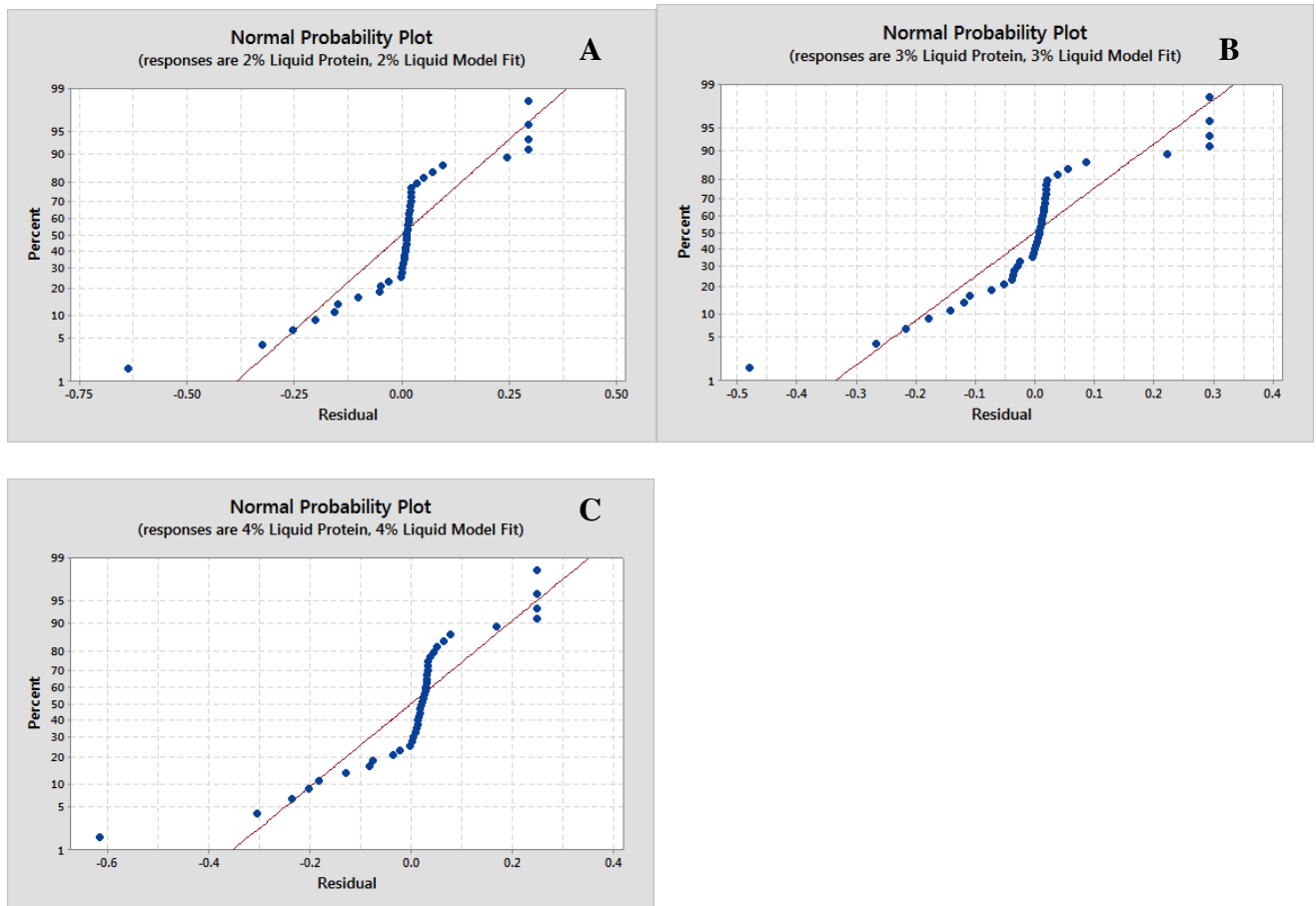


Figure C 3 Residual Data Analysis with fitted model for 2 (A), 3 (B), 4 (C) %w/v alginate beads with liquid protein.

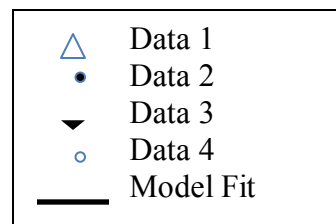
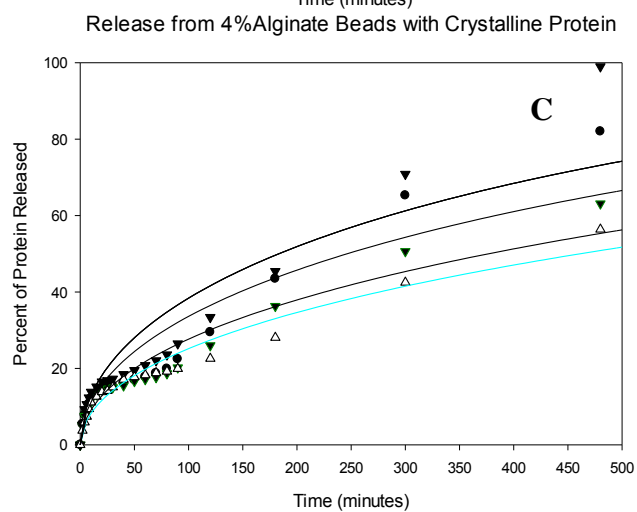
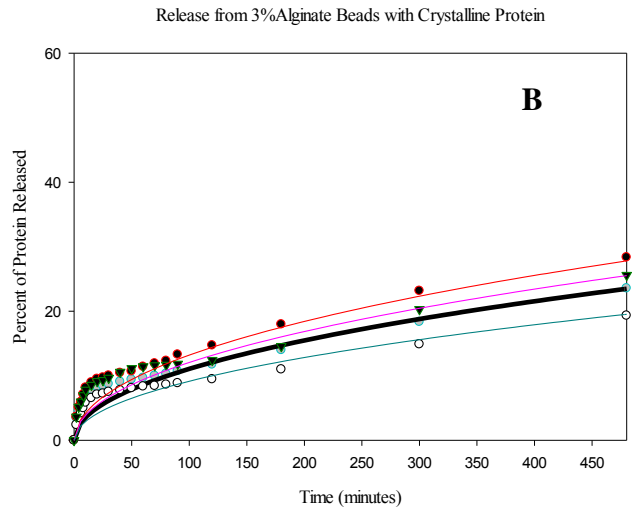
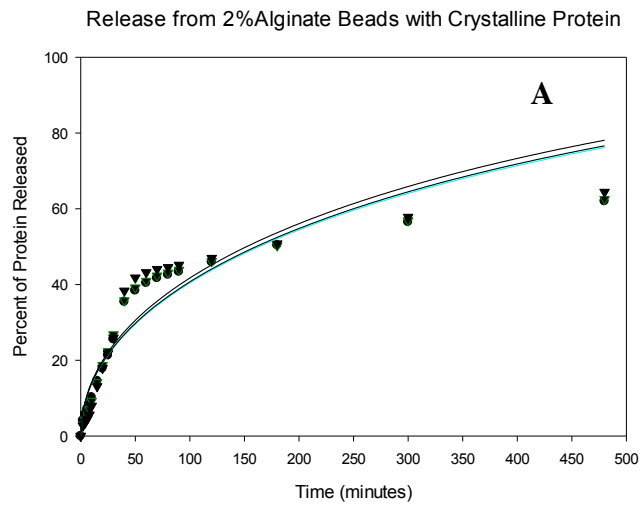


Figure C 4 Protein Release Profiles with fitted model for 2 (A), 3 (B), 4 (C) % w/v alginate beads with crystallized protein. Line corresponds to model. Symbol corresponds to data different runs of the data.

Residual Data Analysis of Results with Model Fit:

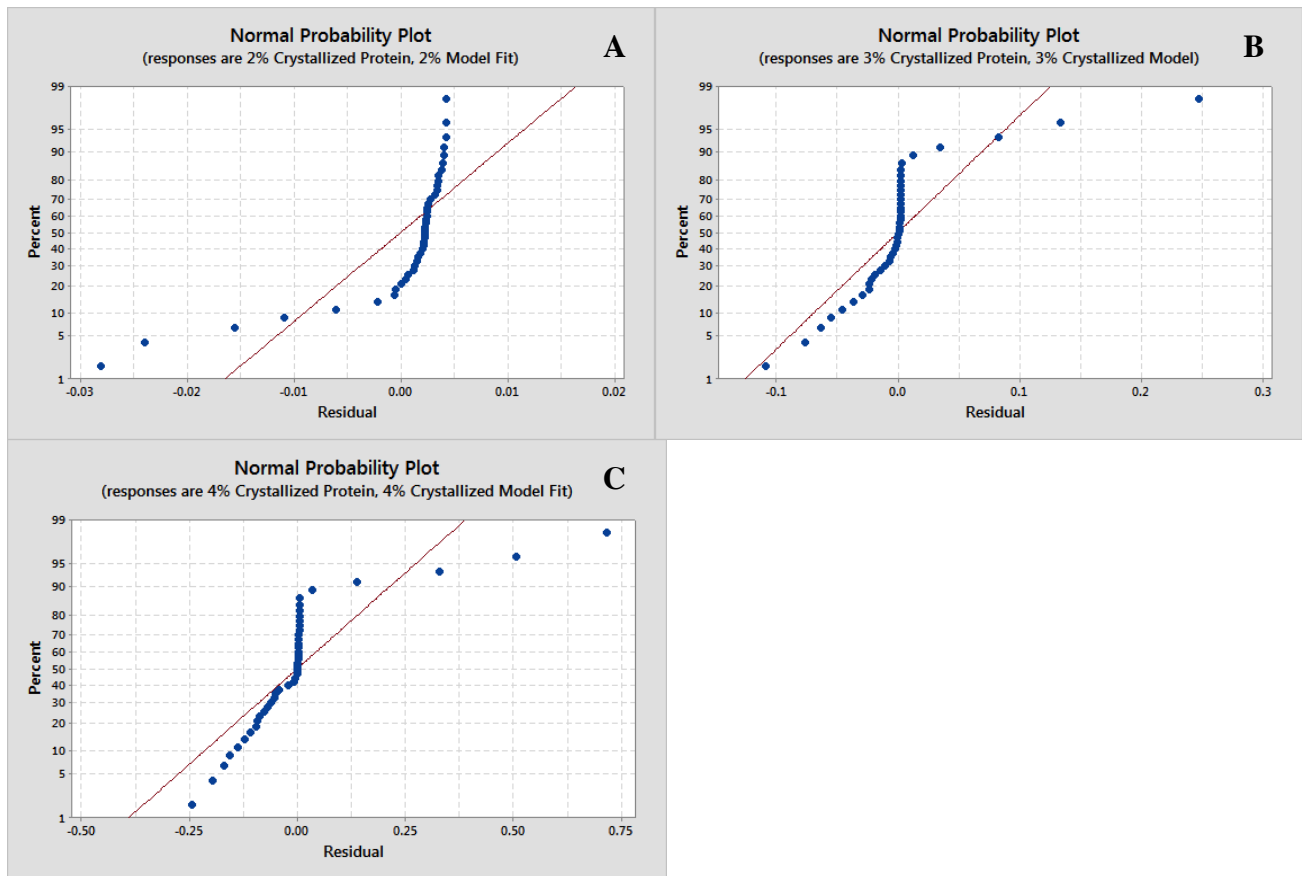


Figure C 5 Residual Data Analysis with fitted model for 2 (A), 3 (B), 4 (C) % w/v alginate beads with crystallized protein.

Appendix D: Insulin Crystallization via Hanging drop method and in Alginate Beads

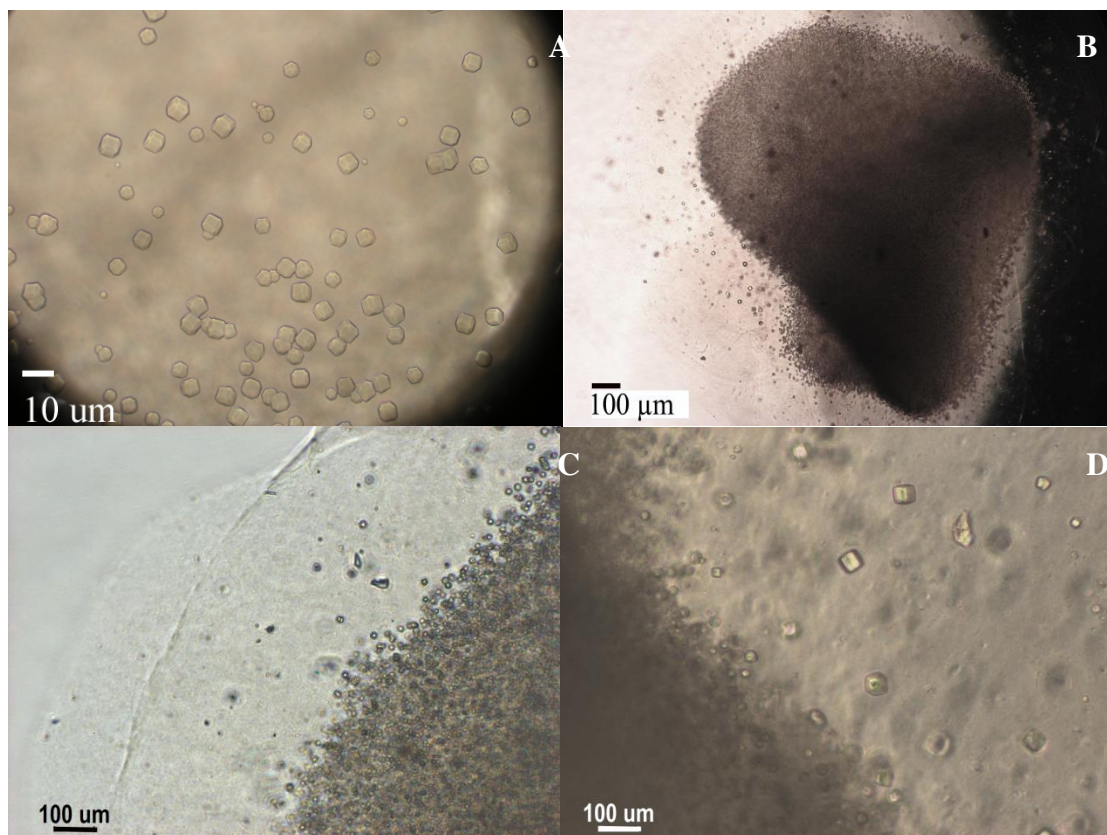


Figure D.1 Insulin Crystals by hanging drop and inside alginate beads

Appendix E: Ovalbumin Crystallization

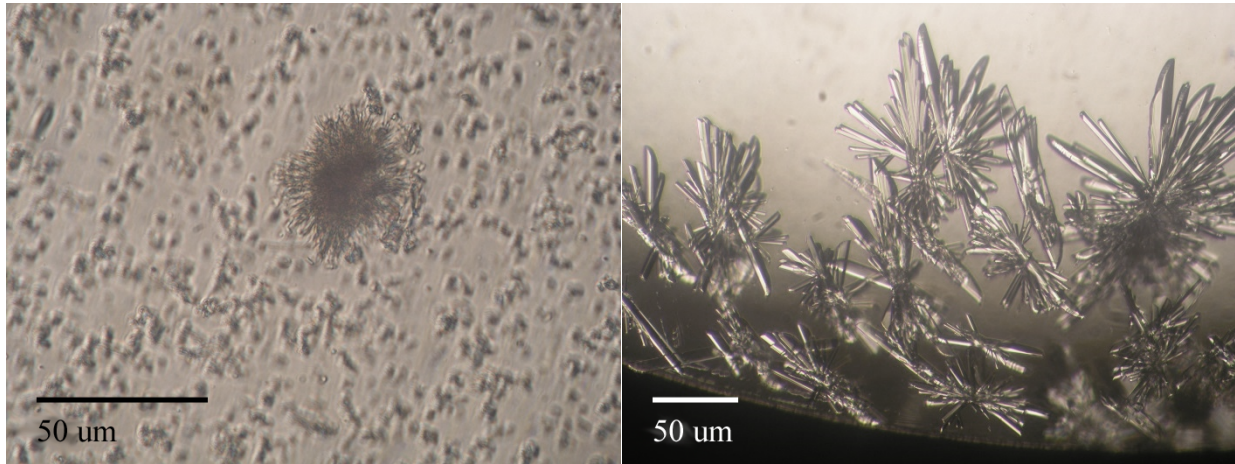


Figure E.1 Ovalbumin Crystallization